Drescher Adrian, BSc

Development of Honeycomb Pd-catalysts for Heterogeneous Cross-Coupling Reactions in Flow

Master's Thesis

to achieve the university degree of

Dipl.-Ing. / Master of Science (MSc)

Master's degree programme: Chemical and Process Engineering

submitted to

Graz University of Technology

Supervisor

Ass.Prof. Priv.-Doz. Dipl.-Ing. Dr.techn. Heidrun Gruber-Wölfler

Institute of Process and Particle Engineering
Head: Univ.-Prof. Dipl.-Ing. Dr.techn. Johannes Khinast

Graz, May 2018

Affidavit

I declare that I have authored this thesis independently, that I have not used other than the declared sources/resources, and that I have explicitly indicated all material which has been quoted either literally or by content from the sources used. The text document uploaded to TUGRAZonline is identical to the present master's thesis.

_____   _____
Date   Signature

Eidesstattliche Erklärung

Ich erkläre an Eides statt, dass ich die vorliegende Arbeit selbstständig verfasst, andere als die angegebenen Quellen/Hilfsmittel nicht benutzt, und die den benutzten Quellen wörtlich und inhaltlich entnommenen Stellen als solche kenntlich gemacht habe. Das in TUGRAZonline hochgeladene Textdokument ist mit der vorliegenden Masterarbeit identisch.

_____   _____
Datum   Unterschrift

Danksagung

An dieser Stelle möchte ich mich gerne bei all den Menschen bedanken, die mich bei der Erstellung der Diplomarbeit, beim Bewältigen meines Studiums und meines Lebens immer unterstützt haben.

Der erste Dank geht natürlich an meine Eltern, die mich ihr ganzes Leben lang unterstützt und immer an mich geglaubt haben. Mit dem Wissen, eure Unterstützung zu haben, habt ihr mir immer große Lasten von den Schultern genommen. Ich kann euch dafür gar nicht genug danken.

Ein besonderer Dank gilt auch meiner Schwester, meinen Großeltern und meiner restlichen Familie, die immer für mich da waren und mich unterstützt haben.

Meiner Freundin, die mich trotz meiner vielen Mängel nicht nur aushält, sondern auch dafür liebt, danke ich dafür, dass sie mein Leben besser macht und an mich glaubt.

Auch meinen Freunden und Studienkollegen danke ich für ihre Unterstützung und ihre Freundschaft, die für mich nicht selbstverständlich ist.

Für die Betreuung der Arbeit möchte ich mich herzlichst bei Ass.Prof. DI Dr. Heidrun Gruber-Wölfler, DI Dr. Georg Johannes Lichtenegger und Christoph Neubauer bedanken. Ihr alle habt mich toll aufgenommen und mich bei meiner Arbeit sehr unterstützt.

Liebe Heidi, ich danke dir besonders für die Möglichkeit, die Diplomarbeit bei dir schreiben zu dürfen und für die Unterstützung und die Geduld während des Schaffensprozesses. Mein Dank richtet sich nicht nur an deine Unterstützung fachlicher Natur, sondern du hast mit deiner herzlichen Art eine tolle Arbeitsgruppe aufgebaut, in der man sich vom ersten Moment an sehr wohl und willkommen fühlt.

Für die fachlichen Gespräche, sowie die Hilfe möchte ich mich gerne bei der ganzen Arbeitsgruppe bedanken.

Abstract

Catalysis plays a major role in the synthesis of pharmaceuticals and fine chemicals. In the last years a lot of effort was put into the development of heterogeneous continuous processes. Nevertheless, most pharmaceuticals processes are still carried out discontinuously which costs more time and increases the risk of a varying product quality. In the last years, a major change was the beginning exchange of homogeneous catalysts, which have drawbacks, for example, in terms of recoverability, stability and product contamination, with novel developed heterogeneous catalysts.

The goal of this thesis was the development of a Pd-immobilized cordierite monolith which can be implemented in continuous flow systems for the Suzuki-Miyaura synthesis of biphenyls with a various number of substrates.

The first step of the thesis included the development of novel leaching-resistant and highly reactive single step coated honeycombs, the characterization of the monolithic surface and the recyclability as well as the heterogeneity in batch. The new developed immobilization process turned out to be very efficient, economical, easy and fast to synthesize. The catalytic surface area could be increased by a factor of three for single coated monoliths and by six for multiple coated honeycombs. Most substrate reactions could be completed within 30 min for the first six runs. To ensure a long durability of the catalyst, a new recycling procedure was developed. Based on the batch experiments it turned out that honeycombs are highly suitable for continuous Suzuki-Miyaura reactions.

The second step was the implementation of the honeycombs into a continuous catalytic system and the testing of the monoliths in flow. To achieve this goal a new reactor had to be built. The novel honeycomb housing was planned as a modular system. For example, new flow regimes or additional process steps, such

as ion-exchangers, filters or membranes, can be easily implemented if needed. The connections of the reactor are standard HPLC-fittings, which makes it suitable to the implementation in current setups. The continuous experiments were performed with a stack of three honeycombs and p-bromotoluene as substrate. The catalytic reactivity in the monolithic system is highly dependent on the temperature, pressure and flow rate. Higher temperature and pressure and a reduced flow rate turned out to be desirable.

The novel developed honeycombs offer a high potential for Suzuki-Miyaura reactions in flow as well as for other cross-coupling reactions. The high durability, the leaching and thermal resistance of the immobilized catalysts and the shape versatility of the monoliths are some examples for the advantages of cordierite based honeycombs.

Kurzfassung

Die Katalyse ist eine der Hauptakteure in der Herstellung von Pharmazeutika und Feinchemikalien. In den letzten Jahren wurden große Anstrengungen der Entwicklung von heterogenen kontinuierlichen Prozessen unternommen. Dennoch werden eine Hauptzahl aller pharmazeutischen Prozesse in diskontinuierlichen Operationsweisen durchgeführt, obwohl damit höhere Standzeiten und Produktionsschwankungen einhergehen. In den letzten Jahren wurde damit begonnen, homogene gegen heterogene Katalysatoren auszutauschen, da homogene einige Nachteile aufweisen, wie zum Besispiel eine geringere Wiederverwendbarkeit, Stabilität und Produktreinheit.

Ziel dieser Arbeit war die Entwicklung eines Monolithen mit immobilisierten Palladiumkatalysatoren für die kontinuierliche Synthese von Biphenylen mit Suzuki-Miyaura Kreuzkupplungsreaktionen.

Im ersten Schritt wurde ein neues leaching-resistentes und hochreaktives System auf Basis von Monolithen entwickelt, auf dem mittels eines Ein-Weg-Verfahrens Palladiumkatalysatoren immobilisiert wurden. Des Weiteren wurde die Charakterisierung der katalytischen Oberfläche durchgeführt, sowie die Wiederverwendbarkeit und Heterogenität in Batchexperimenten bestimmt. Die katalytisch aktiven Wabenkörper erwiesen sich in der Herstellung als kostengünstig, unproblematisch, einfach und zeitsparend. Die Oberflächenanalyse ergab einen Flächenzuwachs von 300% für die einfache und 600% für die mehrfache Immobilisierung von Katalysatorpartikel. Sowohl die Reaktivität, als auch die Reaktionsrate wurden mit mehreren Substraten getestet. Die meisten Reaktionen konnten innerhalb der ersten sechs Zyklen nach 30 min abgeschlossen werden. Um eine lange Lebensdauer der Waben zu garantieren, wurde für die Aktivitätserhaltung ein Wiederherstellungsprotokoll entwickelt. Basierend auf den Batchergebnissen kon-

nte gezeigt werden, dass sich Wabenkeramikmonolithe für kontinuierliche Suzuki-Miyaura-Reaktionen eignen.

Der zweite Schritt beinhaltete die Implementierung der neu entwickelten Monolithe in ein kontinuierliches System und die experimentelle Durchführung zur Bestimmung ihrer Eignung. Um die Waben in kontinuerlicher Weise testen zu können, musste zunächst ein neuer Reaktor für die Waben entwickelt werden. Der Reaktor wurde als ein modulares System entwickelt, um nach erfolgreicher Durchführung den Aufbau um weitere Prozessschritte erweitern zu können. Einige mögliche Änderungen und Erweiterungen wären die Strömungsführung oder das Zuschalten von Ionentauschern, Filtern und/oder das hinzufügen von Membranen. Für die Verbindungen des Reaktors wurden standardisierte HPLC-Anschlüsse verwendet. Für die kontinuierlich durchgeführten Experimente mit p-Bromtoluol als Edukt wurde festgestellt, dass sowohl erhöhte Temperatur und Druck, als auch eine erniedrigte Strömungsgeschwindigkeit von Vorteil sind.

Abschließend kann gesagt werden, dass die entwickelten Katalysatoren ein hohes Potential für Kreuzkupplungsreactionen aufweisen. Die Langlebigkeit, die Resistenz gegen Leaching und thermische Einflüsse, sowie die Flexibilität bei der Herstellung der Form sind nur einige der großen Vorteile von Wabenmonolithen.

Contents

List of Figures

List of Tables

List of Equations

List of Symbols

Sign	Description	Unit
A	Pre-exponential factor	$[(mol/m^3)^{1-n} \cdot s^{-1}]$
$E, E(t)$	external residence time distribution, probability density function	$[s^{-1}], [min^{-1}], [h^{-1}]$
E_A	Activation energy	[J/mol]
$F, F(t)$	cumulative distribution function	[-]
F_V	Volume flow	$[m^3/s]$
MM	Molar mass	[g/mol]
N, n	Amount of substance	$[mol]$
R	Universal gas constant	$[J/(mol/K)]$
S	Selectivity	[-]
TOF	Turnover frequency	$time^{-1}$
TON	Turnover number	[-]
T	Temperature	[K],[°C]
V	Volume	$[m^3]$
X_A	Relative conversion	[-]
Θ	Dimensionless time	[-]
$\tau, \bar{t}$	Mean residence time	[s],[min],[h]
c	Concentration	[mol/l]
k	Reaction rate constant	$[(mol/m^3)^{1-n} \cdot s^{-1}]$
m	Mass	[g]
r_A	Reaction rate	$[mol/(s \cdot m^3)]$
t	Time	[s],[min]

Acronyms

ACN   ammonium cerium(IV) nitrate.
EtOH   ethanol.
HNO_3 nitric acid.
MeOH   methanol.
$Pd(NO_3)_2$ palladium(II)nitrate.
$PdCl_2$ palladium(II) chloride.
$Sn^{2+}O_x$ tin(II) oxalate.

BET   Brunauer-Emmet-Teller Theory.
Bo   Bodenstein number.

CSTR   continuous stirred tank reactors.

HPLC   high pressure liquid chromatography.

ICP/MS   inductively coupled plasma - mass spectrometry.

PFR   plug flow reactor.

RTD   residence time distribution.

SCS   solution combustion synthesis.

TWC   three-way-catalyst.

1 Introduction

The easy handleability and the development history of most chemicals and pharmaceutical drugs make batch reactors attractive to use. Over decades, organic synthesis can be described as flask chemistry. These chemicals and especially their reactions were developed, studied and synthesized in laboratory scaled flasks. When it comes to the implementation in industry, the behavior of the reaction in a flask is well known - therefore, it is easy to be implemented in a batch reactor. The classical way of performing reactions in batch is more and more superseded by continuous processes. According to many regulatory bodies, continuous manufacturing is supported to be implemented. Continuous manufacturing offers higher safety, shorter processing times, increased efficiency and a smaller ecological footprint according to the constant heating, cooling and the reduction of the amounts of solvents. The most common types of continuous reactors are continuous stirred tank reactors, tubular reactors, packed-bed reactors and fluidized beds. As batch reactors, continuous reactors can also be operated with homogeneous and heterogeneous catalysts. Heterogeneous catalysts are more recommended because they are easier to separate after the reaction is finished. The homogeneous catalysts can be immobilized on different types of surfaces like metal foams. Macroporous monolithic materials, like cordierite honeycombs or silica gel, with high surface areas gained a lot of attraction as carriers for catalysts and their usage in microporous technology for chemical syntheses in flow. This attraction is basically related to the general advantages of heterogenous catalysts, the high surface-to-volume ratio, based on the interconnected network, and the very efficient mixing. One of the main advantages of monoliths is the high versatility. Size and shape of the monolith, diffusion length and wall thickness of the channels and the regime and flow configuration are very easy to modify.[1,2]

Therefore, the goal of this thesis is the development of monolithic immobilized Pd-catalysts that can be recycled several times and easily implemented in continuous flow setups.

2 Theoretical background

In this chapter a brief insight of the thesis' background will be presented. The short overview includes catalysis, immobilization, coupling reactions, solution combustion synthesis, batch and continuous operational modes and monolithic reactors.

2.1 Catalysis

Catalysis is one of the most industrially used production mechanisms. The theoretically background will be discussed in this section.

2.1.1 Definition

Catalysts are compounds which accelerate chemical reactions and make them more likely to perform.
If a catalyst accelerates a reaction by decreasing the activation energy E_A, it is defined as a positive catalysis. Negative catalysts are also called inhibitors, which slow down reactions and therefore are used to control fast and strong exothermic reactions.
The equilibrium of a reaction is not affected by the presence of a catalyst. By forming an intermediate complex with a lower activation energy, as shown in Figure 2.1, a reaction is more likely to perform. Especially at lower temperatures the presence of a catalyst makes reactions possible, increases the reaction rate and helps to save energy. The effect of a catalyst is illustrated in Figure 2.2.[5,6]

Figure 2.1: Scheme of a catalytic cycle.[3]
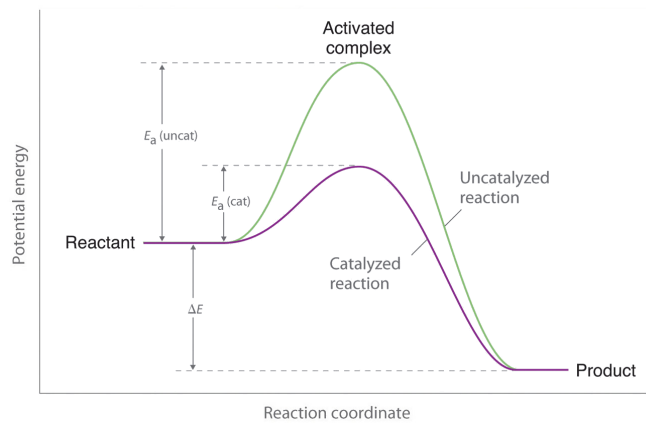
Figure 2.2: The effect of a catalyst on the activation energy of a chemical reaction[4]

The temperature dependence of the reaction rate is described by the Arrhenius equation (Equation 2.1).[5,6]

During the catalytic process, the catalyst is theoretically not changed or consumed. After completing the chemical reaction, the same amount of catalyst should be present in the reaction mixture or the reactor. However to non-ideal behavior, a catalyst is deactivated over time by various effects, which also can lead to a drop in weight.[7]

4

$$k = A * e^{-\frac{E_A}{R*T}} \qquad \begin{aligned} &\text{k} = \text{Constant rate} \\ &\text{A} = \text{Pre-exponential factor} \\ &E_A = \text{Activation energy} \\ &R = \text{Universal gas constant} \\ &T = \text{Temperature} \end{aligned} \qquad (2.1)$$

Equation 2.1: Arrhenius equation

2.1.2 Performance

The performance of a catalyst is defined by its

- Productivity

- Activity

- Selectivity

- Durability

Productivity

The productivity of a catalyst can be described with the turnover number (TON), which can be seen in Equation 2.2. It is the number of moles of substrate that a mole of catalyst can convert before becoming inactivated. For an economical process of precious metal catalysts, the TON should be higher than 1000.[7,6]

$$TON = \frac{\text{moles of substrate converted}}{\text{moles catalyst used}} \qquad (2.2)$$

Equation 2.2: Turnover number

Activity

The turnover frequency (TOF), presented in Equation 2.3, is described by the number of molecules produced divided by the number of active sites and the time.

It is easier to calculate the TOF for enzymatic processes and for homogeneously catalyzed reactions than for heterogeneously catalyzed reactions, because it is difficult to determine the active sites of a heterogeneous catalyst. To compensate the lack of knowledge of active sites for a heterogeneous catalyst, the mass or the surface are used as a substitute.[7,6]

$$TOF = \frac{\text{molecules of product}}{\text{(moles of catalyst used)*(time)}} \qquad (2.3)$$

Equation 2.3: Turnover frequency

Selectivity

The selectivity describes the ability of a catalyst to favor the production of the desired product against the formation of side products. The equation is shown in Equation 2.4.[7]

$$S = \frac{\text{moles of desired product}}{\text{moles of all products formed}} \qquad (2.4)$$

Equation 2.4: Selectivity

Durability

Durability is defined as the time of usage while the activity and the selectivity are not falling under a pre-defined limit. It also includes the stability and the mechanical strength of a catalyst. The durability is affected negatively by fouling, sintering, poisoning and leaching.[7]

2.1.3 Classification of catalysts

Catalysis in general can be divided in different types:[8,7]

- Homogeneous catalysis
- Heterogeneous catalysis

- Electrocatalysis

- Photocatalysis

- Biocatalysis

- Organocatalysis

Homogeneous catalysis

A catalysts can be described as homogeneous, if the catalyst and the reacting partner are situated in the same phase. Usually this phase consists of a gas or a liquid. To have a high economic benefit from the usage of a homogeneous catalyst, it should show a high activity (TOF) to allow a low reactor volume and a low catalyst concentration. In general, homogeneous catalysts show a high activity and a high selectivity.

The main disadvantages of homogeneous catalysts are the necessary post-processing down-stream separation to recycle/reuse the catalyst and to avoid product contamination. The loss of catalyst mass during the recycling process also leads to a shorter lifetime. For the separation two industrial methods, distillation and liquid-liquid extraction, are common. Both methods are associated with a complexity of the instruments.[6,9]

Heterogeneous catalysis

A heterogeneous catalyst is in a different phase state than the reactants, which practically means that it is usually operated with a solid heterogeneous catalyst and a gaseous or liquid reaction phase, as shown in Figure 2.3. The solid catalyst is represented by the bed of catalyst particles and especially the porous carrier. The fluid phase consists of the reactants and the formed products. Solid heterogeneous catalysts offer a lot of potential advantages for the industry:[7]

- environmentally friendly

- safer to be manipulated

- easier recyclability

- improved process control

- reduction of metal traces in the product

Common devices for heterogeneous supported reactions are packed-bed reactors, fluidized beds, continuous stirred tank reactors (CSTR) and slurry reactors.
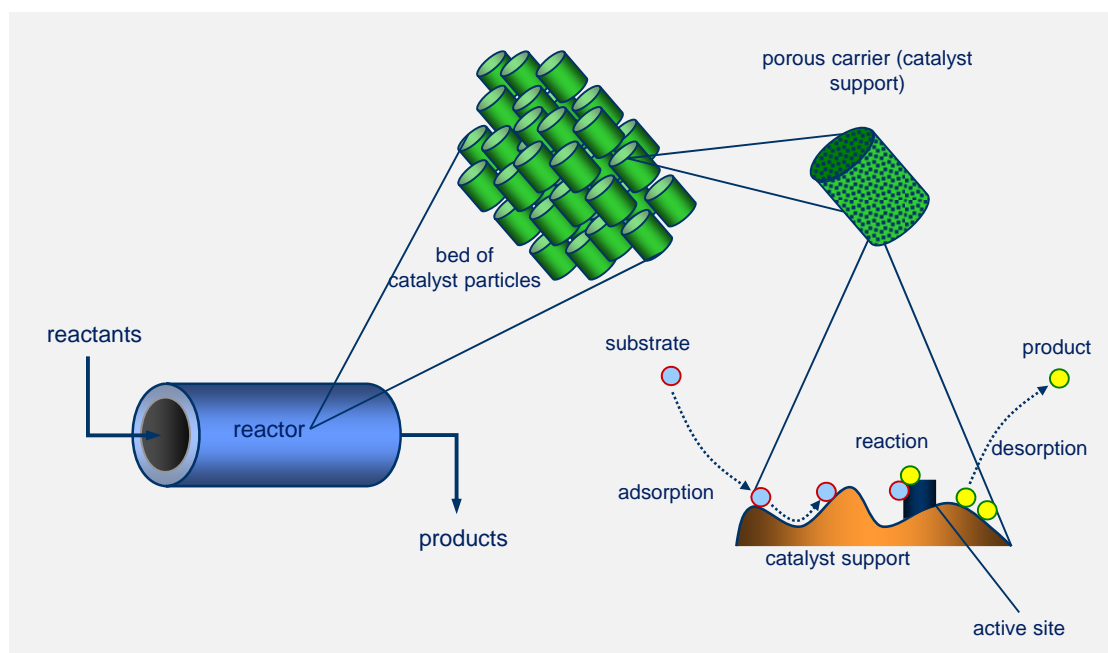
Figure 2.3: The scheme shows the technical setup of a process involving heterogeneous catalysts and the steps of heterogeneous catalysis according to the Langmuir-Hinshelwood mechanism.[10]

A not commonly used type of reactor, which has to be mentioned, is the trickle bed reactor. The heterogeneous reaction takes place on the surface of the catalyst and includes five steps:[7,11]

1. Transport of the reactants from the bulk to the surface of the catalyst

2. Adsorption of one or more reactants to the surface of the catalyst

3. Reaction of adsorbed species on the active sites to form the product

4. Desorption of product from the surface of catalyst

5. Transportation of product back in the fluid phase

Step one and five are physical transportation processes which can be rate limiting. Steps two to four describe processes which occurring on the surface of the catalyst. These steps are often labeled as microkinetics. Step three is the relevant chemically product forming step. The process is illustrated in Figure 2.3.[6,11]

The deactivation of heterogeneous catalysts is based on non-ideal behavior. Deactivation mechanisms are presented in Figure 2.4.[8,12,13]

- Poisoning

- Fouling

- Thermal degradation/sintering

- Volatilization of active compounds/leaching

- Mechanical deactivation
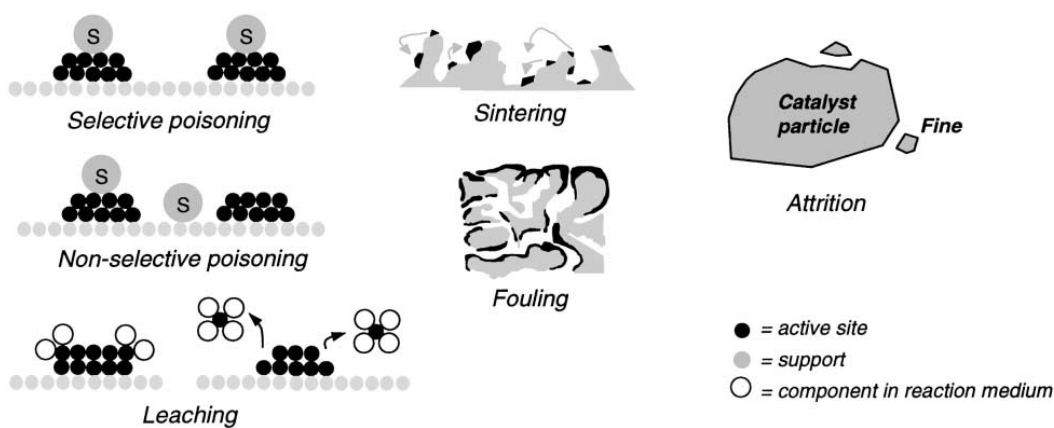
Figure 2.4: Different catalyst deactivation mechanisms.[13]

The loss of activation over time can also cause decreasing selectivity. Sometimes the loss of activity can be compensated by increasing the reaction temperature and reaction rate, otherwise the catalyst must be regenerated. The regeneration

process is limited to the fact that some deactivation processes are irreversible, like the volatilization of active compounds, poisoning and sintering. Fouling or some types of poisoning can be reversible processes.[11,8]

Catalyst Poisoning

Poisoning is the one of the main causes of catalyst deactivation. It can be classified as the blocking of active sites by a certain element associated with a formation of complexes or by chemisorption. A weak chemisorption can lead to a reactivated catalyst. If the chemisorption is too strong, deactivation will become permanent. Catalyst poisoning can be separated in:[8,12]

- Group 15 and 16 elements

- Metals and ions

- Molecules with free electron pairs

- NH_3, H_2O and organic bases

- Compounds which react with active sites

Catalyst fouling

Pores which are blocked by organic compounds or hydrocarbons can cause fouling and catalyst deactivation. For example, at temperatures above $700\,K$, polymeric compounds tend to form black carbonaceous materials on the surface of the catalyst. Organic compounds, such as methane, ethanol (EtOH) or arenes, can also form carbonaceous material on the surface of the monoliths. The carbon forms a layer and therefore it is not possible for reactants to reach the active sites and the reaction slows down or stops completely. For example: In a system of methane, the formation of such polymeric layer can be minimized by a high steam/methane ratio or by the alkalization of the carrier.[11,8,12]

Thermal Degradation/Sintering

Sintering is the first form of thermal degradation and describes the agglomeration of metal crystallites below the melting point of the metal. In the presence of steam by increasing the temperature the rate of sintering increases. Above the temperature of $970\,K$ a solid-solid reaction can occur and favors the formation of inactive metal-carrier compounds, for example metal-aluminates, which describe the second type of thermal degradation. The third type of degradation is caused by phase changes. An example for the reduction of the surface area is the phase change of γ-alumina to α-alumina. The surface area shrinks by the factor of 250.[11,8,12]

Volatilization of active compounds/leaching

During conversion, the noble metals escape from the catalyst and lead to an irreversible deactivation process. For example the deactivation process for continuous cross-coupling reactions is attributed to its special reaction mechanism. The cross-coupling reaction mechanism requires free palladium complexes as active species and therefore the mechanism is based on a homogeneous reaction process. After the reaction occurs most of the Pd-complexes are caught by its support. Complexes, which are not caught, lead to leaching. If leaching occurs in a bigger scale during the reaction, an ion exchanger can be implemented in the downstream processes to catch the leached ions and to avoid product contamination. The determination of leached Palladium can be done for example with inductively coupled plasma - mass spectrometry (ICP/MS) measurements.[11,8,12]

Mechanical deactivation

Catalyst particles force a high amount of mechanical stresses during their life time cycle. In fluidized-bed reactors, high attrition can be studied. In fixed-bed reactors attrition will occur less, but thermal influences and tensions will also result in a higher forming of very small particle parts, which can lead to reactor blocking and

polluted products. Mechanical strength of catalyst particles are caused by shape, porosity, pressure-drop, rapid temperature changes and fluid velocities.[12,13]

2.2 Immobilization

The development of a honeycomb based catalytic system requires different immobilization methods. The most important methods are described in this section. The immobilization of homogeneous catalysts on heterogeneous solid surfaces combines the advantages of homogeneous and heterogeneous catalysts. The used immobilization method is based on the interaction between the catalyst and the solid support.[7]

2.2.1 Methods

Four immobilization methods can be determined:[14]

- Covalent binding

- Electrostatic interaction

- Adsorption

- Encapsulation

Covalent binding

Covalent binding, or tethering, involves the covalent fixation of a catalytic active compound on a surface. The solid support has several requirements. It should provide stabilization, an enhancement of the selectivity to the metal complex and an easy recoverability. The well-defined silanol groups of ordered mesoporous silica offer for example an ideal anchoring site for homogeneous and enzyme catalysts and make them very suitable for covalent tethering.[7,14,15]

Electrostatic interaction

Electrostatic interaction is a well-explored and well-established method of immobilization. The main requirement to use this method is the surface ionizability of the solid support. Studies have shown that the interaction between the catalyst and the surface is strong enough to minimize leaching.[7,14,15]

Adsorption

The driving force for the adsorption is the Van-der-Waals-Interaction. The unmodified type of the interaction is quite weak and will make leaching and deactivation inexorable. Ways of improving the performance of the interaction are modifying the stability of the catalyst and implementing hydrogen bonds.[7,14]

Encapsulation

Encapsulation uses the pore size diameter of the support and the diameter of the catalyst particles to entrap them in the free pore space. Therefore, the pore size opening has to be smaller than the diameter of the pore space. The smaller pore size prevents the catalyst from leaching. As a side effect, the small pore diameter rises the mass transfer resistance for the reactants as well as for the product.[14]

Coating

Coating is a special form of immobilization. It combines the methods of covalent binding, adsorption and encapsulation. In the automobile industry, coating is a wide spread immobilization technique. Usually three-way-catalysts (TWCs) are coated and used for exhaust gas after-treatment systems. In most cases the supporting system is a honeycomb, like a monolithic ceramic body, which is first coated with γ-Al_2O_3 to expand the surface area and it is working as a binder.
For washcoating different procedures exist. One commonly used method is the Sol-gel routine. The active phase, which is applied on the washcoat, consists of a

slurry of particles. The process steps for the washcoat are dripping of the monolith into the slurry, blowing air to remove the liquid, drying at high temperature and calcination. The second way of immobilize catalysts on a ceramic monolith is the in-situ growth of nano-crystals via a solution combustion routine on the cordierite honeycomb surface. Therefore a solution of precursors are impregnated onto the surface and dried in a furnace to force the in-situ growth. The in-situ method is a complex, dense layered formation of inter-crystalline porous particles, which has the disadvantage that diffusion limitation can occur. The main advantage is the stronger adhesion. A combination of both, washcoat and in-situ growth, results in a higher adhesion than the coating with just the slurry phase.[7,16,17,18,19]

2.3 Coupling reactions

In this thesis the novel monolithic catalytic system should be applied for Suzuki-Miyaura cross coupling reactions. A short introduction to the coupling reactions is given in this section.

In organic chemistry, a coupling reaction describes a variety of reactions between two hydrocarbons in the presence of a metal catalyst. In cross-coupling reactions an aryl, vinyl or alkyl halide is replaced by a nucleophile (which can be an olefin or organometallic), to form a new carbon-carbon bond. Equation 2.5 shows the reaction equation of a cross-coupling reaction.

$$R-M + R'-X \xrightarrow{\text{Palladium catalyst}} R'-R + M-X \qquad (2.5)$$
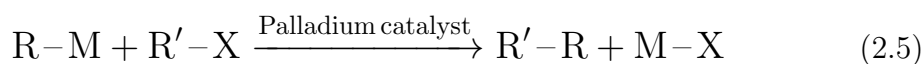
Equation 2.5: Cross-coupling reaction

Two types of coupling reaction can be defined:[3,20]

- The cross-coupling reaction couples two different partners
- The homo-coupling process forms a bond between two identical partners

2.3.1 Palladium catalyzed cross-coupling reactions

Richard F. Heck, Ei-ichi Negishi and Akira Suzuki were awarded with the 2010 No-
bel Prize in Chemistry for the development of Palladium catalyzed cross-coupling
reactions. In the production of fine chemicals, palladium cross-coupling reactions
are widely used for the formation of C–C bonds.

R–R' L_nPd^0 R'–X

Step 3: reductive   Step 1: oxidative
elimination   addition

$L_nPd\overset{R'}{\underset{R}{\diagup}}$ $L_nPd\overset{R'}{\underset{X}{\diagdown}}$

R–M   Step2:   M–X
      transmetallation
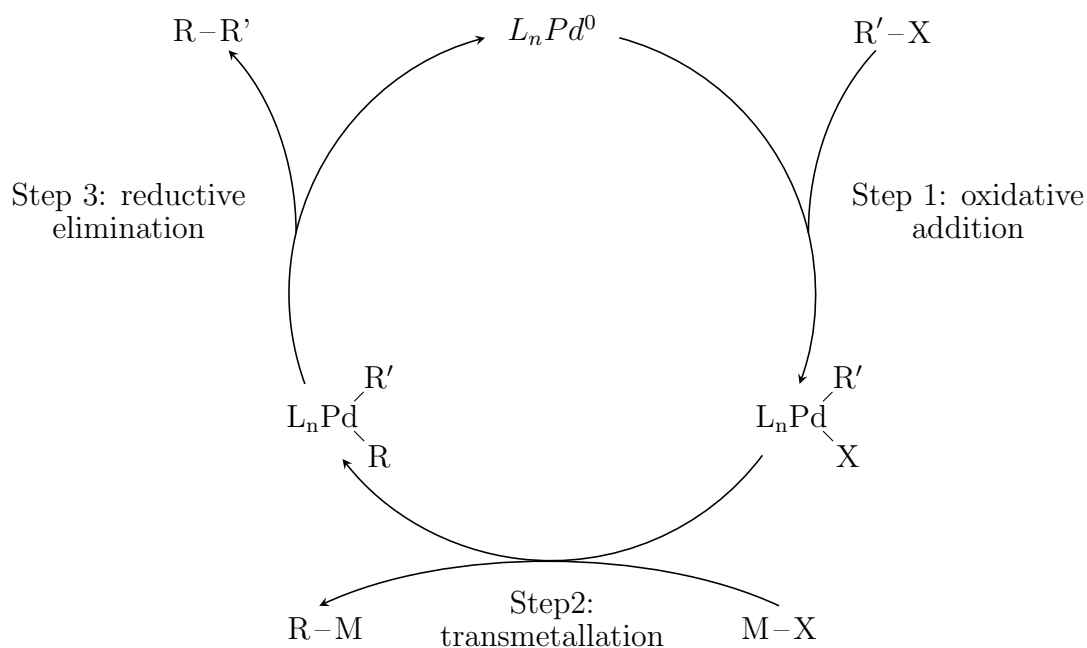
Figure 2.5: Scheme of a palladium catalyzed cross-coupling cycle.[adopted from:21]

Figure 2.5 describes the principle of a palladium catalyzed cross-coupling reaction.
Two molecules are coupled with the help of the metal by the formation of metal-
carbon bonds. Via the assembly of the carbon with the metal, the two carbon
atoms can be brought very close to each other, so a new carbon-carbon single
bond can be formed.
The types of cross-coupling reactions, which operate according to this principle and
have become very important in the field of organic synthesis, are the Heck and the
Suzuki-Miyaura reaction. In both reactions palladium is present in a zerovalent
state. The reaction between an electrophilic partner, which is an organohalide
R–X (or an analogous compound), and a nucleophilic partner. This nucleophilic
partner can be either an olefin (e.g. for the Heck reaction) or an organometallic

compound (e.g. for the Suzuki-Miyaura reaction) $R-M$.[21,22,23]

2.3.2 Suzuki-Miyaura reactions

Suzuki-Miyaura reactions couple organoboron compounds with an organohalide in the presence of a base, needed for the activation of boronic acids, and a zerovalent palladium complex. The reaction scheme of a palladium catalyzed Suzuki-Miyaura reaction cycle is shown in Equation 2.6.

$$R-B(OH)_2 + R'-X \xrightarrow[\text{Base}]{\text{Pd}} R'-R + B(OH)_2-X \qquad (2.6)$$
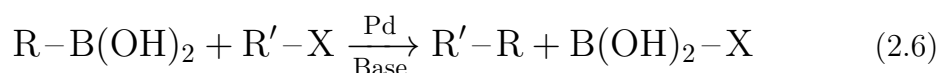
Equation 2.6: Suzuki-Miyaura reaction

The whole cycle involves three steps, which are illustrated in Figure 2.5:
The first step is an oxidative addition of $R'-X$ to the palladium(0), which leads to an organopalladium compound. In the second step, which is called transmetallation, the R compound of the $R-X$ molecule is transferred to the palladium and forms the metal intermediate $R'-R-Pd$. The intermediate is the assembly of the organic groups on the same palladium atom. The final step is called reduction elimination. During this step, the two carbon groups on the intermediate complex couple with each other and a new $C-C$ single bond is formed and released from the palladium. Following from this the Pd^{II} is reduced to Pd^0. The mild running and non-toxic reaction conditions, its high chemoselectivity and a wide range of possible functional groups are big advantages of the Suzuki-Miyaura cross-couplings.[21,22,23]

2.4 Solution combustion synthesis

In the thesis a new direct coating process was tested via a solution combustion routine. The new routine does not need a pre-applied binder and only involves one synthesis step. The solution combustion synthesis (SCS) is a very simple and rapid process for the synthesis of nano particles. It involves a homogeneous solution of

different oxidizers and fuels. The fuel depends on the used metal nitrates. For chromium and related oxides, glycine is used as fuel. The purposes of fuels are to provide heat and C and H-atoms, which form CO_2 and H_2O during the combustion and to form metal complexes with the metal ions in the solution. The SCS co-operates with properties of the synthesized nano-material. The uniform and precise formulation of the composition of particles is referable to the mixing of reactants in the initial reaction media. The high synthesis temperature of 500-900 °C leads to a high product purity and crystallinity. The temperature and the nature of the combustion (flaming to non-flaming) depend on the exothermity of the used fuel. The ignition point for self-propagating reaction are usually below 500 °C. The short process duration supports the growth and the formation of nano-sized powders with high surface areas.[24,25,26]

2.5 Batch and Continuous Operation

The honeycombs were tested for batch and continuous operation modes. To determine the peculiarities of each operational mode a short introduction is given here. Chemical reactors are vessels to perform chemical reactions in a controlled and safe environment. Reactors are designed to ensure highest efficiency of desired outputs and the highest yield of product with lowest energy and financial input. The two main operation types:[27,28]

- Batch operations
- Continuous operations

2.5.1 Ideal chemical reactors

According to the two operation types, three main basic models (Figure 2.6) of ideal chemical reactors can be determined:[27]

- Batch reactor
- Continuous stirred tank reactors (CSTR)
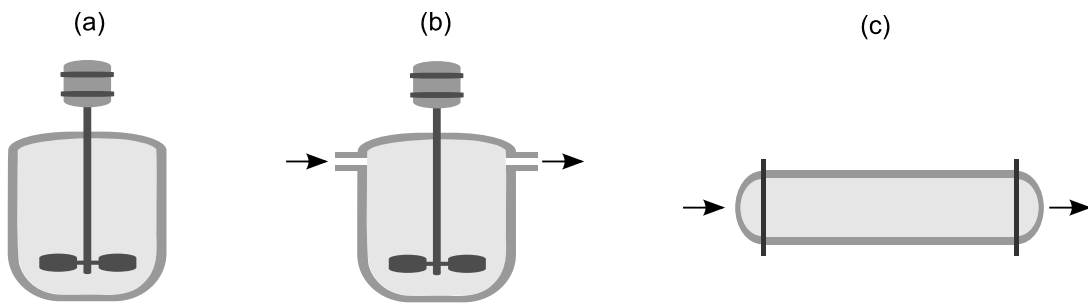
Figure 2.6: Schemes of reactor designs: (a) Batch reactor, (b) CSTR, (c) PFR[29]

- Plug flow reactor (PFR)

Batch reactor

Batch reactors are widely used in industry and laboratories. In a batch reactor the composition of components is uniform at any location. After the vessel is filled with reactants the reaction performs until one reactant is totally consumed or the reaction is aborted. Afterwards the vessel is discharged, cleaned and used again.[27]

Continuous reactors

As mentioned before, the two basic types of continuous reactors are the CSTR and the PFR. A CSTR is a continuously operating well stirred vessel showing a perfect back-mixing similar to the batch reactor. The composition over place and time is constant. The PFR is based on a differential volume element because the composition varies from point to point throughout the entire length of the reactor.[27]

2.5.2 Batch vs. Continuous operation

Batch operations as well as continuous operations have advantages and disadvantages which are determined in tables 2.1 and 2.2.

Table 2.1: Batch operation[28]

Advantages	Disadvantages
Simple and flexible equipment and operation	Varying product quality
Low investment costs	High energy costs (heating/cooling)
Well known processes	Difficult to automate
Easy to clean	Labor intensive
	Down time between batches
	Scale-up is challenging

Table 2.2: Continuous operation[28]

Advantages	Disadvantages
Uniform product quality	Lack of process knowledge
Low personnel costs	Lack of qualified personnel
Online monitoring and control in real time	Complex monitoring equipment
Production of dangerous chemicals in small scale	
High selectivity	
Small economic footprint	
Automation feasible	
Smaller facility size	
Easier scale-up	
24/7 production	

2.5.3 Residence time distribution

The residence time τ is the quotient of the reactor volume V_R and the feed volume $F_{V,0}$:

$$\tau = \frac{V_R}{F_{V,0}}$$

It is necessary, due to non-ideal behavior of the flow profile in a reactor, to investigate the hydrodynamics to fix the gap between the theoretical and the real behavior. One test method to describe the complex flow profile is the residence time distribution. This method is based on the residence time quantification of molecule assemblies or particle aggregates in a reactor. The residence time distribution (RTD) forms the basis for the calculation and the reactor performance.

Two ways for the experimental determination of the RTD can be described:

- Pulse function

- Step function

For both methods the current input condition is manipulated and the response of the reactor output is recorded as shown in Figure 2.7. The RTD of a PFR, shown as number 1 in Figure 2.7, is characteristic for its mixing.

Input signal
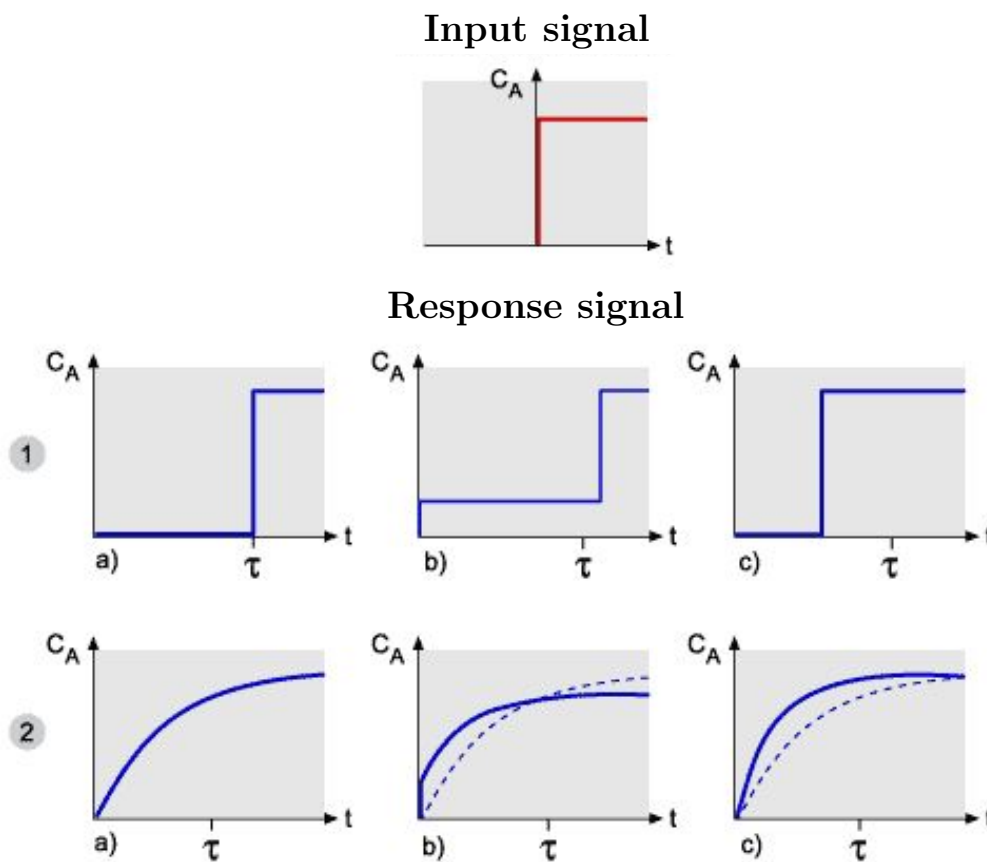
Response signal

Figure 2.7: The figure shows the response signals for a residence time distribution using a step function. The concentration at the input is changed immediately. (1) PFR, (2) CSTR. (a) ideal, (b) short-circuit flows, (c) with dead zones.[30]

Batch and idealized plug-flow reactors have a very sharp RTD because all atoms in the reactor have the same residence time. For a CSTR, presented as number

2, the concentration change is slowly and therefore a mean residence time has to be calculated. Some atoms remain long in the reactor and some are leaving very early. This can be manipulated by the flow regime inside the stirred vessel.

Three cases are presented in Figure 2.7. The first case (a) shows ideal flow behavior. Case (b) illustrates a short-circuit flow, whereas case (c) shows a reactor with dead zones. To determine the residence time it is important that the change of the input is easily measurable and must not lead to a different flow behavior inside the reactor.
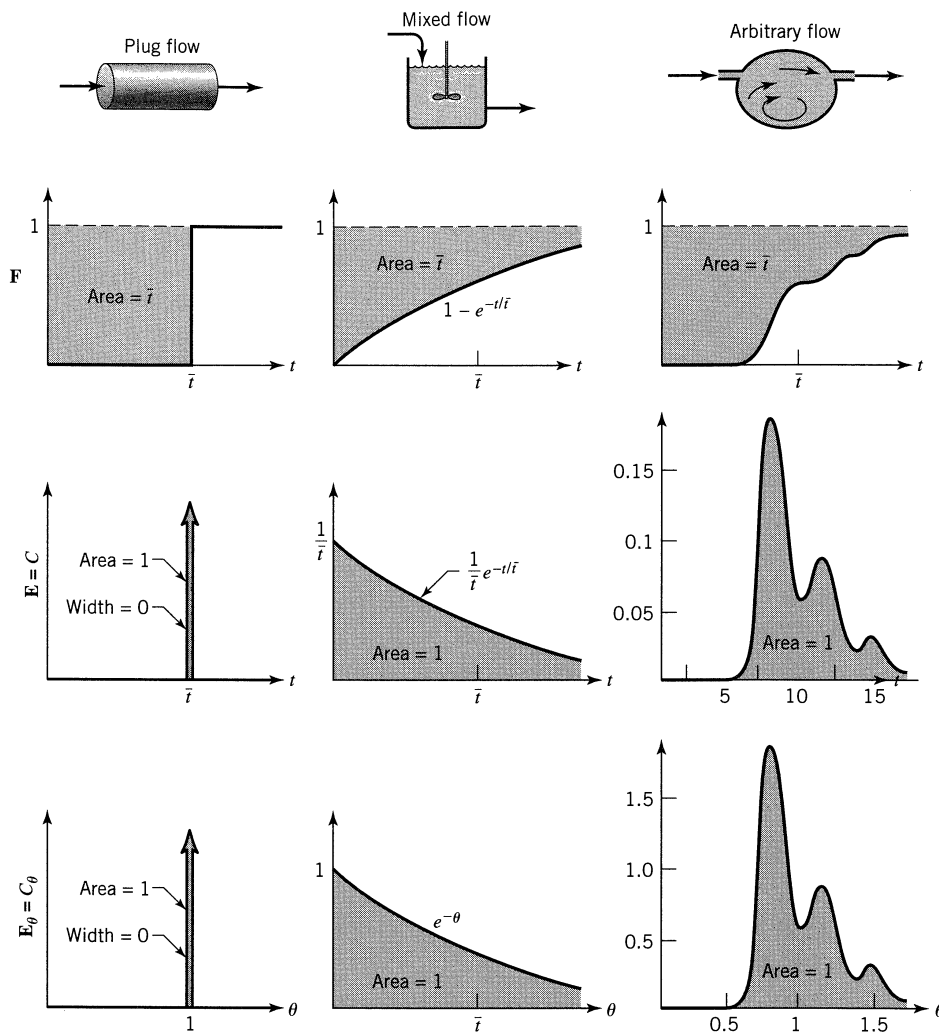
Figure 2.8: The E- and F-function for various flows with ordinary and dimensionless time scale.[27]

21

The exit age function, also called E-function (Equation 2.7), describes the time distribution a fluid element has spend inside of the reactor.

$$\int_0^\infty E(t) \cdot \mathrm{d}t = 1 \tag{2.7}$$

Equation 2.7: Exit age function

The cumulative distribution function F(t)(Equation 2.8) defines the leaving fraction of a fluid with an age time less than t.

$$F(t) = \int_0^t E(t) \cdot \mathrm{d}t \tag{2.8}$$

Equation 2.8: Cumulative age function

The illustration for the E- and the F-function for various flows and ordinary and dimensionless time are presented in Figure 2.8. The mean residence time $\bar{t}$ can be calculated with Equation 2.9 and is necessary to calculate the variance σ^2 (Equation 2.10). The variance is the expectation of the deviation of a variable from its mean value. A high variance leads to a high dispersion inside the vessel.[31,32,28]

$$\bar{t} = \frac{\sum t_i c_i \Delta t_i}{c_i \Delta t_i} = \int_0^\infty t \cdot E(t) \cdot \mathrm{d}t \tag{2.9}$$

Equation 2.9: Mean residence time

The Bodenstein number (Bo) is a dimensionless ratio between convective mass transfer to axial dispersion (Equation 2.11) and can be calculated with the variance. The Bo provides a measure for the backmixing. A higher Bo indicates a lower backmixing and a low diffusion coefficient (PFR). A very small Bo leads to a high diffusion coefficient and to ideal backmixing (CSTR).

$$\sigma^2 = \int_0^\infty (t - \bar{t})^2 \cdot E(t) \cdot \mathrm{d}t \tag{2.10}$$

Equation 2.10: Variance

L = Characterisic length of the reactor

$$\mathrm{Bo} = \frac{u \cdot L}{D_{ax}} \qquad \text{u = Flow rate} \tag{2.11}$$

D_{ax} = Axial diffusion coefficient

$$
\begin{array}{lll}
Bo \to \infty & D \to 0 & \text{PFR / no backmixing} \\
Bo \to 0 & D \to \infty & \text{CSTR / ideal backmixing}
\end{array}
$$

Equation 2.11: Bodenstein number

2.5.4 Design equations

In the next subsection the design equations of the three ideal reactors are explained. All design equations are based on the material balance:

$$\text{input} = \text{output} + \text{disappearance reaction} + \text{accumulation} \tag{2.12}$$

Equation 2.12: Material balance

Batch reactor

Due to the fact that the vessel is sealed after filling, the input and output of the material balance are nulled.[27,29,31]

$$\cancel{\text{input}}^{0} = \cancel{\text{output}}^{0} + \text{disappearance reaction} + \text{accumulation} \tag{2.13}$$

$$0 = (-r_A) \cdot V + \frac{dN_A}{dt} \tag{2.14}$$

$$(-r_A) \cdot V = \frac{-dN_A}{dt} \tag{2.15}$$

with $N_A = N_{A,0} \cdot (1 - X_A)$ and its derivation

$$\frac{dN_A}{dt} = \frac{N_{A,0} \cdot dX_A}{dt}$$

we obtain

$$(-r_A) \cdot V = N_{A,0} \cdot \frac{dX_A}{dt} \tag{2.16}$$

By integrating Equation 2.16 over time we receive the design equation of a batch reactor:

$$t_R = N_{A,0} \cdot \int_0^{X_A} \frac{dX_A}{(-r_A) \cdot V} \tag{2.17}$$

Equation 2.17: Design equation batch reactor

Continuous stirred tank reactor

By definition no accumulation is occuring in a CSTR, which leads to its elimination in the material balance.[27,31]

$$\text{input} = \text{output} + \text{disappearance reaction} + \underbrace{\text{accumulation}}^{0} \tag{2.18}$$

$$F_{A,0} \cdot (1 - X_{A,0}) = F_A + (-r_A) \cdot V \tag{2.19}$$

with $F_A = F_{A,0} \cdot (1 - X_A)$ and $F_{A,0} \cdot (1 - X_{A,0}) = F_{A,0}$
we get

$$F_{A,0} \cdot X_A = (-r_A) \cdot V \tag{2.20}$$

$$\frac{V}{F_{A,0}} = \frac{X_A}{(-r_A)} \tag{2.21}$$

The transformation of Equation 2.21 leads to the CSTR design equation:

$$\tau = \frac{V}{F_{V,0}} = \frac{V \cdot c_{A,0}}{F_{A,0}} = \frac{X_A \cdot c_{A,0}}{-r_A} \tag{2.22}$$

Equation 2.22: Design equation CSTR

Steady-state Plug Flow Reactor

The mass for the PFR is fed and released continuously. The reactor content is moving like a plug and therefore a differential volume element is considered in the mass balance:[27,31]

$$\text{input} = \text{output} + \text{disappearance reaction} + \text{accumulation} \xrightarrow{\quad} 0 \tag{2.23}$$

$$F_A = (F_A + dF_A) + (-r_A) \cdot dV \tag{2.24}$$

by replacing with $dF_A = d[F_{A,0} \cdot (1 - X_{A,0})] = -F_{A,0} \cdot dX_A$
we obtain

$$F_{A,0} \cdot dX_A = (-r_A) \cdot dV \tag{2.25}$$

separating and integrating result in

$$\int_0^V \frac{dV}{F_{A,0}} = \int_0^{X_A} \frac{dX_A}{(-r_A)} \tag{2.26}$$

Converting Equation 2.26 leads to the PFR design equation:

$$\frac{V}{F_{A,0}} = \frac{\tau}{c_{A,0}} = \int_0^{X_A} \frac{dX_A}{-r_A} \tag{2.27}$$

Equation 2.27: Design equation PFR

2.6 Monolithic reactors

Monolithic reactors are widely used for environmental applications, like the automobile exhaust treatment, ozone destruction, catalytic combustion or other cat-

alytic processes. The structure of these monoliths consists out of small parallel ordered with catalyst coated channels. Big advantages of these reactor types are the reduced dimensions and the low pressure drop combined with high flow, heat and mass transfer rates, very flexible and well-defined structuring possibilities and high selectivity. Some possible structures are presented in Figure 2.9. The devel-
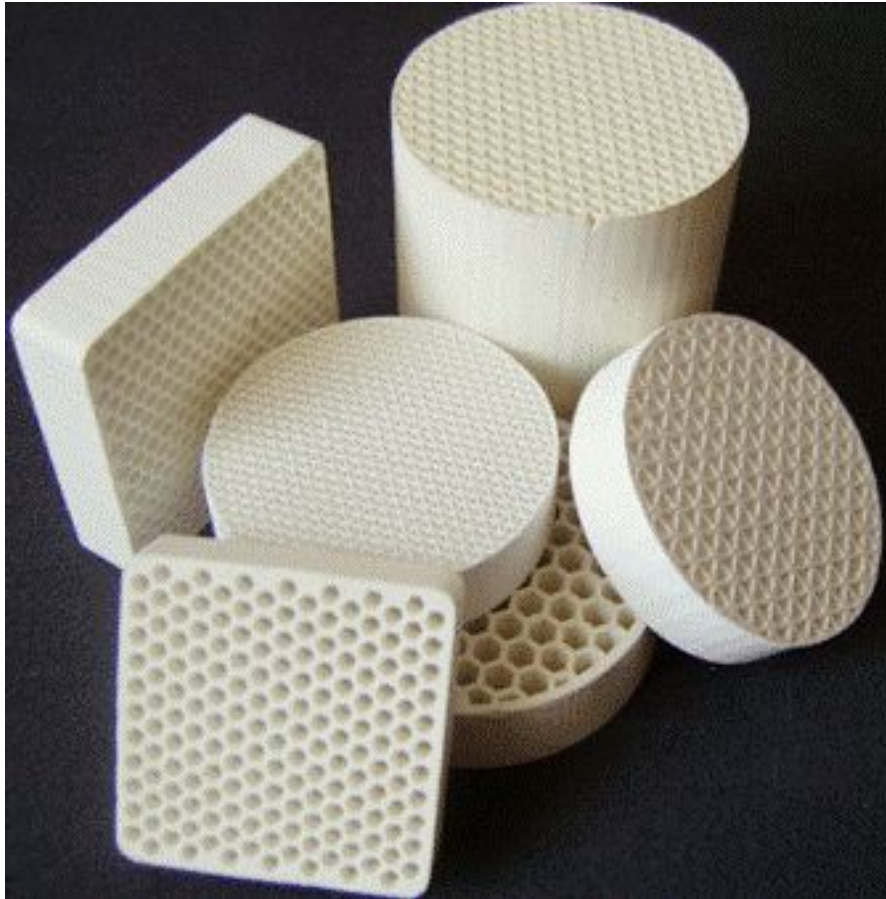
Figure 2.9: Monolithic structures[33]

opment of dies for a continuous production of ceramic honeycombs was one key factor for the success. Another key factor was the high cell density ($\sim$ 1600 cpsi), which was achieved by the progressive perfection of dies. With new and more precise extrusion processes pressure drop, different shapes, fluid dynamics, mass and heat transfer phenomena could be improved.[19,34]

2.6.1 Types of ceramic monoliths

Three types of extruded catalytic monoliths can be distinguished:

- Low surface area monolith

- High surface area monolith

- Integral monolith
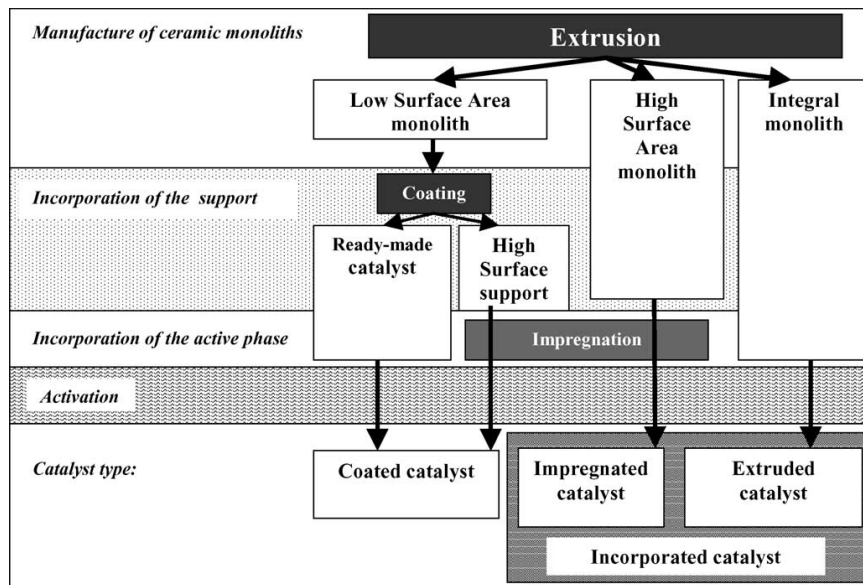
Figure 2.10: Extrusion of monoliths[19]

The three types of extruded monoliths and their usage and post-processing possibilities are shown in Figure 2.10.

Low surface area monoliths

Low surface area monoliths with less than $1\,\mathrm{m^2\,g^{-1}}$ are likely used as carriers, for example for automotive exhaust emission control. The surface should offer a roughness suitable for washcoat immobilization, mechanical strength, thermal stability and a high resistance for temperature changes. A widely used material

for low surface area monoliths is cordierite. Cordierite honeycombs are produced by mixing (kneading) the raw materials, cordierite powders, water and an agglomerate agent or kaolin or clays or talc with alumina. The desired shape is formed by the extruder. The extruded strand is burned and calcined at $1300-1400\,°C$ for $3-4\,h$. By adding other additives, for example zirconia, mullite or alumina, properties can be improved. A mixture of talc, kaolin and alumina hydroxide is the most frequently used mixture.[19,34]

High surface area monoliths

High surface area monoliths are in the range between $200-400\,m^2g^{-1}$. Thermal stability and thermal shock resistance is less important. They are mostly manufactured out of alumina, silica, titania, zirconia zeolites or activated carbon. The monoliths offer a high porous structure and a low mechanical strength. The mechanical strength can be increased by high thermal treatment which also leads to a reduction of porosity.[19,34]

Integral monoliths

Integral monoliths are produced out of a composition of dough and included corresponding compound or precursors. The active sites are distributed through the whole monolith which is one of the biggest advantages. This type of monolith is insensitive against the deactivation of the catalyst by erosion and abrasion.[19,34]

3 Motivation

Ceramic monoliths have been successfully used for multiphase reaction systems. Many globally operating companies, like Unilever or Shell, use monoliths for their processes. Very famous applications are gas-phase processes, like the automotive exhaust gas cleaning. Especially the ability to handle multiple kinds of substances simultaneously makes honeycombs valuable for the conversion of volatile organic compounds and the reduction of NOx. Another field of development of honeycombs is the reduction of nitrates and nitrites in water. The excessive use of fertilizers, the effluent outfall from urban residues or the industry, which are harmful for humans make the treatment of water necessary. Distillation and adsorption processes could also be performed successfully.[35,36,37,38]

New applications with a high potential of the novel Pd-immobilized honeycomb catalyst system are Suzuki-Miyaura reactions in batch and in flow. The aim of this thesis is the development of a Palladium based monolithic catalytic system for Suzuki-Miyaura reactions in flow with long durability and high selectivity. The monolithic system is forced to be leaching-free, versatile, mechanically and thermally stable.

The first goal of this thesis was the direct immobilization of the pre-developed, with solution combustion synthesis produced catalysts on the surface of the cordierite monolith. As well as the investigation of the coating and the determination of catalytic activity, durability and selectivity in batch experiments with a various number of substrates.

The second goal of the thesis was the implementation of the honeycombs for testing their catalytic abilities in a continuous synthesis process. To achieve this, a housing for the honeycombs had to be built. The reactor is planned with PTC:CREO and manufactured in the workshop of the institute. For the continuous reactor, a

residence time distribution has determined to study the characteristic flow behavior inside the vessel. The performance of the reactor and the catalyst have to be investigated with several continuous experiments.

4 Methods and Materials

4.1 Analytical balance

To measure the mass and to calculate mass differences a Mettler HK 160 analytical balance was used. The measuring is based on the proportionality of the weight to the mass in a gravitational field. The weighted object has to be at room temperature to avoid natural convection. Furthermore, the balance has to be leveled to avoid tilting and the doors of the balance have to be closed to minimize the influence of air flow and dust accumulation.

4.2 Microscopy

For the optical determination of the honeycomb surface a Leica DM4000 M with transmitted and reflected light microscopy mode was used. Light microscopy is one of the most well-known and used methods to view small objects. Two different types of light microscopes are common:

- Transmitted light microscope

- Reflected light microscope

The mechanics of the two microscopes are delineated in Figure 4.1. Nowadays microscopes usually support both types alternately or simultaneously for conduct investigations.

(a) Scheme of a Transmitted light microscope

(b) Scheme of a Reflected light microscope
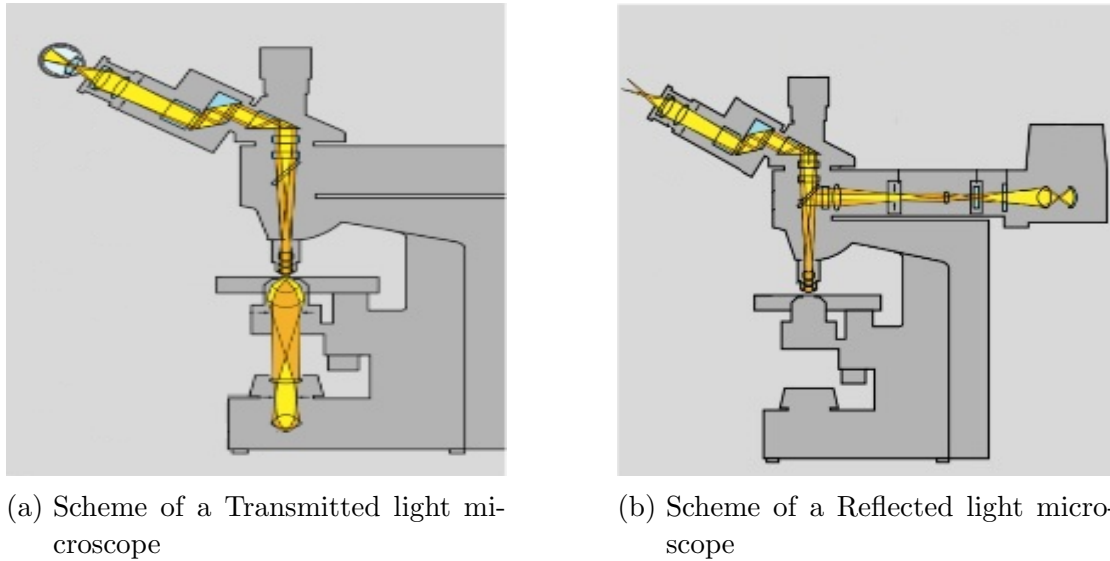
Figure 4.1: Scheme of light microscope[39]

Transmitted light microscopy

Transmitted light microscopy is commonly used for optically permeable samples. The working principle of a transmitted light microscope is shown in Figure 4.1a. According to the principle samples require more care in preparation than sample for reflected light microscopy. These samples have to be naturally thin or processed to be light permeable. The light source for transmitted light microscopy is placed directly on the opposite site of the specimen. The light passes a condenser, which focus the light on the object. The image of the samples passes the lens and hits the port for photomicrography. The image is created by absorbed light due to stains, pigments or different dense areas.[40,41]

Reflected light microscopy

Reflected light microscopes are used to investigate opaque samples, for example most metals, ores, ceramics and polymers. The opaque properties of these specimen require a light source which is directed onto the surface. The light has to return to the microscope objective by a specular or diffused reflection (Figure 4.1b). The reflected light from the specimen's surface re-enters the objective

and passes through the binocular head to a port for photomicrography. Reflected light microscopy is the domain method for industrial scale in semiconductor areas, metallography and many other applications.[42,43]

4.3 High pressure liquid chromatography

The high pressure liquid chromatography (HPLC) is an analysis technique which separates a mixtures of substances into their components. The molecular structure and molecular composition are the main factors for the separation. The mixture dissolved in a mobile phase is forced to flow under a pressure up to 400 bar through a stationary phase. The interaction between the single components and the stationary phase are the driving forces for the analysis. The stronger the interaction, the slower the components are moving through the column and the later the components are reaching the detector. The principle of a chromatography column is illustrated in Figure 4.2. The retention time and the peak area give information about the type of the component and the concentration.[44]

Figure 4.2: Chromatography principle[45]

In this thesis an Agilent 1100 series HPLC System was used. The system is

equipped with a quaternary pump, an autosampler, an online degasser, a thermostated column and a UV-vis detector. As stationary phase a reversed phase column was used. The mobile phase consisted of methanol and a 300:1 aqueous phosphoric acid. The method is given in Table 4.1. The sample measurement temperature was set to 25 °C. Over the method's duration of 15 min the UV-Vis detector was working at wavelengths of 237 and 270 nm. The time started after a 2 µL sample was injected into the HPLC system.

Table 4.1: HPLC method

Time [min]	% A (v/v)	% B (v/v)	Flow [ml/min]
0	60	40	1
10	80	20	1
12	60	40	1

The retention times and wavelengths of the internal standard, substrates, products and side products are presented in Table 4.2 and in Table 4.3.

Table 4.2: HPLC substrate wavelength

Chemical	Retention time [min]	Wavelength [nm]
Anisol	1.56	270
Phenylboronic acid	0.88	237
p-Bromotoluene	4.74	237
4-Bromoacetophenone	1.78	237
2-Bromobenzonitrile	1.23	237
4-Bromobenzonitrile	1.23	237
4-Bromobenzyl alcohol	1.23	237
4-Bromobenzotrifluoride	4.94	237
5-Bromo-1-indanone	1.72	237
4-Bromoanisole	1.44	237

Table 4.3: HPLC product wavelength

Chemical	Retention time [min]	Wavelength [nm]
Product		
4-Methylbiphenyl	8.81	237
4-Acetylbiphenyl	3.59	237
Biphenyl-2-carbonitrile	2.29	237
Biphenyl-4-carbonitrile	2.29	237
4-Biphenylmethanol	2.32	237
4-Trifluoromethylbiphenyl	8.44	237
5-Phenylindan-1-one	3.37	237
4-(4-Methoxyphenyl)benzene	2.99	237
		237
Sideproduct		237
Biphenyl	5.87	237
Phenol	0.81	270

4.4 Inductively Coupled Plasma - Mass Spectrometry

ICP/MS (Agilent 7700x) is an elemental determination analytical technique. Concentrations of metals and non-metals at detection limits at or below parts per trillion (ppt) can be analyzed.
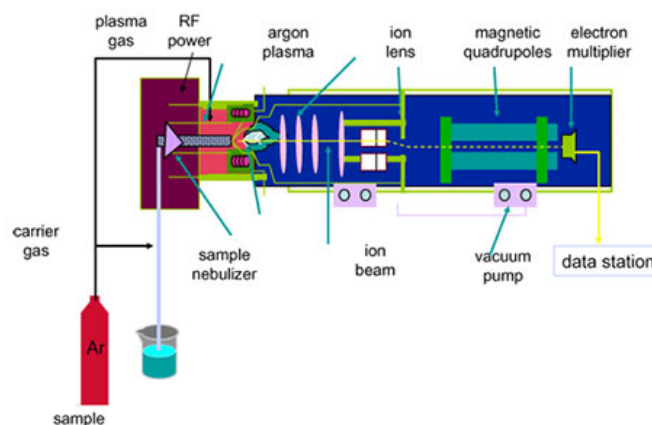
Figure 4.3: ICP/MS[46]

The method uses inductively coupled plasma (for example Argon) to ionize the

sample, which is seperated and quantified in a mass spectrometer. Most commercial mass spectrometers work with the mass-to-charge ratio to split the ions. All ions with the chosen mass-to-charge ratio, which is set by the magnetic quadrupoles, are allowed to pass the mass spectrometer to the detector (electron multiplier). The process is presented in Figure 4.3.[47]

4.5 TriStar II 3020

The analytical method of the TriStar II 3020 is based on Brunauer-Emmet-Teller Theory (BET) and used to determine the specific surface area and the material porosity with nitrogen as analytical gas. First of all micropores are filled. In the next step the free surface gets covered completely. Finally capillary condensation fills the larger pores. The desorption process is started with the systematically reduction of the pressure which results in the liberation of the absorbed molecules. The sets of generated data are used to describe the isotherms. The shapes of the isotherms give conclusions about the surface and internal pore characteristics.[48]

4.6 Materials

In this section the used materials and chemicals are listed in Table 4.4

Table 4.4: Chemicals

Name	Manufacturer	Formula	Purity
Ammonium cerium(IV) nitrate	Sigma-Aldrich	$Ce\,H_4\,N_8\,O_{18}$	98.5%
Tin (II) oxalate	Sigma-Aldrich	$Sn\,C_2\,O_4$	98%
Palladium (II) chloride	Aldrich	$Pd\,Cl_2$	99%
Glycine	Sigma-Aldrich	$C_2\,H_5\,N\,O_2$	99%
Potassium carbonate	Sigma-Aldrich	$K_2\,C\,O_3$	99%
Phosphoric acid	Roth	$H_3\,PO_4$	85%
4-Bromotoluene	Aldrich	$C_7\,H_7\,Br$	98%
4-Bromobenzonitrile	Aldrich	$C_7\,H_4\,Br\,N$	99%
2-Bromobenzonitrile	Sigma-Aldrich	$C_7\,H_4\,Br\,N$	99%

Table 4.4: Chemicals

Name	Manufacturer	Formula	Purity
4-Bromoanisol	Sigma-Aldrich	$C_7 H_7 Br O$	99%
4-Bromoacetophenone	Fluka	$C_8 H_7 Br O$	98%
4-Bromobenzyl alcohol	Sigma-Aldrich	$C_8 H_7 Br O$	99%
4-Bromobenzotrifluoride	Sigma-Aldrich	$C_7 H_4 Br F_3$	99%
5-Bromo-1-indanone	Sigma-Aldrich	$C_9 H_7 Br O$	97%
Ethanol	Roth	$C_2 H_6 O$	99,8%
Acetone	Brenntag	$C_3 H_6 O$	100%
Methanol	Roth	$C H_3 O$	HPLC Grade
Phenylboronic acid	Fluka	$C_6 H_7 BO_2$	97.0%
Anisole	Sigma-Aldrich	$C_7 H_8 O$	99%

5 Experimental

5.1 Preparation of the cordierite

The cordierite monolith, based on its form also called 'honeycomb' (MK20, $\varnothing 1$ inch), was produced by Porzellanfabrik Hermsdorf GmbH and provided as a 20 cm extruded strand by CTP Chemisch Thermische Prozesstechnik GmbH. The honeycomb consists out of 14% MgO, 35% Al_2O_3 and 51% SiO_2 according to the provided information of the manufacture. The strand was cut into fifteen 1.0 cm pieces (Figure 5.1) with a band saw shown in Figure 5.2.
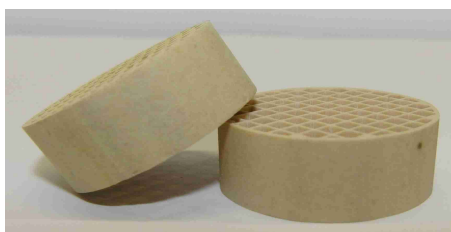
Figure 5.1: Pieces of honeycombs

Figure 5.2: Band saw

To remove residues on the surface the pieces were cleaned with acetone, dried at room temperature and stored in 1.3 cm high plastic Petri dishes. Before the monoliths were used for the immobilization of the catalyst, they were washed with acetone, dried for at least 1 min in a furnace at 100 °C and cooled down.

5.2 Preparation of the catalyst

For each honeycomb a batch of about 3 g of catalyst had to be prepared by using a modified SCS reported by Lichtenegger et al.[49] Figure 5.3 illustrates the synthesis of the catalyst and the coating process of the honeycombs. To provide 3.000 g of catalyst 4 ($Ce_{0.49}Sn_{0.49}Pd_{0.01}O_{2-\delta}$) a theoretical composition of 5.000 g ammonium cerium(IV) nitrate (ACN), 1.861 g tin(II) oxalate ($Sn^{2+}O_x$), 3.294 g glycine and 0.033 g palladium(II) chloride ($PdCl_2$) were weighted (Figure 5.3a) and blended by grinding the particles to a fine powder (Figure 5.3b) using a mortar and a pestle.[49,50] This catalyst composition is used for catalyst 1-6 and 9-16.

(a) Weighing compounds   (b) Blending and grinding   (c) Dissolving in water

(d) Catalyst liquid   (e) Filling in honeycomb   (f) Pressing in honeycomb

(g) SCS   (h) Cleaning   (i) Immobilized catalyst
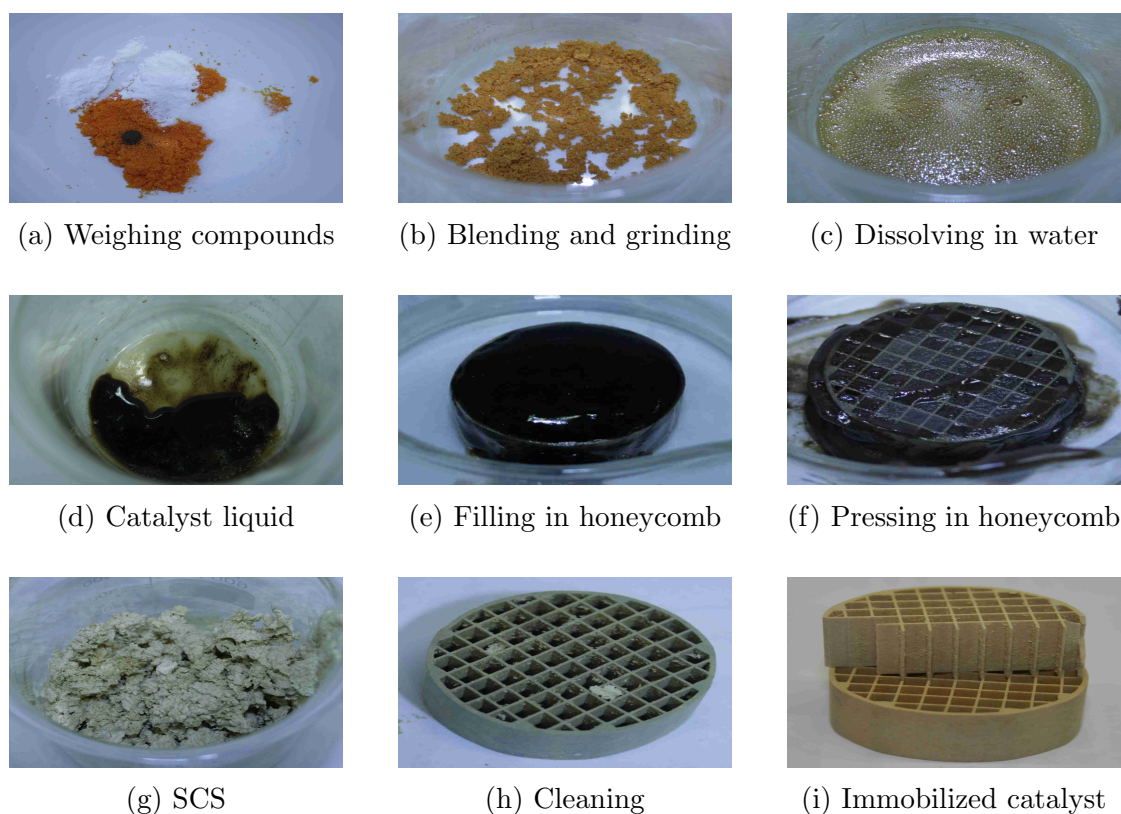
Figure 5.3: Catalyst synthesis process.

For the synthesis of a 3.000 g batch of catalyst 2 ($Ce_{0.79}Sn_{0.20}Pd_{0.01}O_{2-\delta}$), which was used for honeycomb 7 and 8, 5.000 g ACN, 0.469 g $Sn^{2+}O_x$, 2.1625 g glycine and 0.020 g $PdCl_2$ were blended and synthesized. The fine solid crystals were

transferred into a 600 ml borosilicate beaker and 2 ml deionized water was added while the beaker was swiveled until the solid powder was completely dissolved. (Figure 5.3c) The light orange solution in the beaker was treated in an ultrasonic bath, until a viscous, honey like, puce liquid was achieved.(Figure 5.3d) This process step takes up to 30 min. The honeycomb was placed into a borosilicate 5.0 cm high crystallizing dish and the liquid was filled into the channels of the honeycomb.(Figure 5.3e) The crystallizing dish with the honeycomb was immediately put into a desiccator and a pressure of 50 mbar was applied for about 30 s. For honeycomb 3 this step was skipped. The desiccator was de-pressurized and the paste like solution was pressed into the channels of the honeycomb with a scoop as presented in Figure 5.3f. The desiccator was pressurized again for several seconds until the solution mixture was dark brown and highly viscous. Afterwards, the pressure was slowly adjusted to atmospheric pressure, the monolith was removed from the desiccator and placed in a 600 ml borosilicate beaker.

Table 5.1: First coating Catalyst 4

Component	Nominal [g]	Honeycomb [g]					
		1	2	3	4	5	6
ACN	5.000	5.0018	5.0056	5.0021	5.0009	5.0061	5.0021
SnO_x	1.861	1.8621	1.8639	1.8621	1.8617	1.8644	1.8610
$PdCl_2$	0.033	0.0342	0.0331	0.0331	0.0338	0.0351	0.0350
Glycine	3.294	3.2944	3.2956	3.2949	3.2950	3.2934	3.2954
		9	10	11	12	13	14
ACN	5.000	4.9992	4.9997	5.0009	5.0058	5.0011	5.0050
SnO_x	1.861	1.8624	1.8635	1.8611	3.2939	1.8620	1.8633
$PdCl_2$	0.033	0.035	0.0328	0.0338	0.0347	0.0346	0.0379
Glycine	3.294	3.2945	3.2957	3.2950	3.2939	3.2950	3.2986
		15	16				
ACN	5.000	5.0003	5.0012				
SnO_x	1.861	1.8623	1.8618				
$PdCl_2$	0.033	0.0384	0.0348				
Glycine	3.294	3.2944	3.2951				

The beaker was transferred to a 350 °C muffle furnace, which reached the ignition point within less than 5 min.[49,50] The honeycomb remained in the furnace for about 5 h. By the solution combustion a fine and high volumetric foam was formed

which is presented in Figure 5.3g. After that time it was removed, cooled down to room temperature and cleaned with high pressured air, deionized water and EtOH shown in Figure 5.3h. The cleaned honeycomb was placed back in the muffle furnace for about 19 h, removed from the furnace, cooled down and stored in a small plastic Petri dish.(Figure 5.3i) This procedure secured a good immobilization of the catalyst on the surface of the monolithic material. Some honeycombs were coated several times. All honeycomb coatings are presented in tables 5.1 to 5.3.

Table 5.2: Second coating Catalyst 4

Component	Nominal [g]	9	10
ACN	5.000	5.0026	5.0023
SnO_x	1.861	1.8606	1.8623
$PdCl_2$	0.033	0.0343	0.0341
Glycine	3.294	3.2936	3.2936

Table 5.3: Coating Catalyst 7

Component	Nominal [g]	Honeycomb [g]	
		7	8
ACN	5.000	4.9998	4.9999
SnO_x	0.469	0.4690	0.4692
$PdCl_2$	0.020	0.0201	0.0204
Glycine	2.163	2.1625	2.1619

5.2.1 Re-coating

The re-coating was performed in two different ways. The first one was a direct re-coating without the dissolution of Pd in nitric acid (HNO_3). The second procedure includes three steps. The first step was the dissolution of the immobilized palladium. Palladium dissolves in HNO_3 with the formation of palladium(II)nitrate ($Pd(NO_3)_2$). Therefore each honeycomb was transfered into a round bottom flask with a magnetic stirrer inside and the flask was filled with HNO_3. It was assumed

that after 48 h in a stirred vessel the palladium is dissolved and therefore the process was aborted after 48 h by washing the honeycombs with deionized water and EtOH. The second intermediate step for the re-coating were drying for 24 h in a muffle furnace at 350 °C, washing and drying again. The last step includes the new coating process for the honeycombs. The direct re-coating process was chosen for honeycomb 3 after the forth run and the first re-coating of honeycomb 4 after the seventh run. The second re-coating of honeycomb 4 was performed after the eighth run by including the dissolution of the immobilized Pd. The honeycombs 4 and 5 were treated with HNO_3 and tested afterwards. Honeycomb 5 was tested immediately after the treatment with HNO_3, whereas honeycomb 4 was re-coated and then tested.

Table 5.4: Re-coating of Catalyst 4

Component	Nominal [g]	Honeycomb [g]		
		3	4 / 1	4 / 2
ACN	5.000	5.0021	5.0122	5.0018
SnO_x	1.861	1.8608	1.8845	1.8617
$PdCl_2$	0.033	0.0344	0.0338	0.0334
Glycine	3.294	3.2935	3.2950	3.2950

5.3 Characterization of honeycombs

The characterization of the uncoated and coated monoliths was performed by light microscopy, with an analytical balance and the surface area measurements.

5.3.1 Mass

After the pre-treatment of the cordierite monolith, the honeycombs were weighted with an analytical balance to define the starting mass. Afterwards the honeycombs were coated, cleaned, dried, cooled down and weighted to define the mass after the immobilization procedure.

5.3.2 Light microscopy and specific surface area

The preparation of the honeycombs for light microscopy and TriStar are similar. For both analysis techniques the honeycomb has to be destroyed. For the measurements ceramic bridges were needed, so they were broken out of the ceramic honeycomb formation. Light microscopy requires 4-5 bridges, whereas the adsorption requires about 20-25 ceramic bridges for accurate results. The specific surface areas were determined by degassing the samples with nitrogen for about 4h under vacuum at ambient temperature. The absorbed volume of nitrogen was recorded over a relative pressure range between 0.01 and 0.99.

5.4 HPLC-Calibration

The calibration curve is necessary to produce solutions with known molarity to link the peak areas of the HPLC measurements to the concentration in the sample. Different solutions are made out of a 50 ml 8 mM to 40 mM stock solutions via a dilution series. The solvent is a mixture of EtOH and ultra pure water at a volume ratio of 6:4. The stock solutions are shown in Table 5.5. Equation 5.1 is used for calculating the concentration, number of substance and mass of the used stock solutions and dilution series.
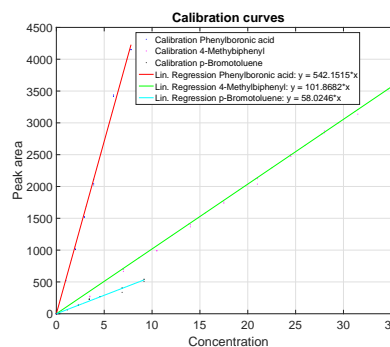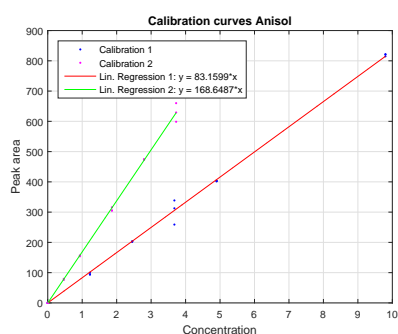
Figure 5.4: Calibration curves Anisol

Figure 5.5: Calibration curves for phenylboronic acid, 4-methylbiphenyl and p-bromotoluene

5 Experimental

The starting materials were weighted with an analytical balance into a volumetric flask and filled up with the solvent. The other solutions were diluted with graduated pipettes as presented in Table 5.6.

Solution samples were transfered to HPLC vials with a 1 ml piston pipette and analysed with HPLC.

$$c = \frac{n}{V} \qquad\qquad n = c \cdot V \qquad\qquad m = n \cdot MM \qquad\qquad (5.1)$$

Equation 5.1: Determination of concentration, number of substance and mass

Table 5.5: Stock solutions

Component	MM $[\frac{g}{mol}]$	V [ml]	calculated		real amounts	
			c $[\frac{mmol}{l}]$	m [mg]	m [mg]	c $[\frac{mmol}{l}]$
Anisole	108.14	50	8	43.256	52.9886	9.8
		50	40	216.28	221.5610	40.9839
p-Bromotoulene	171.04	50	8	68,416	78.3363	9.16
Phenylboronic acid	121.93	50	8	48.772	47.5527	7.8

Table 5.6: Dilution series

c $[\frac{mmol}{l}]$	$V_{solvent}$ [ml]	V_{stock} [ml]	V_{total} [ml]
8	0	20	20
6	5	15	20
4	10	10	20
3	12.5	7.5	20
2	15	5	20
1	17.5	2.5	20
40	0	20	20
30	5	15	20
20	10	10	20
10	15	5	20
5	17.5	2.5	20

Table 5.7: Accurate concentration dilution series

c [$\frac{\text{mmol}}{\text{l}}$]			
Anisole		p-Bromtoluene	Phenylboronic acid
First series	Second series		
9.8	3.7258	9.16	7.8
4.9	2.7944	6.87	5.968
3.675	1.8629	4.58	3.9
2.45	0.9315	3.435	2.925
1.225	0.4657	2.29	1.9893
		1.145	0.975

Each solution was measured two to three times to consider fluctuations. The second anisole dilution series (Figure 5.4) were completed after the column was changed. Therefore a 40 mM stock solution was produced and each sample (100 µl) was diluted with 1 ml of methanol (MeOH). Calibration curves are presented in Figure 5.5. In Table 5.7 the accurate concentrations of the produced dilution series are listed.

5.5 Recrystallization of phenylboronic acid

To remove impurities from the phenylboronic acid it had to be recrystallized. This was done by dissolving 2 g of phenylboronic acid in a flask with 200 ml of ultra pure water. The solution was stirred with a magnet stirrer in an oil bath at 60 °C until all particles were dissolved. The over-saturated solution was immediately filtered with a vacuum frit and the remaining solution was put into the fridge at 5 °C over night. On the next day the solution was filtrated with a vacuum frit to separate the gained crystals from the aqueous solution. The crystals were dried for about 72 h in a desiccator at a pressure of 50 mbar. Afterwards the crystals were stored in a flask.

5.6 Suzuki-Miyaura reactions

All batch experiments were carried out using a varying amounts of bromoarene with phenylboronic acid, potassium carbonate as base, anisole as an internal standard and a 6:4 solvent mixture of EtOH and water.
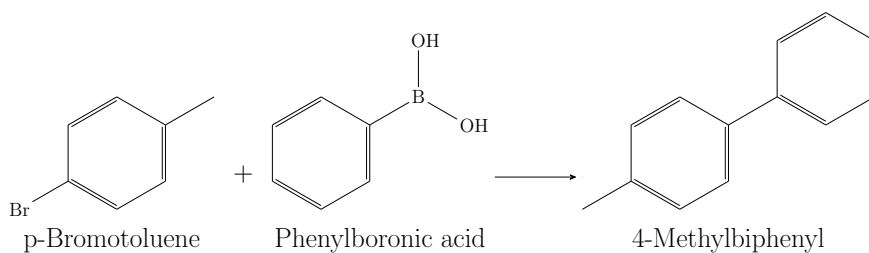
Figure 5.6: Suzuki-Miyaura coupling of p-Bromotoluene with Phenylboronic acid
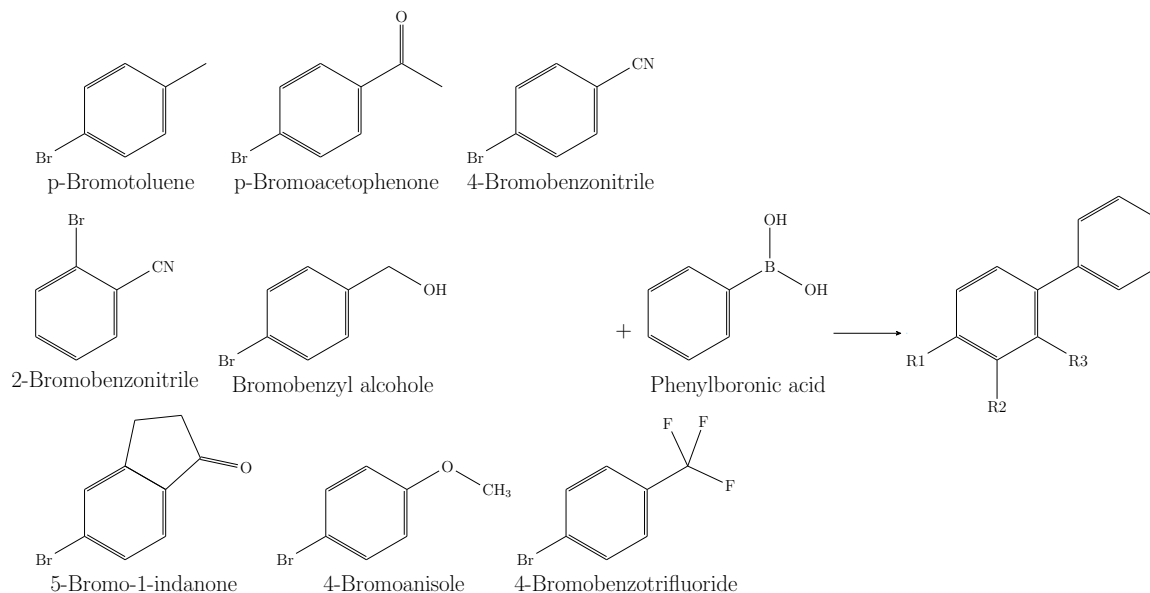
Figure 5.7: Performed Suzuki-Miyaura coupling reactions with various bromoarenes and phenylboronic acid

Figure 5.6 shows the theoretical coupling reaction of p-bromotoluene with phenylboronic acid. The different performed reactions are shown in Figure 5.7. The mass of the weight compounds for the reactions are displayed in Table 5.8. The temperature was set to 75 °C, the solvent was a 6:4 mixture of EtOH and water and the volume was 30 ml. In Table 5.9 the performed reaction is linked to the

used honeycomb, its cycle and the reaction type (batch B or continuous C).

Table 5.8: Theoretical reaction compositions

		Bromoarene	Phenylboronic acid	Potassium carbonate	Anisol
		[mol]			
Mol eqvivalent		**1**	**1.8922**	**2.4917**	**0.7955**
Nr.	Reaction	[mg]			
1	p-Bromotoluene	222.4			
2	4-Bromoacetophenone	258.8			
3	4-Bromobenzonitrile	236.67			
4	2-Bromobenzonitrile	236.67			
5	4-Bromobenzyl alcohol	243.18	300	450	111.87
6	4-Bromobenzotrifluoride	222.4			
7	5-Bromo-1-indanone	274.42			
8	4-Bromoanisole	243.18			

Table 5.9: Overview of the batch/continuous reactions

Reaction (Type Nr)	Batch/Continuous experiment								
Honeycomb	1	2	3	4	5	6	7	8	9
uncoated 6	B 1								
uncoated 10	B 1								
1	Light microscopy / Specific surface								
2	B 1	B 1	B 1						
3	B 1	B 1	B 1	B 1	B 1				
4	B 1	B 1	B 1	B 1	B 1	B 1	B 1	C 1	B 1
5	B 1	B 1	B 1	B 1	B 1	B 1	B 1	B 6	B 4
6	B 1	B 1	B 1	B 1	B 1	B 1	B 1	B 6	B 4
7	Light microscopy / Specific surface								
8	B 1	B 1	C 1						
9	B 1	B 1	B 2	B 3	B 5	C 1	C 1	C 1	
10	B 1	B 2	B 3	B 7	B 1	C 1	C 1	C 1	
11	B 4	C 1	C 1	C 1	C 1	C 1	C 1		
12	B 4	C 1	C 1	C 1	C 1	C 1			
13	B 8	C 1	C 1	C 1	C 1	C 1			
14	C 1	B 1	C 1	C 1	C 1	C 1			
15	C 1	B 1	C 1	C 1	C 1				
16	C 1	B 1	C 1	C 1	C 1				

5.6.1 Batch reaction

Each batch was prepared separately in a 50 ml round bottom flask. For each batch the procedure was performed similar. The reactants and the internal standard, which was used for subsequence analysis in a HPLC-Column, were weighted into a 50 ml round bottom flask. Afterwards 30 ml of the solvent mixture (EtOH/Water in a ratio of 6:4) and a magnetic stirrer were added. The round bottom flask was transferred into a preheated (40 °C) oil bath. The oil bath was heated up to 75 °C and the temperature was controlled by a PT100 measuring resistance, which was dipping into the oil bath. The process can be seen in Figure 5.8.

Figure 5.8: Setup batch experiments
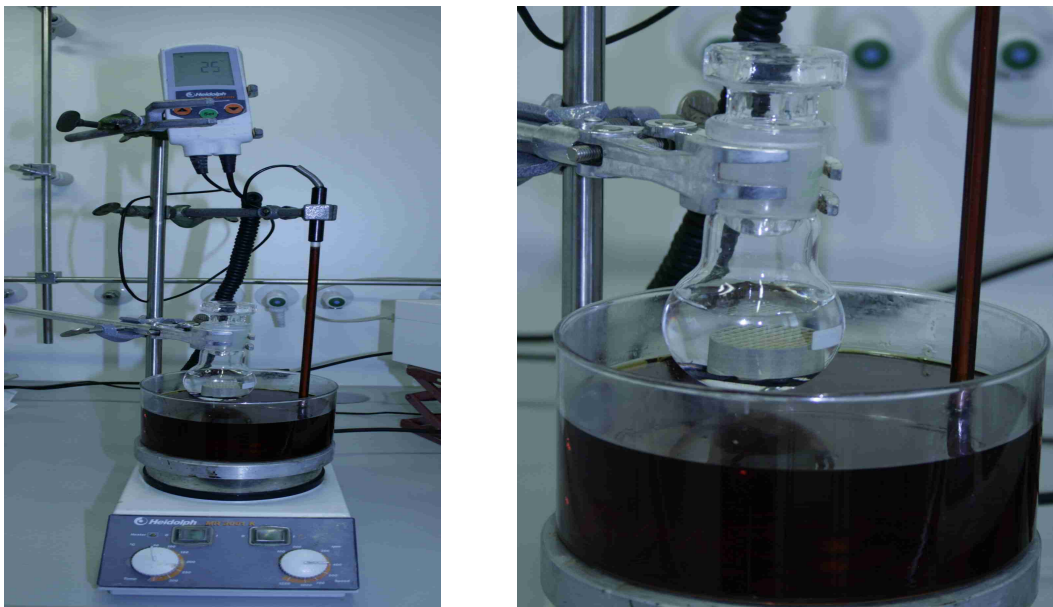
When the reaction solution was well mixed, all solid components were dissolved and the solution reached the required temperature a 100 µl sample (reference sample) was taken with a piston pipette and the sample was transferred into a 1.5 ml vial. Afterwards the sample was diluted with 1 ml HPLC graduated MeOH and moved to the HPLC for analysis. Three 4.5 cm stainless steel pipes were added to

the round bottom flask. The function of the pipes was to keep a sufficient distance between the magnetic stirrer and the coated honeycomb. This was necessary to avoid abrasion by the moving stirrer. After the pipes were set up, the honeycomb was placed on the pipes. As a standard sampling time 15 min was scheduled. At the defined sampling time a 100 µl sample was taken out of the round bottom flask, transferred into a 1.5 ml vial, diluted with HPLC graduated MeOH and analyzed with HPLC. The reaction solution was stored in the fridge at 5 °C after the reaction was canceled or completed. Some over-saturated reaction solutions were crystallized to gain products for further investigations, such as leaching. Therefore, the cooled down samples were filtrated over a frit after about 24 h and the detached crystals were dried in a desiccator for about another 72 h. The dried crystals were filled into roll glasses and stored in the fridge. The honeycomb was recycled and stored. The recycling process is described below in the sub-section Recyclability. Table 5.9 shows the performed reaction depending on the used honeycomb and recycling cycle.

5.6.2 Continuous reactions

The continuously performed synthesis processes were carried out with reaction 1, which is described in Table 5.8. The reaction solution was filled in a 100 ml measuring flask with the portions of reaction 1. The solution was pumped with the HPLC-pump (Knauer P 4.1S) with a rate of 0.15 to 0.5 ml min^{-1}. The reaction vessel was placed in the oil bath, which was heated up to 75 °C to 84 °C. The back-pressure regulator was set up between 1 bar to 40 bar.

The first test setup, shown in Figure 5.9a, consists of a storage for the reaction solution, an analytical balance, which works as a mass flow controller, a HPLC-pump, a magnetic stirrer, an oil bath, a PT100 measuring resistance for temperature control, a reaction vessel and a back-pressure regulator. The reaction vessel consists of brass. A magnetic stirrer was located at the bottom of the vessel to stir and to increase the residence time of the reaction solution inside the vessel. Above the stirrer three covered honeycombs are stacked. The second continuous reaction setup, shown in Figure 5.9b, includes a HPLC-pump, a heating plate, a heated oil

(a) First setup continuous experiments

(b) Second setup continuous experiments

Figure 5.9: Setup continuous experiments

bath, a PT100 thermal controller, a storage for the reactants and for the reaction solution, a heated oil bath and a back-pressure regulator. Inside the stainless steel reactor three honeycombs were stacked.

Residence time distribution

The residence time distribution (RTD) was performed with a step function. The experiment was carried out with the second reactor setup. For the experiment a 200 ml reaction solution with 6.67 mM anisole and a solvent of EtOH and water with the ratio of 6:4 was produced. The solution was split up to two volumetric flasks. One flask was connected to HPLC-pump and the reaction solution was pumped with a rate of $0.15\,\text{ml}\,\text{min}^{-1}$. The other one was used to produce a 9.27 mM p-bromotoluene reaction solution. Anisole was used as an internal standard. p-Bromotoluene fulfilled two tasks. The first task was to determine the concentration. The second one was the testing if the substrate itself is getting caught by the catalyst. The first 40 min the samples were taken in a range of

2 min. Afterwards the samples were taken every 4 min because the concentration change became smaller. After 64 min the samples were taken every 6 min until the experiment was stopped after 88 min.

5.6.3 Heterogeneity of the catalyst

For the testing of heterogeneity and to determine the recyclability of the produced catalytic monoliths the leaching had to be determined with a hot filtration test. Other test procedures are three phase tests and poisoning test.

Recyclability

The honeycombs were washed several times, after the reaction was completed, alternately with pure EtOH and deionized water. This procedure should ensure that all organic and ionic compounds were removed. Afterwards the honeycombs were dried in a muffle furnace at 550 °C. The monoliths were removed 48 h later. They were cooled down and stored until they were used again. For the determination of the recyclability and the adequate recycle process, several experiments were performed with honeycombs 3 and 4. After the reaction was completed, the honeycombs were removed from the reaction solution. The monoliths were washed with pure EtOH and deionized water as described above. The second and third run was carried out the same way as the first one. The honeycombs were washed between the runs and immediately used again. After the third run, the honeycombs were alternately washed with pure EtOH and deionized water and dried for about 48 hours. Honeycomb 4 was dried at a temperature of 550 °C and honeycomb 3 was dried at a temperature of 350 °C. Afterwards they were cooled down and reused again. Honeycomb 4 was reused two times and dried again at a temperature of 550 °C. After batch 4 honeycomb 3 was washed and re-coated. The samples which are compared for the recyclability were taken 40 min after the reaction was started.

Hot filtration test

For three honeycombs (4,5 and 6) at the 7th run a hot filtration test was performed. The hot filtration test was carried out with reaction 1, which is described in table 12. All components were weighted with an analytical balance into a 50 ml round bottom flask. The same procedure as described for the Suzuki-Miyaura reaction was used. Before the catalyst was added a reference sample was taken. After 60 min the coated honeycomb was removed with a tweezer from the reaction solution and the reaction and the sample taking was continued. The samples were taken after 5, 10, 20, 40, 60, 100, 120, 160 and 180 minutes. If the bromoarene was totally consumed earlier the sampling and the reaction were stopped.

6 Results and Discussion

6.1 Mass analysis

In Table 6.1 the masses and the mass differences of the honeycombs are reported. The mass of honeycomb 9 and 10 were determined after the second coating. With this data and the data from the TriStar II, the increased surface area can be calculated. The average immobilized catalyst mass is $0.0899\,\mathrm{g}$ per honeycomb. The average amount of palladium per kg honeycomb is $314.46\,\mathrm{mg/kg}$.

Table 6.1: Immobilized catalyst mass

Honeycomb	uncoated mass	coated mass	Catalyst mass	Pd mass	$\dfrac{\mathrm{Pd}}{\mathrm{Honeycomb}}$
		[g]		[mg]	$[\dfrac{\mathrm{mg}}{\mathrm{kg}}]$
1	2.7683	2.8318	0.0635	0.6998	246.66
2	2.7703	2.8462	0.0759	0.8349	293.34
3	2.7617	2.8349	0.0732	0.8052	284.03
4/1	2.7672	2.8211	0.0539	0.5929	210.17
4/2	2.8179	2.8742	0.0563	0.6193	215.47
4/3	2.8709	2.9436	0.0727	0.7997	271.67
5	2.7630	2.841	0.0780	0.8580	302.01
6	2.7651	2.8588	0.0937	1.0307	360.54
7	2.7206	2.8021	0.0815	0.8965	319.94
8	2.7636	2.8596	0.0960	1.056	369.28
9	2.7627	2.8873	0.1246	1.3706	474.69
10	2.7631	2.8806	0.1175	1.2925	448.69
11	2.7613	2.8543	0.0930	1.0230	358.41
12	2.7721	2.8715	0.0994	1.0934	380.78
13	2.7753	2.8603	0.0850	0.9350	326.89
14	2.7810	2.8704	0.0894	0.9834	342.60
15	2.7684	2.8236	0.0552	0.6072	215.05
16	2.7727	2.8346	0.0619	0.6809	240.21

6.2 Surface analysis

The surface of the monoliths changes significantly by color and roughness after the treatment with the novel developed catalysts. To determine the scale of the changes, the surface was analyzed with light microscopy and with surface area measurements.

6.2.1 Specific surface area

The specific surface areas of the honeycombs were determined with the TriStar II 3020. The measured surface areas are displayed in Table 6.2. The measurement of the uncoated suggests that the honeycomb is a low surface monolith. The analyzed samples are shown in Table 6.1. The surface area per g and the mass of the honeycomb result in the m^2 gain of each honeycomb. The m^2 of honeycombs 1, 2, 3, 4 and 7 are calculated with measured mass and surface areas. The results are presented in Table 6.3.

The areas of the other honeycombs shown in Table 6.4 are predicted with the average surface area gained from Table 6.2 of $0.8382\,m^2/g$ for single coated honeycombs and an approximated surface area of $1.2021\,m^2/g$ for double coated honeycombs. The average gain of m^2 per coating is about $1.4879\,m^2$.

Table 6.2: TriStar

Honeycomb	Surface area $[\frac{m^2}{g}]$
uncoated	0.2503
1	0.9016
2	0.6777
3	0.8707
4	1.566
7	0.9026

Figure 6.1: Ceramic bridge

Table 6.3: Immobilized catalyst surface area

Honeycomb	m^2 uncoated	m^2 coated	m^2 Catalyst
1	0.6929	2.5531	1.8602
2	0.6934	1.9288	1.2354
3	0.6912	2.4683	1.7770
4	0.7185	4.4128	3.6942
7	0.6809	2.5291	1.8482

Table 6.4: Approximated immobilized catalyst surface area

Honeycomb	m^2 uncoated	m^2 coated	m^2 Catalyst
5	0.6915	2.3811	1.6896
6	0.6921	2.3961	1.7039
8	0.6917	2.5810	1.8893
9	0.6915	3.3209	2.62946
10	0.6916	3.3214	2.6298
11	0.6912	2.3923	1.7011
12	0.6938	2.4067	1.7128
13	0.6946	2.39736	1.7027
14	0.6960	2.4058	1.7097
15	0.6929	2.3666	1.6736
16	0.6940	2.3758	1.6818

6.2.2 Immobilization

In Figure 6.2 the different states of honeycombs during the preparation and usage are figured. On the left of Figure 6.2a an uncoated honeycomb is presented. It has a light beige-color and a very smooth surface. After the SCS (honeycomb in the middle) the honeycomb gets a light yellow color and in the inner channels particle growth, shown in Figure 6.2b, can be reported. Furthermore the surface gets a little bit more structured. The growth of the particles varies per combustion batch. The right honeycomb was used nine times. During the usage a re-coloring could be observed. The dark gray to black color implies a decomposition of the catalyst and a formation of palladium black.[51] The change is irreversible and leads to a loss of catalytic activity over time. Figure 6.3 shows inner channel particle growth located on the wall surface.

The catalyst forms little tiles, which are directed to the inner area of the monolith's channel. This tiles can also act as flow breakers near the surface and increase the
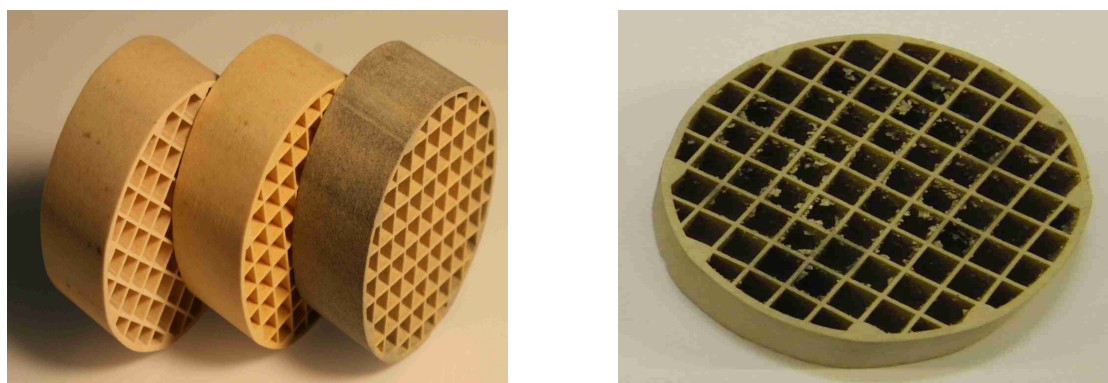
(a) Three states of honeycombs are displayed. Uncoated(left), freshly coated(middle) and used(right)

(b) Particle immobilization

Figure 6.2: Honeycomb

Figure 6.3: Particle growth

turbulence and the back-mixing. Especially the corners are covered with tiles.

6.2.3 Light microscopy

To investigate the surface changes pictures of the uncoated cordierite monolith were taken. Figure 6.4 presents a very light and smooth surface area. No significant areas can be spotted. The immobilization and covalent tethering of the catalyst particles can be observed in Figure 6.5. In Figure 6.5a, the distribution of Pd on the surface of the honeycomb and the formation of Pd-clusters can be
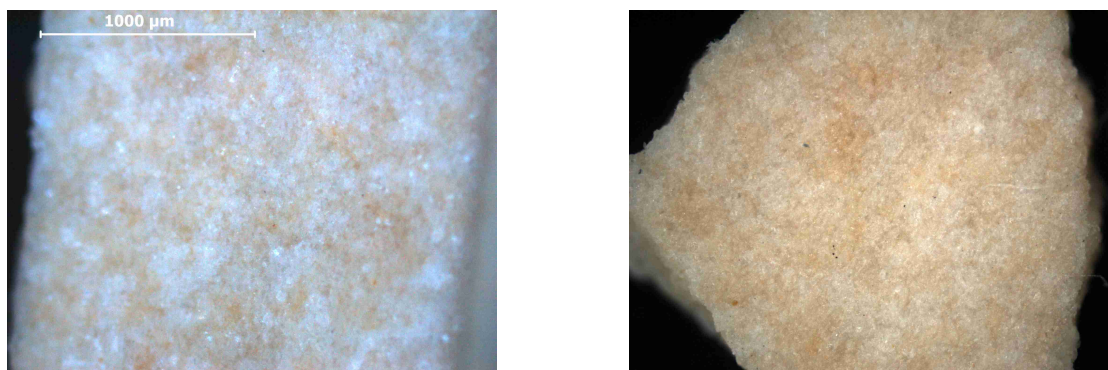
Figure 6.4: Uncoated cordierite surface

discovered. The structure of the surface is visible in Figure 6.5b. It can be studied that particle growth happened and a rough and porous surface is formed.

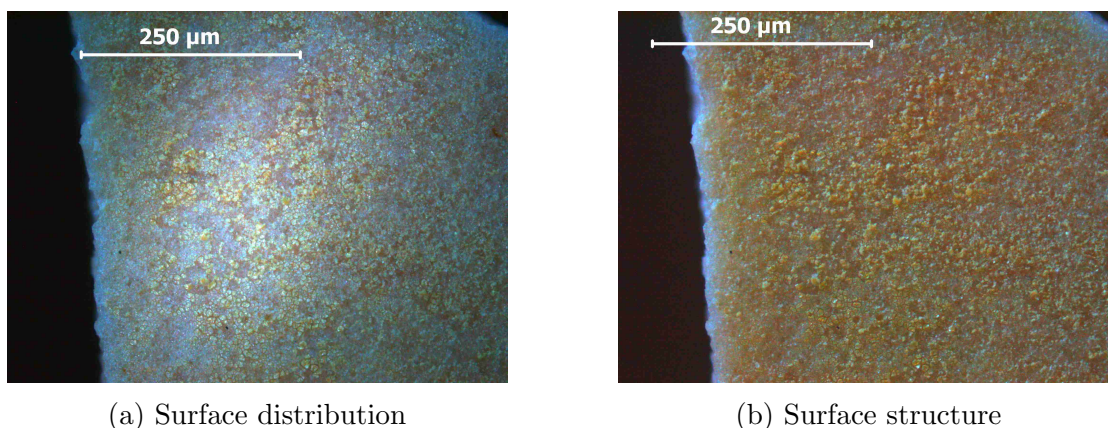
(a) Surface distribution
(b) Surface structure

Figure 6.5: Coated cordierite surface

The pictures of Figure 6.5 were taken with two different light settings. The left picture was taken with fully light level. Therefore some percentages of the light was passing through the monolith. The right shot was recorded with a low light level. A single coated cordierite still offers a lot of open space for catalysts. In Figure 6.5a the open space can be seen as blue areas. With a double coating procedure the free uncoated area can be reduced. The double coated honeycomb is shown in Figure 6.6. Although the Pd-catalyst is better distributed over the surface, cluster formation and denser populated catalyst areas can be recognized,
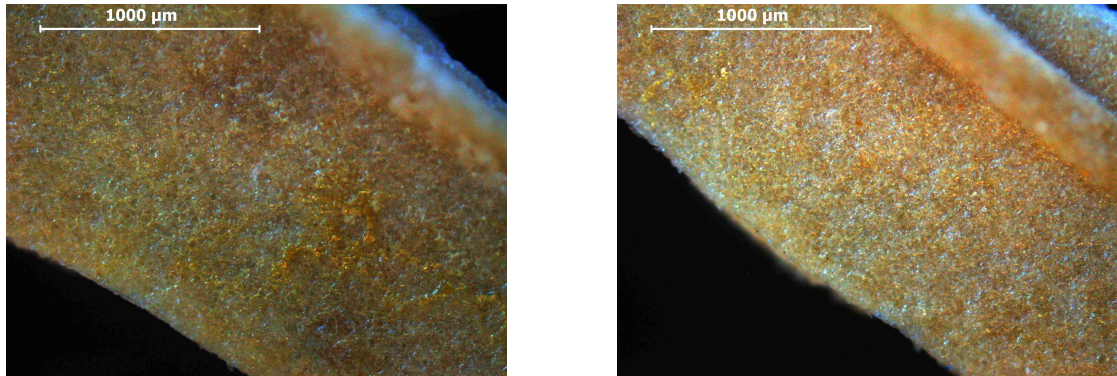
which can be seen in Figure 6.6.

Figure 6.6: Double coated cordierite surface

Figure 6.7 shows a detailed picture of the surface of honeycomb 4. In Figure 6.7a the picture was taken with reflected light microscopy. The catalyst particles can be seen as copper colored particles. The cordierite has a blue color. The catalyst is distributed over the whole area. Figure 6.7b presents the same picture with transmitted light microscopy. According to the low density of the cordierite material the monolith offers a higher transparency. The catalyst particles are represented as black areas whereas the cordierite gleams weak red. The particles of the catalyst have approximately the same size and are uniformly distributed.
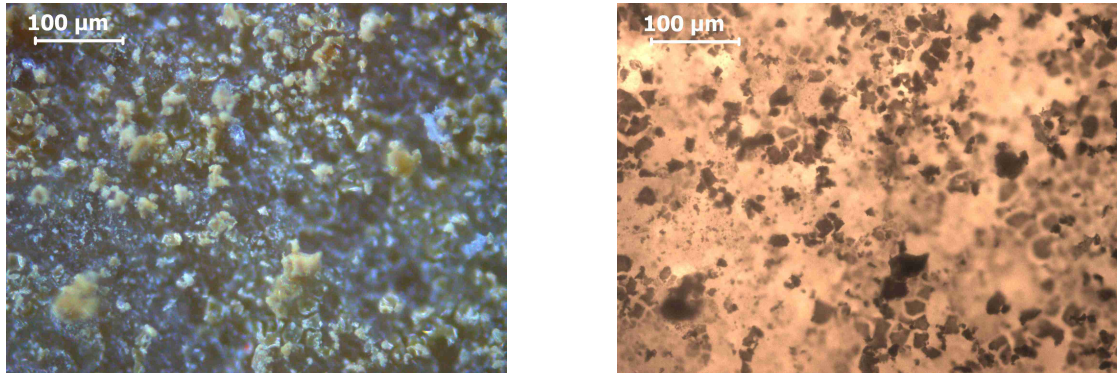
(a) Reflected light microscopy

(b) Transmitted light microscopy

Figure 6.7: The figure shows a very detailed picture of the surface of honeycomb 4.

6.2.4 Conclusion

Honeycombs are highly suitable solid supports for the immobilization of catalysts. The rapid synthesis of the catalyst via a one-step solution combustion synthesis within 2 hours offer an inexpensive way of producing very versatile, durable and handable catalysts with a high surface area. To reduce the uncoated space, the honeycombs should be coated twice. The direct one-step coating process reduces time and makes the synthesis very easy. The novel honeycomb catalytic system has a high potential for Suzuki-Miyaura cross-coupling reactions. According to the flexibility in shape and size, the honeycombs can be used as catalysts for batch operations, as inlets for a CSTR or as PFR.

6.3 Batch experiments

In batch experiments, the novel catalyst system was used for heterogeneity experiments and for testing a various number of bromoarenes. All batch reactions were performed at 75 °C in a stirred round bottom flask. The results from the batch reactions are presented in Table 6.5. In the table the conversion, yield, selectivity and TOF after the first 60 min are shown. For reaction which were completed before the 60 min were reached, the last sample was counted.

Table 6.5: Batch reaction results. The reactions were carried out at 75 °C. The samples were taken after 60 min. Reactions which were completed faster were aborted and the last value was considered.

Honeycomb	Run	Substrate	Conversion [%]	Yield [%]	TOF [h^{-1}]	Selectivity [%]
	1	p-Bromotoluene	13.09	3.34	12.09	100
2	2	p-Bromotoluene	11.66	6.30	16.76	100
	3	p-Bromotoluene	15.46	24.26	62.07	98.88
	1	p-Bromotoluene	100	100	-	-
	2	p-Bromotoluene	11.04	0.58	0.48	100
3	3	p-Bromotoluene	4.46	4.10	10.91	100
	4	p-Bromotoluene	47.16	48.16	129.37	98.71
	5	p-Bromotoluene	80.16	80.45	218.96	98.25

Table 6.5: Batch reaction results. The reactions were carried out at 75 °C. The samples were taken after 60 min. Reactions which were completed faster were aborted and the last value was considered.

Honeycomb	Run	Substrate	Conversion [%]	Yield [%]	TOF $[h^{-1}]$	Selectivity [%]
	1	p-Bromotoluene	100	100	774.68	95.51
	2	p-Bromotoluene	14.44	13.09	58.79	97.68
	3	p-Bromotoluene	17.91	4.92	17.09	100
4	4	p-Bromotoluene	90.81	27.97	105.09	97.68
	5	p-Bromotoluene	7.87	8.73	32.03	100
	6	p-Bromotoluene	9.14	9.14	33.73	100
	7	p-Bromotoluene	60.55	60.91	223.07	98.31
	9	p-Bromotoluene	90.76	88.14	156.51	97.23
	1	p-Bromotoluene	100	100	318.70	97.68
	2	p-Bromotoluene	94.25	93.43	235.68	98.20
	3	p-Bromotoluene	60.33	59.56	150.93	98.72
	4	p-Bromotoluene	76.19	84.14	212.15	98.36
5	5	p-Bromotoluene	76.75	76.87	189.08	98.70
	6	p-Bromotoluene	95.08	97.21	248.32	97.74
	7	p-Bromotoluene	59.31	59.18	150.72	98.87
	8	4-Bromobenzotrifluoride	100	100	409.05	98.1
	9	2-Bromobenzonitrile	2.51	6.27	12.76	-
	10	p-Bromotoluene	-	-	-	95.18
	1	p-Bromotoluene	100	100	425.73	98.68
	2	p-Bromotoluene	100	100	220.35	96.10
	3	p-Bromotoluene	79.25	79.88	168.58	98.54
	4	p-Bromotoluene	95.82	97.04	204.79	98.29
6	5	p-Bromotoluene	97.84	98.93	215.73	97.56
	6	p-Bromotoluene	88.40	86.78	182.80	98.08
	7	p-Bromotoluene	56.61	33.60	69.78	97.32
	8	4-Bromobenzotrifluoride	100	100	328.24	96.87
	9	2-Bromobenzonitrile	6.73	8.78	14.58	-
8	1	p-Bromotoluene	77.41	77.91	160.76	98.49
	2	p-Bromotoluene	60.69	61.89	123.12	98.74

Table 6.5: Batch reaction results. The reactions were carried out at 75 °C. The samples were taken after 60 min. Reactions which were completed faster were aborted and the last value was considered.

Honeycomb	Run	Substrate	Conversion [%]	Yield [%]	TOF $[h^{-1}]$	Selectivity [%]
	1	p-Bromotoluene	100	100	475.13	95.61
	2	p-Bromotoluene	100	100	323.73	94.40
9	3	4-Bromoacetophenone	100	100	324.38	-
	4	4-Bromobenzonitrile	100	100	354.93	-
	5	4-Bromobenzyl alcohol	100	35.15	253.55	-
	1	p-Bromotoluene	100	100	509.68	96.70
	2	4-Bromoacetophenone	100	100	673.22	-
10	3	4-Bromobenzonitrile	100	100	345.12	-
	4	5-Bromo-1-indanone	100	100	677.52	97.25
	5	p-Bromotoluene	100	100	261.44	97.24
11	1	2-Bromobenzonitrile	17.06	18.47	39.84	97.55
12	1	2-Bromobenzonitrile	39.42	27.34	54.09	97.62
13	1	4-Bromoanisole	100	100	470.54	-
14	2	p-Bromotoluene	100	100	636.15	97.00
15	2	p-Bromotoluene	100	100	391.11	97.23
16	2	p-Bromotoluene	100	100	967.46	96.70

Depending on the substrate, the number of uses, the number of coatings and re-coatings and the recycling procedure, the conversion, yield and TOF are varying. The in Table 6.5 described results are measurements of samples, which were taken after 60 min. According to the selectivity values of all experiments, the selectivity can be described as stable. The influence of the factors on the TOF and on the conversion are correlating. The influence of the substrate, number of uses, coatings and re-coatings and the recycling procedure will be discussed in own sections below.

6.3.1 Batch reactions - Influence of the substrates

The batch experiments showed that the reaction rates and the performance of the honeycombs are linked to the used substrates and the run in which the reaction is performed. Substrates with electron donors in para-position show a higher reactivity than reactions with substrates with electron donors in ortho- or meta-position.
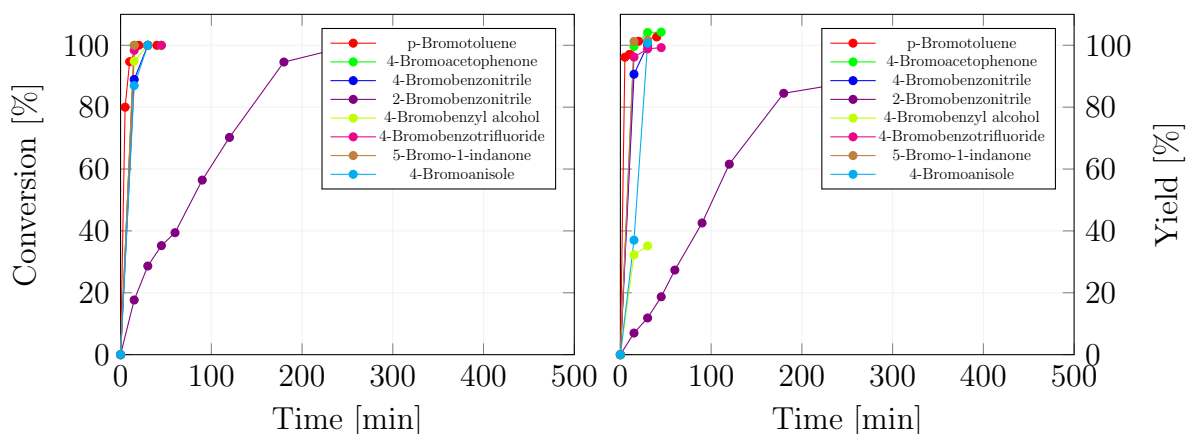

Figure 6.8: Performed reactions with a various number of bromoarenes and phenyl-boronic acid to define the influence of the substrate. The reactions were carried out at 75 °C
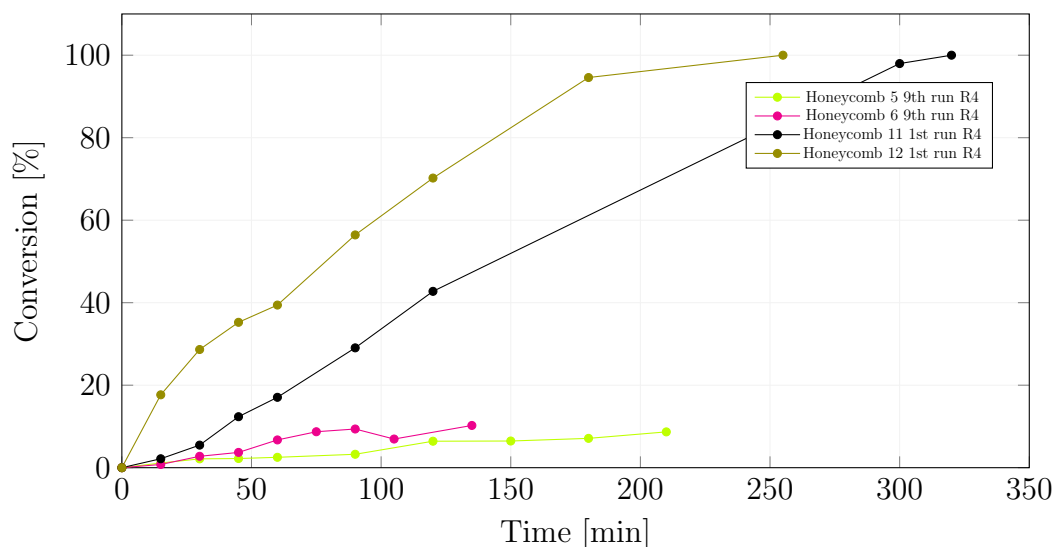

Figure 6.9: Results concerning the re-usability of the honeycombs with 2-bromobenzonitrile and phenylboronic acid at 75 °C.

The results of the reactions are shown in Figure 6.8. The reaction rate of 2-bromobenzonitrile was the lowest. Nevertheless a conversion of 100% and a yield of about 84% of biphenyl-2-carbonitrile for honeycomb 11 and a yield of 100% for honeycomb 12 was reached. The comparison of both runs can be seen in Figure 6.10. As it can be seen in Figure 6.9, the reaction rate of the substrate has a major impact on the re-usability of the honeycomb. The earlier a substrate with a low reaction rate is used, the better the reaction performs. The first runs of the honeycombs 11 and 12 are compared with the ninth run of honeycombs 5 and 6. The high number of re-usages of the two honeycombs make a very slow reaction with progressive usage uneconomical. In Figure 6.10 and Figure 6.11 the catalytic activity of honeycomb 8, which was coated with catalyst 2, can be compared with the other honeycombs (catalyst 4). As expected from previous experiments, performed by other students, the figures show that catalyst 4 is more reactive than catalyst 2. Therefore, no further investigations were performed with honeycomb 8. To investigate the catalytic activity of an uncoated honeycomb, reaction 1 was performed with the uncoated honeycomb 6. The plot is presented in Figure 6.10. As described in section section 6.3.3, the performance of the honeycombs decreases with every run without a recovery process. The comparison of each honeycomb with the run are presented in figs. 6.10 to 6.16. The lowered activity of honeycomb 2 in the first run (Figure 6.10) is lead back to an error of the thermal controller.
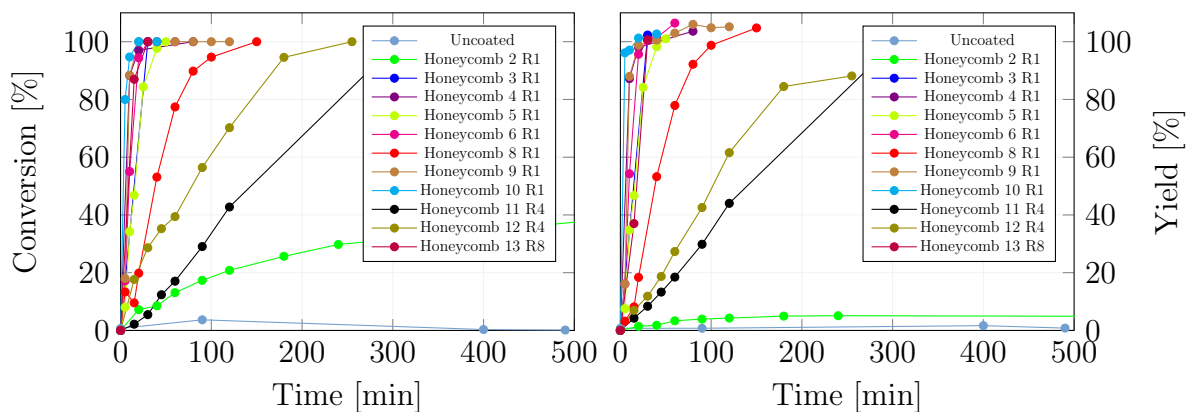

Figure 6.10: Results of the first run of all batch experiments performed at 75 °C with a various number of bromoarenes and phenylboronic acid.
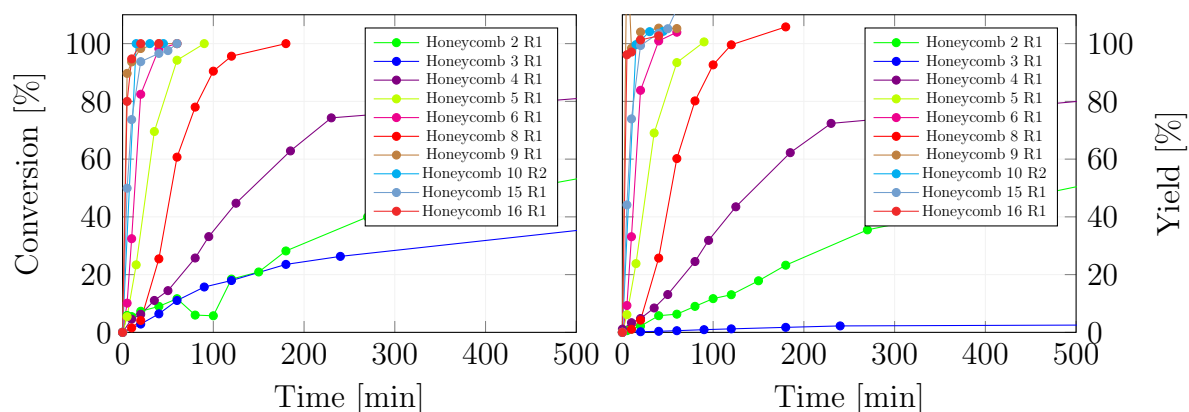
Figure 6.11: Results of the second run of all batch experiments performed at 75 °C with a various number of bromoarenes and phenylboronic acid.
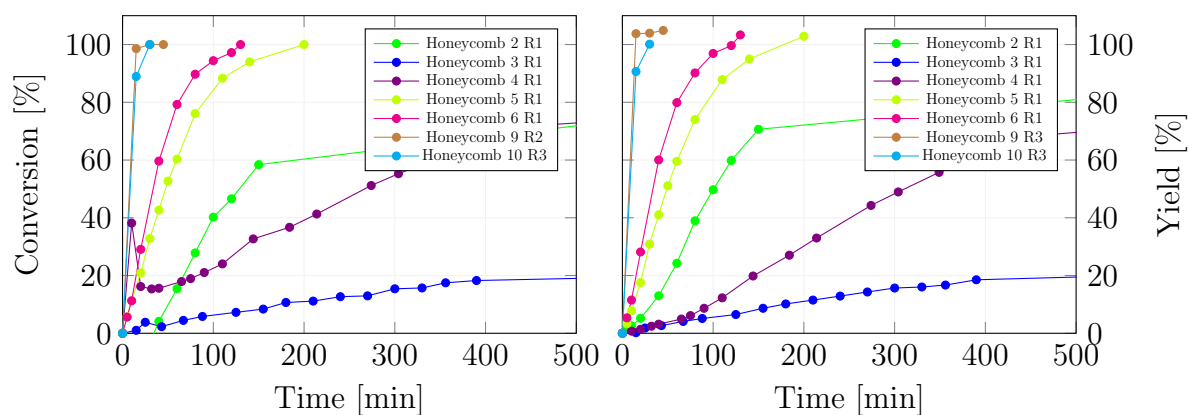

Figure 6.12: Results of the third run of all batch experiments performed at 75 °C with a various number of bromoarenes and phenylboronic acid.

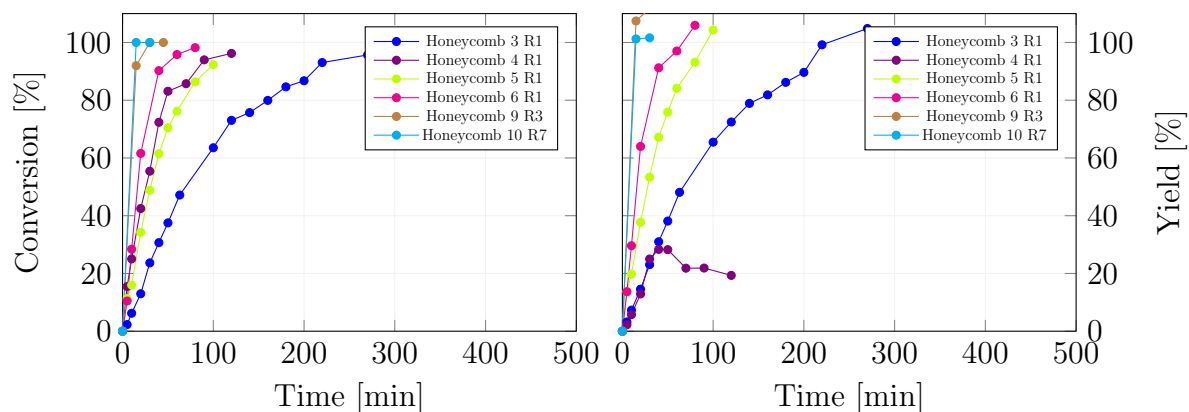

Figure 6.13: Results of the fourth run of all batch experiments performed at 75 °C with a various number of bromoarenes and phenylboronic acid.
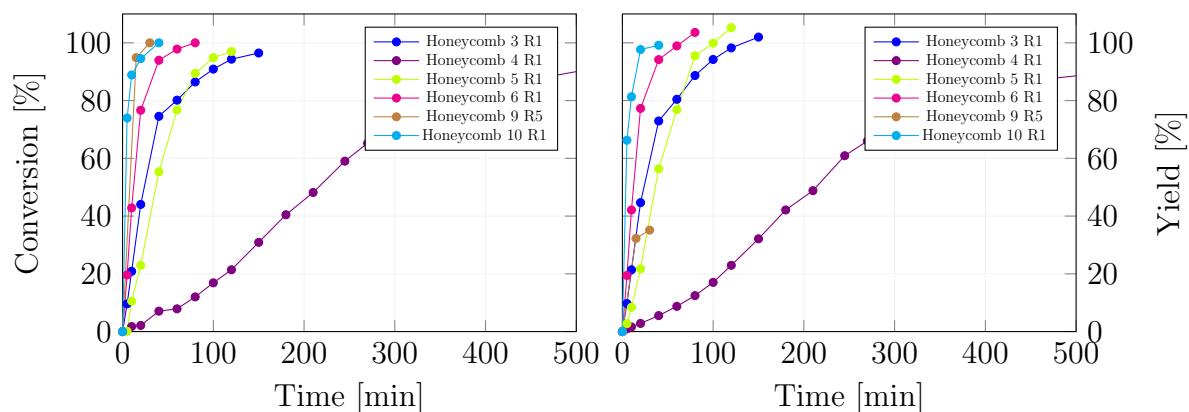
Figure 6.14: Results of the fifth run of all batch experiments performed at 75 °C with a various number of bromoarenes and phenylboronic acid.
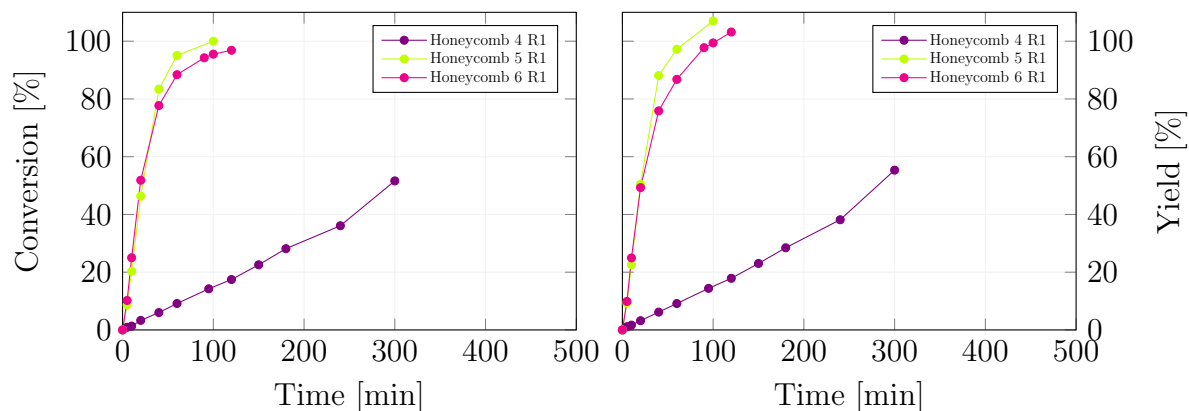

Figure 6.15: Results of the sixth run of all batch experiments performed at 75 °C with a various number of bromoarenes and phenylboronic acid.
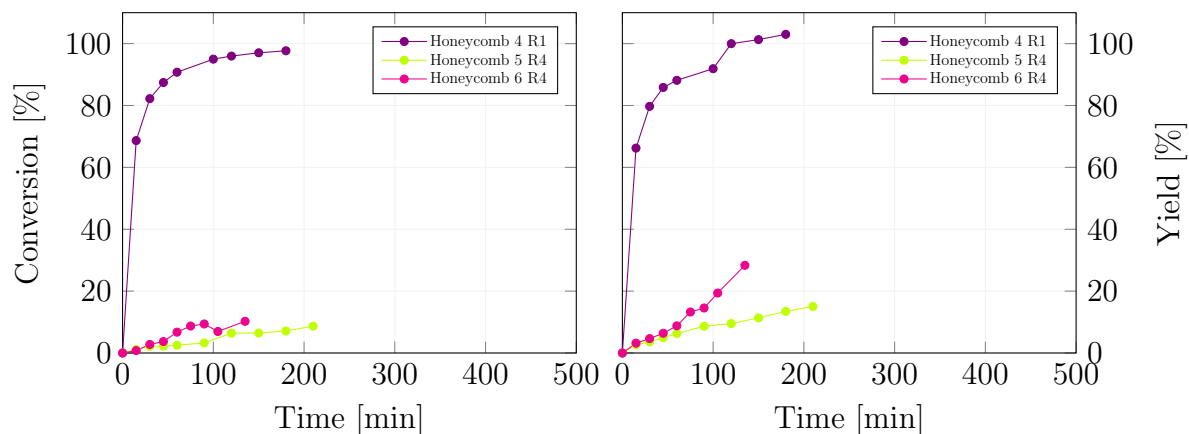

Figure 6.16: Results of the ninth run of all batch experiments performed at 75 °C with a various number of bromoarenes and phenylboronic acid.

The temperature for honeycomb 2 in the first run was set to 65 °C, which had a great influence on the reaction rate. As it is shown in the figs. 6.10 to 6.16 the activity drop over time is highly related to the used substrates, the reaction conditions, the recovery process and to the number of coatings.

6.3.2 Re-coating

Honeycomb 3 was directly re-coated after the fourth run without a dissolution of Pd, whereas the second re-coating of honeycomb 4 was performed after the eighth run and after the Pd was dissolved with HNO_3.
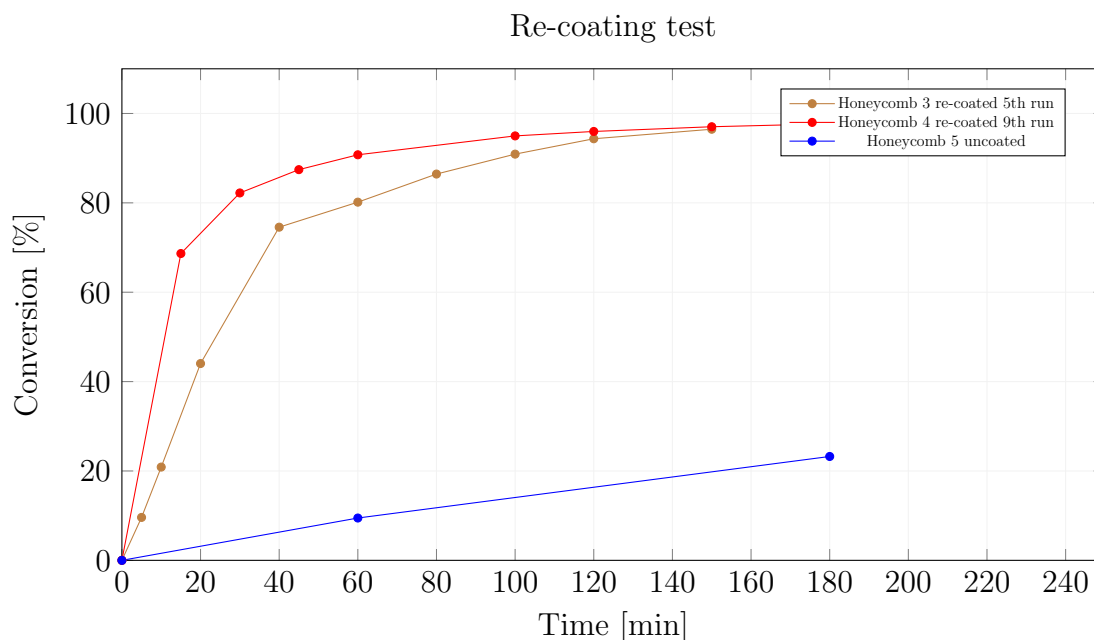
Figure 6.17: Re-coating reactions were carried out at 75 °C with p-bromotoluene and phenylboronic acid.

The first re-coating of honeycomb 4 (not tested) was done after the seventh run in the same way as for honeycomb 3. To check if the Pd was dissolved totally a batch experiment at 75 °C was performed with honeycomb 5. Honeycomb 4 and 5 were selected according to their high re-usage. Honeycomb 4 was re-coated and both honeycombs 3 and 4, were tested with reaction 1 (p-bromotoluene as sub-

strate). Figure 6.17 shows that the activity of the directly re-coated honeycomb 3 is comparable to the activity of honeycomb 4. There is only a small gap between both runs. The conversion of honeycomb 3 after 60 min could be increased from 47% in the 4th run to 80% in the 5th run. By doing the re-coating the activity can be restored, but it is not comparable with a freshly coated honeycomb. As illustrated in Figure 6.17 the Pd could not be dissolved completely with HNO_3. A slight conversion can be observed. The conversion of honeycomb 4 after 60 min in the seventh run was about 60%. The re-coated monolith has a conversion of about 90%. It can be determined that an inactivated honeycomb can be economically reactivated with a re-coating process. The more time consuming three step re-coating procedure can be discarded. The directly re-coating offers a similar outcome in a shorter time.

6.3.3 Heterogeneity

To test the recyclability and the leaching of the new coated honeycombs batch studies with different recyclability procedures and reactions were performed.

Recyclability

The new coating routine and the recyclability of the activity of the catalytic honeycomb system is strongly related to the recycle process. In Table 6.6 the recyclability steps for the honeycombs 3 and 4 are displayed. Washing between the reactions was an essential step. By washing the honeycomb, reactants and products from former batches were removed from the surface of the cordierite. It can be determined that the washing of the honeycombs has no effect on the prevention of the activity drop. A further heating step has to be implemented.

Table 6.6: The recyclability studies for honeycomb 3 and 4 were performed with p-bromotoluene and phenylboronic acid as substrates. The reaction was performed at 75 °C in a stirred round bottom flask.

| Honeycomb | Run | Washing | Recyclability step | | Re-coating | Conversion of p-bromotoluene |
| | | | Recovering temperature | | | |
			350 °C	550 °C		[%]
3	1	Yes	-	-	-	100
	2	Yes	-	-	-	6.42
	3	Yes	-	-	-	2.30
	4	Yes	Yes	-	-	30.67
	5	Yes	-	Yes	Yes	74.56
4	1	Yes	-	-	-	100
	2	Yes	-	-	-	11.06
	3	Yes	-	-	-	15.61
	4	Yes	-	Yes	-	72.35
	5	Yes	-	-	-	7.07
	6	Yes	-	-	-	6.02
	7	Yes	-	Yes	-	44.73

In the case of honeycomb 3 the monolith was washed and dried at 350 °C after the third batch. The conversion is shown in Figure 6.18. According to the conversion, the catalytic activity was slightly recovered by drying at 350 °C.
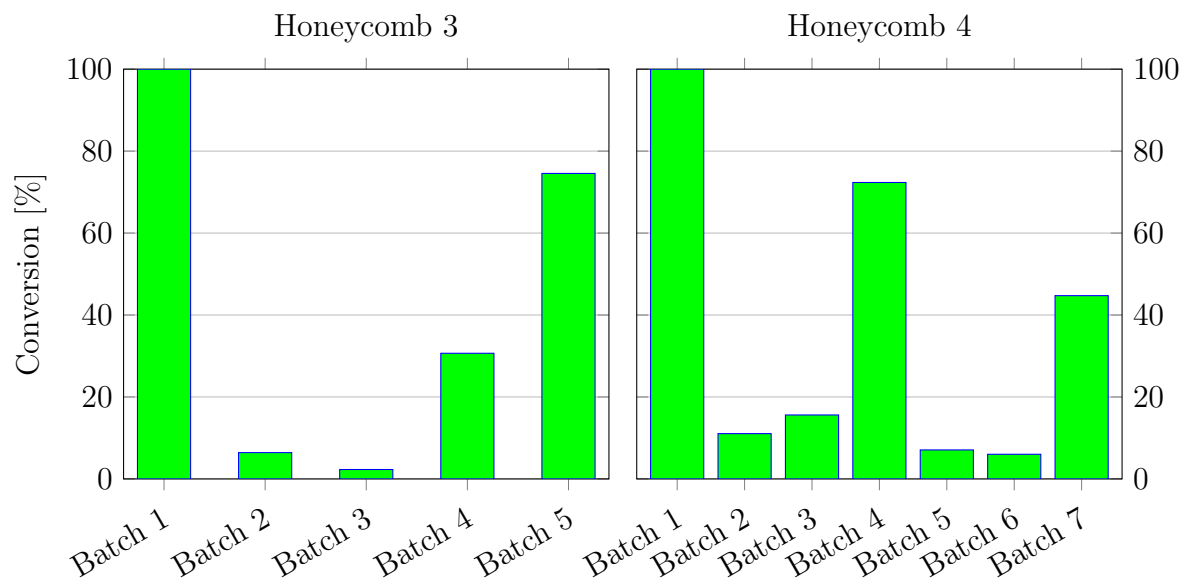
Figure 6.18: Recyclability of honeycombs 3/4 at 75 °C after 60 min with p-bromotoluene and phenylboronic acid
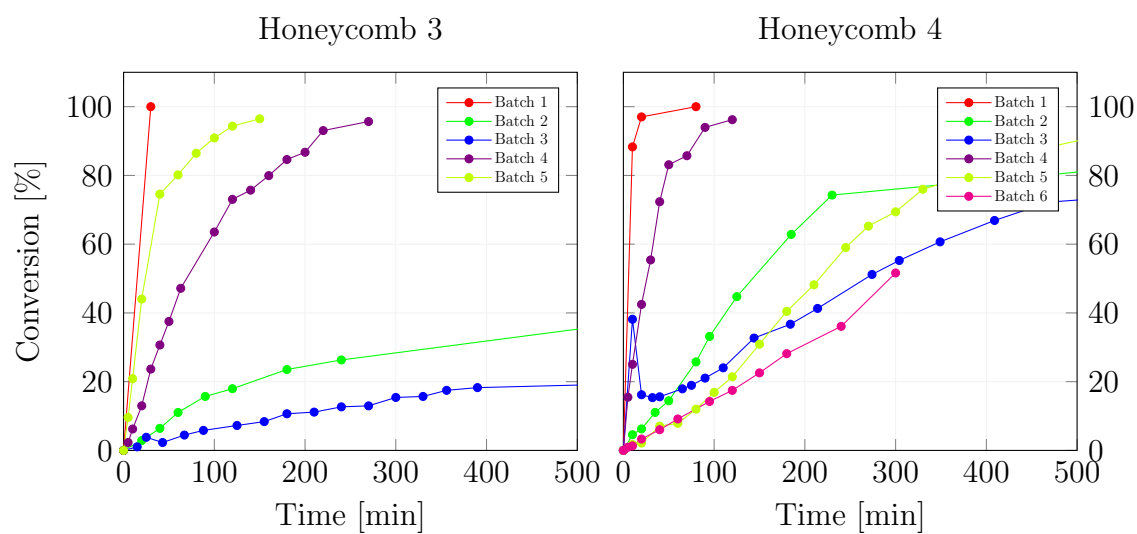

Figure 6.19: Conversion of honeycombs 3/4 at 75 °C with p-bromotoluene and phenylboronic acid

To test if the catalytic activity is totally recovered with a direct re-coating, the honeycomb was re-coated after the fourth batch without a Pd dissolving step.

Table 6.7: The recyclability studies for honeycomb 5 and 6 were performed with p-bromotoluene and phenylboronic acid as substrates. The reaction was performed at 75 °C in a stirred round bottom flask.

Honeycomb	Run	Washing	Recyclability step Recovering temperature 350 °C	550 °C	Re-coating	Conversion [%]
5	1	Yes	Yes	-	-	97.67
	2	Yes	Yes	-	-	69.56
	3	Yes	Yes	-	-	42.65
	4	Yes	Yes	-	-	61.49
	5	Yes	Yes	-	-	55.35
	6	Yes	Yes	-	-	83.40
	7	Yes	Yes	-	-	41.26
	8	Yes	-	Yes	-	100
6	1	Yes	Yes	-	-	100
	2	Yes	Yes	-	-	98.20
	3	Yes	Yes	-	-	59.63
	4	Yes	Yes	-	-	90.24
	5	Yes	Yes	-	-	93.96
	6	Yes	Yes	-	-	77.71
	7	Yes	Yes	-	-	40.63
	8	Yes	-	Yes	-	100

It can be seen in Figure 6.18 and Figure 6.19 that a re-coating can contribute an increase of the activity. Inactive sites are still notable by a lowered activity. Honeycomb 4 shows a quite similar behavior than honeycomb 3. Without drying between the batches (batch 2, 3, 5 and 6) a high blockage of active sites of the catalysts can be observed. Batch 4 and 7 of honeycomb 4 were performed after drying. The reactivity got notably better, but it is still decreasing. The experiments of honeycomb 5 and 6 were performed similar and simultaneously. After each batch, the honeycombs were washed and dried at 350 °C. The recoverability of the monoliths 5 and 6 are shown in Figure 6.20 and 6.21, and are presented in Table 6.7.

According to Figure 6.18 the recyclability of the honeycomb 4, which was recovered every 3rd run with 550 °C, can be described as quite similar to the recovery of honeycomb 5 after every run with 350 °C. The better performance of honeycomb 6, shown in Figure 6.21, possibly underlies the fact that a higher amount of Palladium could be immobilized on the monolith's surface as remitted in Table 6.1.
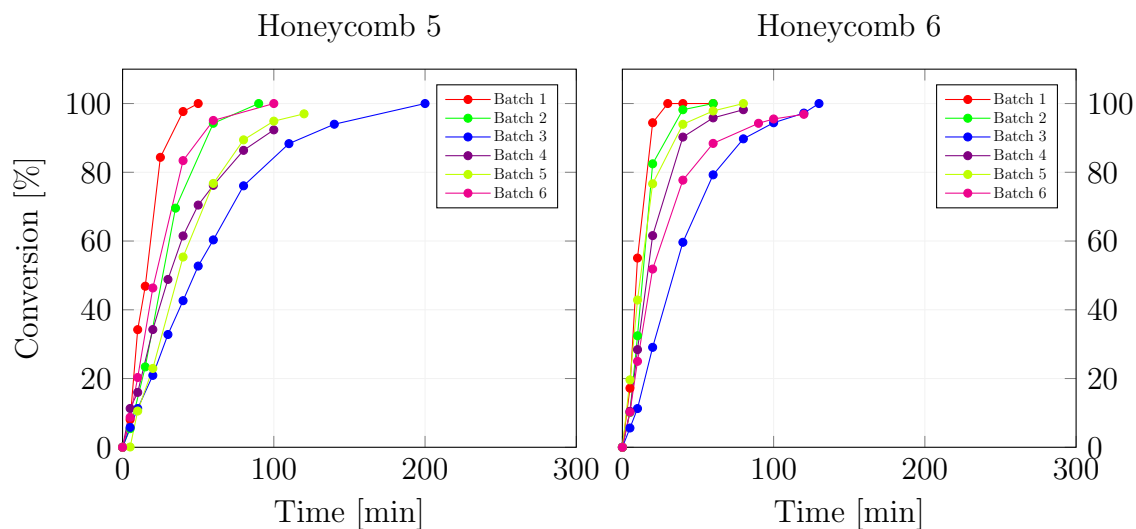
Figure 6.20: Conversion of honeycombs 5/6 at 75 °C with p-bromotoluene and phenylboronic acid
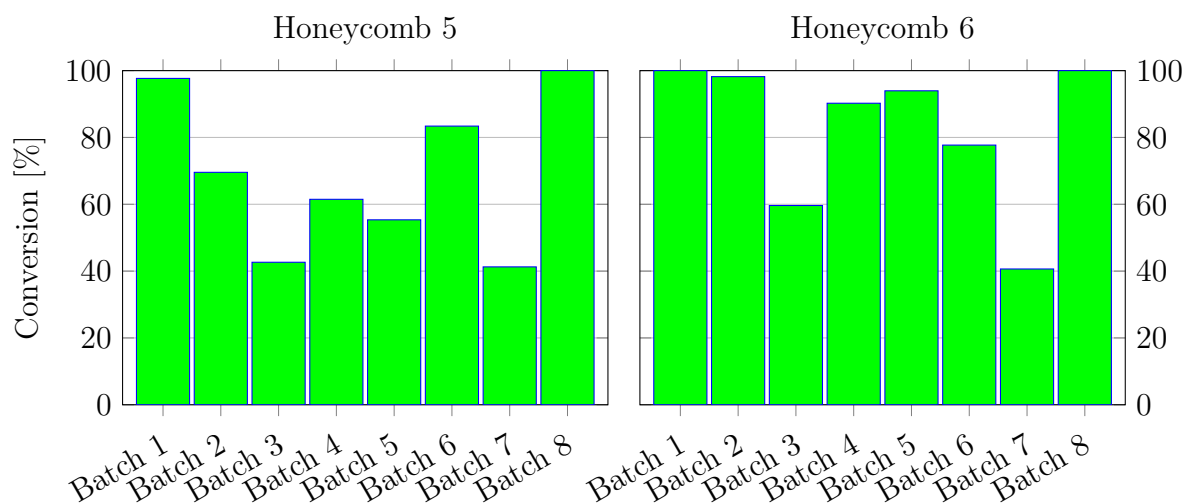

Figure 6.21: Recyclability of honeycombs 5/6 at 75 °C after 60 min. Batch 1 to 7 were carried out with p-bromotoluene and phenylboronic acid. The substrates for batch 8 were 4-bromobenzotrifluoride and phenylboronic acid.

The activity of double coated and regenerated at 550 °C monoliths were tested with the honeycombs 9 and 10. Both honeycombs were checked with various bromoarenes to determine the recyclability as well as the flexibility of the cordierite.

Table 6.8: The recyclability studies for honeycomb 9 and 10 were performed with p-bromotoluene and phenylboronic acid as substrates. The reaction was performed at 75 °C in a stirred round bottom flask.

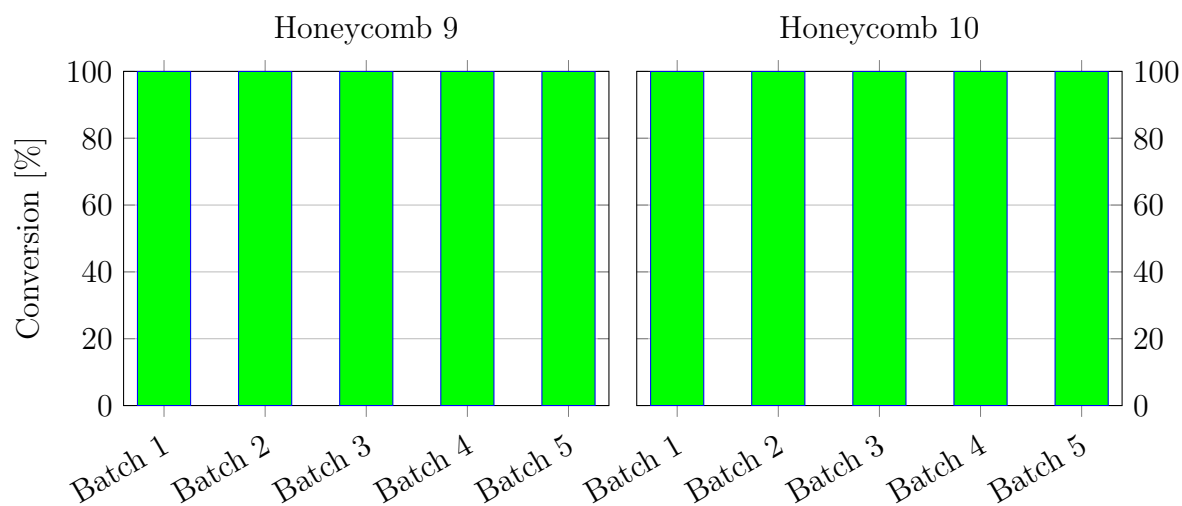| Honeycomb	Run	Washing	Recyclability step Recovering temperature 350 °C	550 °C	Re-coating	Conversion [%]
	1	Yes	-	Yes	-	100
	2	Yes	-	Yes	-	100
9	3	Yes	-	Yes	-	100
	4	Yes	-	Yes	-	100
	5	Yes	-	Yes	-	100
	1	Yes	-	Yes	-	100
	2	Yes	-	Yes	-	100
10	3	Yes	-	Yes	-	100
	4	Yes	-	Yes	-	100
	5	Yes	-	Yes	-	100

Figure 6.22: Recyclability of Honeycombs 9/10 at 75 °C after 60 min with a various number of bromoarenes and phenylboronic acid.

As figured in Table 6.8, the activity could be sustained. The conversion after 40 min is presented in Figure 6.22. The whole reaction curves for the experiments are shown in Figure 6.23.
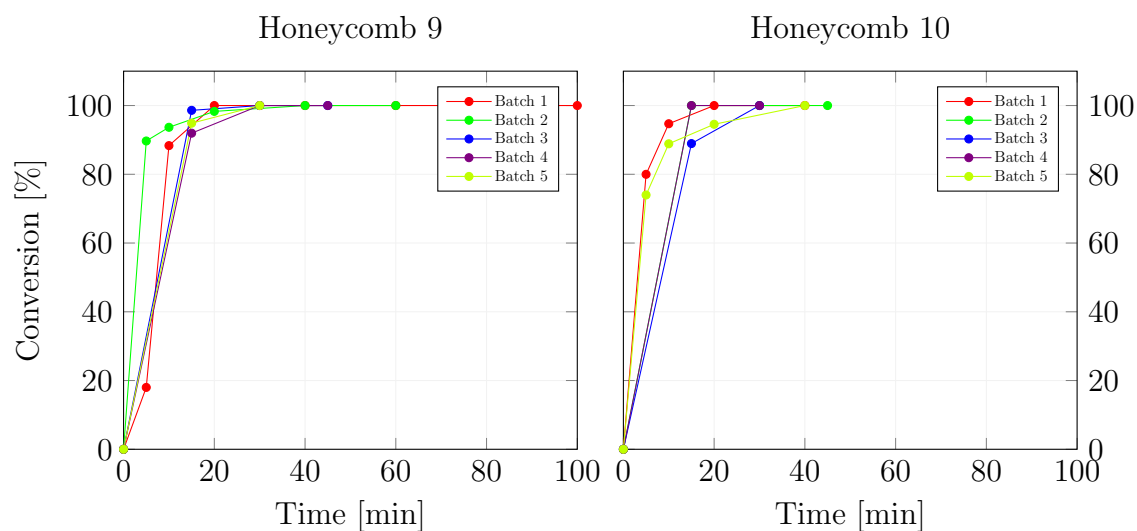
Figure 6.23: Conversion of honeycombs 9/10 at 75 °C with a various number of bromoarenes and phenylboronic acid.

Hot filtration test / Leaching

To test the leaching behavior of the honeycombs, three batch experiments were performed. The tested honeycombs were 4, 5 and 6. It could be observed that the residue in the flask was still catalytically active and proceeded after the removal of the honeycombs after 60 min, as presented in Figure 6.24. The removal of the honeycomb causes a significantly drop in the reaction rate. The reactions were completed after 600 min, which indicates leaching and/or abrasion. Former studies, done by Lichtenegger et al., demonstrated that the reaction is catalyzed by leached Palladium via the performed homogeneous reaction mechanism.

In a very small scale leaching is unavoidable due to the fact that the reaction mechanism supports or requires a short-termed Pd release/capture mechanism. The quite similar performance of all three catalysts encourage the thesis that the recyclability process has an impact on the catalytic activity. To investigate the scale of leaching, ICP/MS studies were made. The analyzed samples are shown in Table 6.9.

The sample of the reaction solution of honeycomb 5 was taken after the third batch experiments was completed. The amount of leached Pd is rather low (0.0069%).
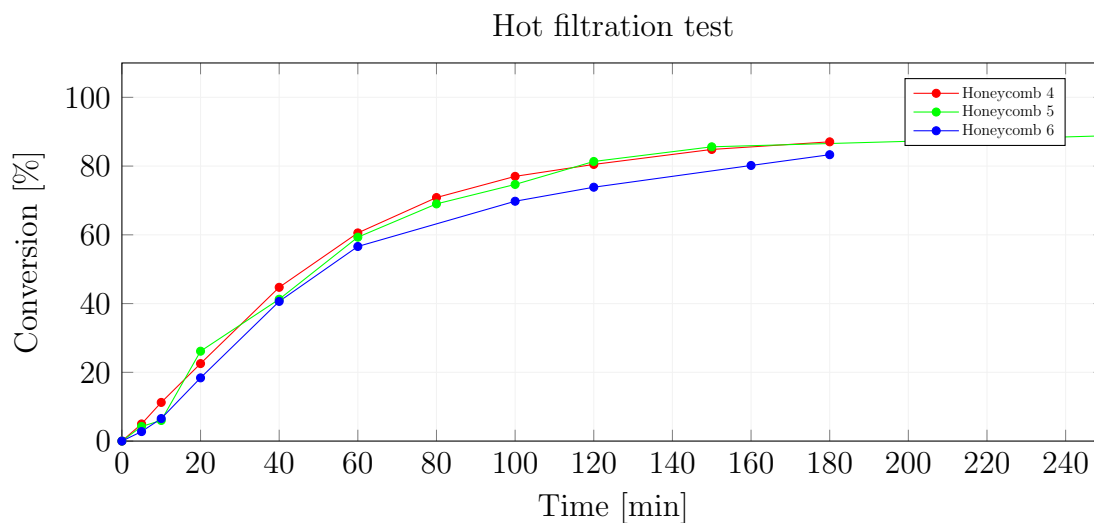
Hot filtration test

Figure 6.24: Hot filtration test, 75 °C

Table 6.9: ICP/MS Samples

Honeycomb	Type	Cycle	State	Reaction
5	Batch	3	Reaction solution	p-Bromotoluene
10	Batch	2	Crystallized product	4-Bromoacetophenone
13	Batch	1	Crystallized product	4-Bromoanisol
14-16	Continuous	1	Reaction solution	p-Bromotoluene
13	Surface	3	Ceramic	

Former experiments, performed by Lichtenegger et al., proved that very low amounts of Palladium are still capable to catalyze Suzuki-Miyaura reactions. Therefore, catalysis is still possible after the main catalyst is removed.

The product of honeycomb 10 was synthesized in the second batch. The batch experiment, which used honeycomb 13 as a catalyst, was the first experiment of honeycomb 13. Therefore, the theory was that the amount of Palladium should be significantly higher than in the other samples because some small particles of catalyst will detach from the surface within the first run. The results of the ICP/MS indicates that detaching of particles is prevented with the washing procedure after the synthesis/immobilization of the catalyst, because the amount of Palladium in the product of honeycomb 10 was higher. After the third run, honeycomb 13 was washed, destroyed and the catalyst was extracted and decomposed with HNO_3

from the carrier to its atoms. The extraction of Pd from honeycomb 13 was not complete, according to the laboratory staff, who carried out the ICP/MS measurements.

Table 6.10: ICP/MS results of different honeycomb runs

Honeycomb	Pd	Sn $[\frac{mg}{kg}]$	Ce
5	$0,069 \pm 0,001$	$0,56 \pm 0,05$	$0,48 \pm 0,07$
10	$10,0 \pm 0,3$	$3,9 \pm 1,7$	14 ± 3
13	$6,6 \pm 0,3$	$7,8 \pm 1,1$	116 ± 11
14-16	$0,17 \pm 0,01$	$0,26 \pm 0,02$	$0,45 \pm 0,02$
13	40 ± 5	58 ± 13	7146 ± 893

The result from the experiment of honeycomb 14-16 was taken from the first continuous experiment's reaction solution, which can be gleaned in Table 5.8. The results indicate that the leaching in batch and in continuous operational modes are quite similar. Leaching does not play an important role for the catalyst's deactivation. Nevertheless, leaching occurs and a technical solution has to be applied to remove contaminations from the final product. All results of ICP/MS can be read up in Table 6.10.

6.3.4 Conclusion

It can be concluded that a recovery process at a temperature of $550\,°C$ is recommendable to maintain the activity of the catalyst. The recovery temperature of $550\,°C$ ensures a long durability and high conversion over all cycles. At least a temperature of $350\,°C$ should be provided. Investigations of colleagues exposed that at temperatures above $600\,°C$ favorable the formation of Pd-black. Therefore, the temperature should not be higher than $550\,°C$. The batch experiments showed a good catalytic activity for Suzuki-Miyaura cross-coupling reactions. The honeycombs can be considered as very versatile and durable. The catalytic monoliths can be reused up to 9 times, depending on the reaction. Without a reactivation process, the honeycomb's activity is destroyed within the first run. Furthermore, the catalytic activity and the long term durability of double coated honeycombs

are significantly higher. Although the honeycombs offer a high recyclability, the activity drop is unstoppable with advanced cycles. The re-coating can restore the reactivity of the honeycombs significantly. The conversion after 60 min for honeycomb 3 could be increased from 47% up to 80% and for honeycomb 4 from 60% up to 90%. According to the quite similar reactivity range of direct re-coating and re-coating with Pd dissolution, the former process is recommendable.

The amounts of leached palladium are as minimal that a full conversion, high yield and high selectivity within two hours can be reached. The release/capture mechanism of palladium on solid supports can explain the good recyclability and the high leaching resistance of the honeycombs. The two attributes indicate that honeycombs are highly suitable for continuous Suzuki-Miyaura cross-coupling reactions.

6.4 Continuous experiments

The continuous experiments were performed in two vessels. The first vessel was an improvised reactor. It was constructed out of stored brass parts, which were originally not considered for a reactor. The second reactor was a self-developed stainless steel reactor, and was manufactured in the institutes workshop.
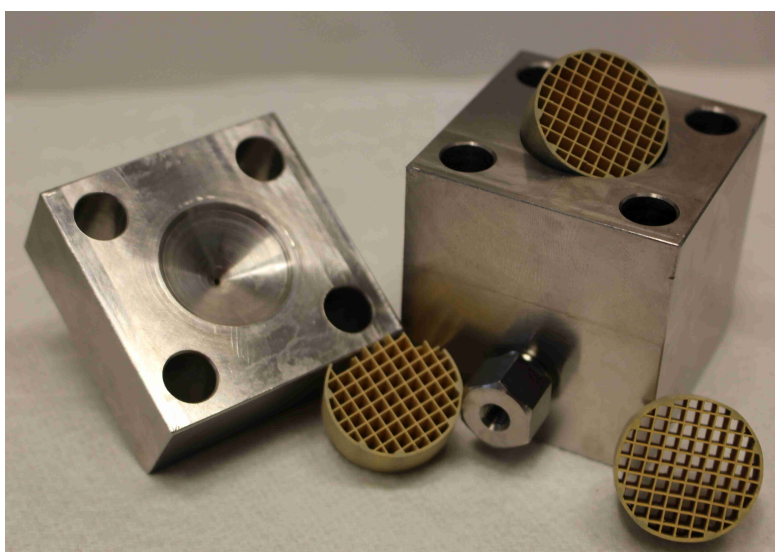
6.4.1 Reactor 2

Figure 6.25: The reactor is a novel developed housing for honeycomb catalysts. It is flexible, handable, compact and modular. The performance was tested with Suzuki-Miyaura reactions on immobilized Pd-catalysts.

The reactor (Figure 6.25) was manufactured for the performance of Suzuki-Miyaura reactions with the novel developed honeycomb catalysts. The catalyst was previously tested in batch experiments. The reactor had several requirements:

- can be implemented easily

- small and compact

- easy to clean

- honeycombs can be easily changed

- modular setup

All enumeration points could be solved with the developed reactor. The reactor offers a high flexibility according to its modular method of construction. The upper performance limits of the continuous reactor are 200 °C and 60 bar. This limits are due to the sealing. Gas/solid, liquid/solid as well as gas/liquid/solid reactions can be performed. The reactor can be used with honeycombs or as a fixed bed reactor with particles. Its small scale of 7 cm x 5 cm x 5 cm (HxBxT) is easily expandable by adding new modules. Possible expansions could be for example ion-exchangers to catch leached metal ions.
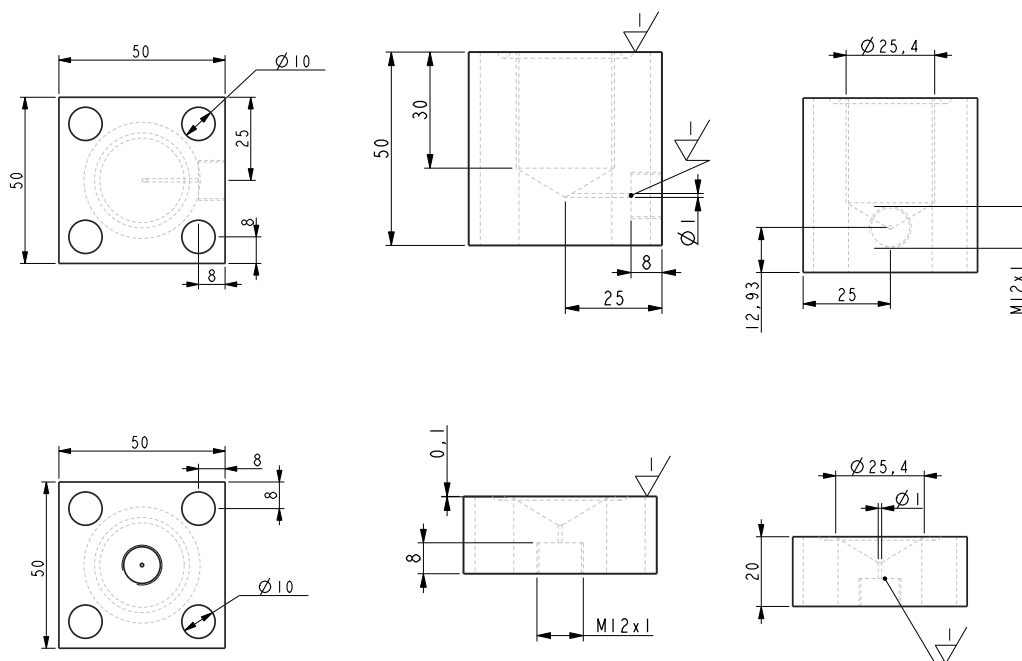

Figure 6.26: Construction plan of the second reactor

Two reactors were built for testing. The first reactor was built "quick and dirty" out of stored brass parts which were not considered for reactor setups. The main problem of the reactor was the small wall thickness at the connections of the vessel with the pipes, which led to leakage. Attributable to the leakage the experiments

were limited to its significance, because the leaked amount of reaction solution could not be determined. Other problems with this reactor were the high dead volume and the slow dissolution of brass by one of the substrates (phenylboronic acid).

Figure 6.27: All parts of the reactor

For the second reactor two other materials were available. Aluminum and 1.4571 stainless steel. According to the dissolution of brass with phenylboronic acid and the dissolution of aluminum by potassium carbonate, a 50 mm quadric profile stainless steel was chosen. 1.4571 is chemically and corrosion resistant. The profile provided enough space for the 25.4 cm reactor drilling as well as for the setting screws. The reactor construction plan is provided in Figure 6.26. The reactor was considered to be the housing for the honeycombs. The honeycomb's channels are predicted to act as PFRs. It was provided that the reactor has to be easily connected with the HPLC-pump. Therefore, it was planned with HPLC-fittings and O-ring sealants. The reactor was designed with PTC:CREO. The reactors assembly is presented in Figure 6.27. It consists out ot four setting screws, two o-ring sealants for the two HPLC-connectors, a surface sealing the reactor body with the inlet, and the reactor cover with the outlet. According to manufacturer issues the volume above and under the honeycombs could not be removed completely.

Therefore, a deviant behavior of an ideal PFR can be predicted. Because it was not possible to cut a groove in the workshop, the sealing between the two parts were changed to a surface sealant.

6.4.2 Residence time distribution

The residence time distribution was determined with a reaction solution based on reaction 1 with p-bromotoluene. Usually RTDs are performed with inert tracers. p-bromotoluene as a compound for the RTD was chosen to exclude the possibility that the substrate bis getting caught by the honeycomb, the reactor or the catalyst. Furthermore, the measured peak areas at the output of the reactor could be related to a known concentration. The setup was the same as for every other continuous experiment. Three honeycombs were placed inside and the vessel was sealed. The preliminary solution, 6.67 mM anisole with EtOH/water in the ratio of 6:4, was pumped through the reactor until the temperature (75 °C), the flow (0.3 ml) and the pressure (34 bar) were constant. Afterwards, the solution was changed to a 9.27 mM p-bromotoluene reaction solution with anisole as internal standard to generate a step function as shown in Figure 6.28.
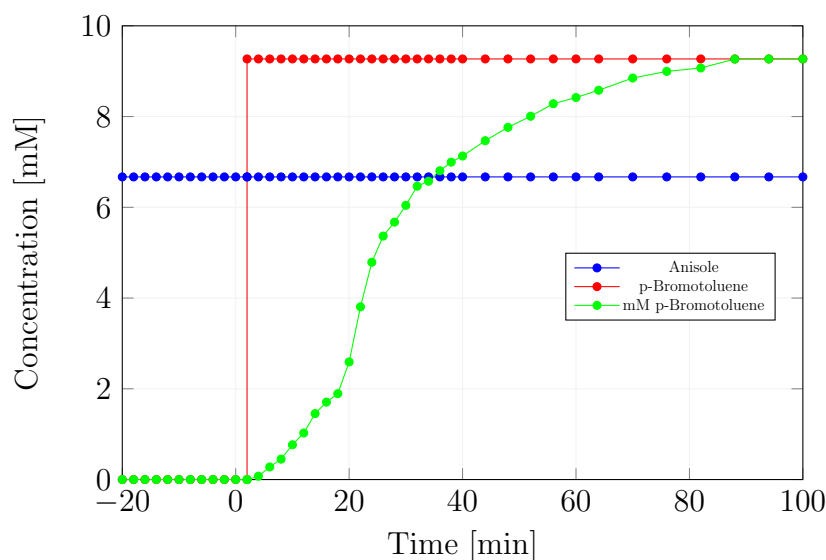

Figure 6.28: Step function, three honeycombs, 0.3 ml, 75 °C, 34 bar

The samples were taken every 2 min. Figure 6.28 shows the progress of the concen-

tration. With the data the exit age distribution E and the cumulative distribution F, presented in Figure 6.29, were determined. The dimensionless exit age distribution $E(\Theta)$ and cumulative distribution $F(\Theta)$ are shown in Figure 6.30.
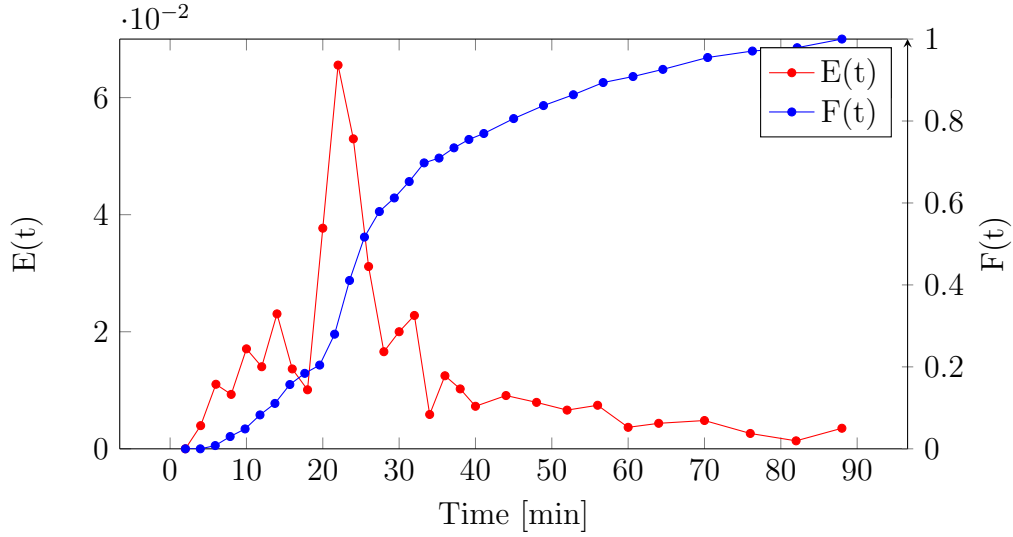

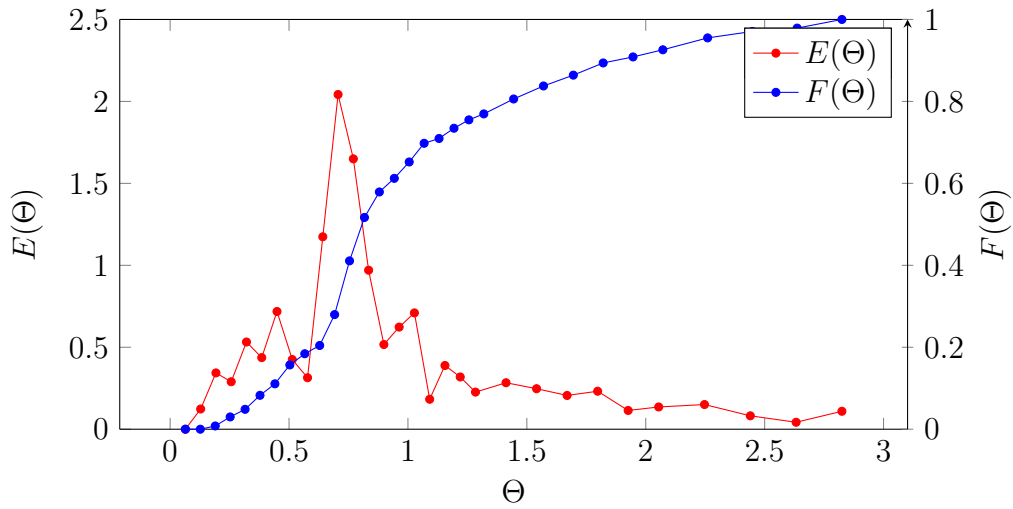Figure 6.29: Exit age distribution E and cumulative distribution F

Figure 6.30: Dimensionless exit age distribution E and cumulative distribution F

As predicted, the exit age distribution as well as the cumulative distribution show a deviant behavior from an ideal PFR. The volume under and above the honeycombs, which were created by the drilling, are acting as reservoirs and as well

as mixing zones. The high volume causes back-mixing at the beginning and the ending of the reactor. The back-mixing is responsible for the flat and unsteady E- and F-curve, which can describe the flow regime as arbitrarily. On the basis of the ferro magnetic material, it was not possible to place a magnetic stirrer inside the reactor to approximately achieve the residence time distribution of a CSTR. The mean time residence was calculated as $\bar{t} = 31.15\,\text{min}$. Furthermore, the variance could be calculated as $\sigma_t{}^2 = 349.91$ and $\sigma_\Theta{}^2 = 0.36$. The dimensionless time Θ was calculated with Equation 6.1.

$$\Theta = \frac{t}{\bar{t}} \tag{6.1}$$

Equation 6.1: Dimensionless time

The Bo was calculated with the dimensionless variance by Equation 6.2. The number is very low and indicates in the direction of a CSTR.

$$Bo = \frac{1}{\sigma_\Theta{}^2} + \sqrt{(\frac{1}{\sigma_\Theta{}^2})^2 + \frac{8}{\sigma_\Theta{}^2}} = 8.24 \tag{6.2}$$

Equation 6.2: Bodenstein number

6.4.3 Continuous reactions

The implementation of the honeycombs was tested with a various number of experiments. The first experiments were performed with reactor one, which was assembled with brass parts. According to the leakage of this reactor, the back-pressure regulator could not be used.

Therefore, the pressure was 1 bar. The settings for reactor one are described in Table 6.11 and the results are illustrated in Figure 6.31. All honeycombs were recovered after every run as described above at 550 °C in the muffle furnace. The reaction solution was prepared with the same molar ratios as for the batch experiments.

Table 6.11: Settings Continuous Reactions reactor 1

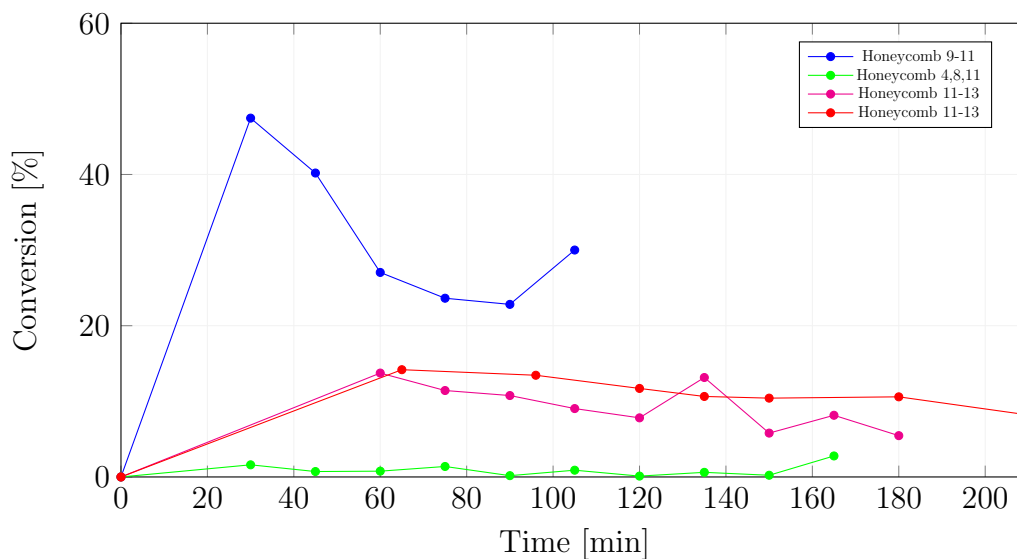| Honeycomb	Temperature °C	Mass flow ml/ min	Pressure bar
9-11	75	1	1
4,8,11	75	1	1
11-13	75	0.6	1
11-13	75	0.6	1

Figure 6.31: Continuous experiments reactor 1, various ml, 75 °C, 1 bar

In Figure 6.31 can be seen, that the catalyst shows a good catalytic reactivity for the first continuous experiment with the honeycombs 9 to 11 (6th run). The recovery process in the batch experiments at 550 °C and the double coating of the monoliths showed positive effects. The reaction had to be aborted according to high leakage. The second experiment with the honeycombs 4, 8 and 11 showed no noteworthy conversion. In tests with the honeycombs 11 to 13 (single coated), the conversion for both runs were low and quite similar but nearly constant over time. It can be assumed that a double coating is beneficial for a continuous setup as it is for batch setups. Nevertheless the leakage at ambient pressure and the high dead volume of reactor one demanded the planning of a new reactor vessel. The results are not significant according to the loss of substrates and products. According of the ability of stirring with a magnetic stirrer inside the reactor, the residence time

distribution can be considered to be the same as for a CSTR.

A various number of experiments were performed with reactor two. The results provide statements to the temperature, pressure and flow rate dependency of the reaction and the reactor. The settings for the experiments are listed in Table 6.12. The pressure was adjusted with different inlets of the back-pressure regulator. The temperature was changed with the oil bath and the flow rate was adapted with the HPLC-pump. The scheme of the reactor setup is shown in Figure 5.9b. The small pipe diameter as well as the low flow rate from the pump to the reactor provides a very good preheating of the reaction solution. The pipe from the back-pressure regulator was isolated with a multiple layer of aluminum foil to suppress crystallization.

Table 6.12: Settings Continuous Reactions reactor 2

Experiment	Honeycomb	Temperature °C	Mass flow ml/ min	Pressure bar
1	9-11	75	1	1
2	10,12,13	75	1	20
3	9,11,12	75	0.6	20
4	14-16	80	0.4	34
5	14-16	80	0.35	34
6	14-16	80	0.3	34
7	13,14,16	84	0.25	25
8	12-14	84	0.2	35

The conversion of the first two experiments (Continuous 1 and 2) of reactor two can be compared with the results of the honeycombs 11 to 13 from reactor one. The conversions are low, but also nearly constant over time. As presented in Figure 6.32, the conversion increases with lowered flow rate, increased pressure and increased temperature. The higher pressure is important for the testing with higher temperatures to increase the boiling point of the solvents. In the case of experiment 3 (Figure 6.32) with a decreased flow rate of about 0.3 ml/ min and a higher pressure the reaction rate could be increased.

The lowered flow rate leads to a higher residence time, which leads to an enhanced contact between the substrates and the active catalytic sites. It turns out that at a temperature of 84 °C, according to the small pipe diameter the solvent starts
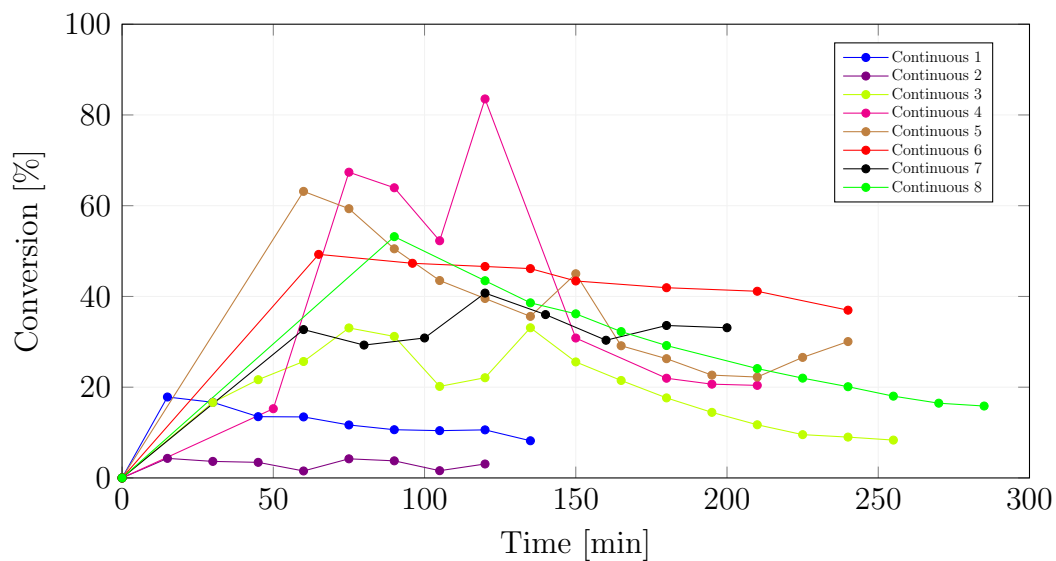
Figure 6.32: The continuous experiments for reactor 2 were carried out at different temperatures, flow rates and pressures. The conditions are shown in Table 6.12.
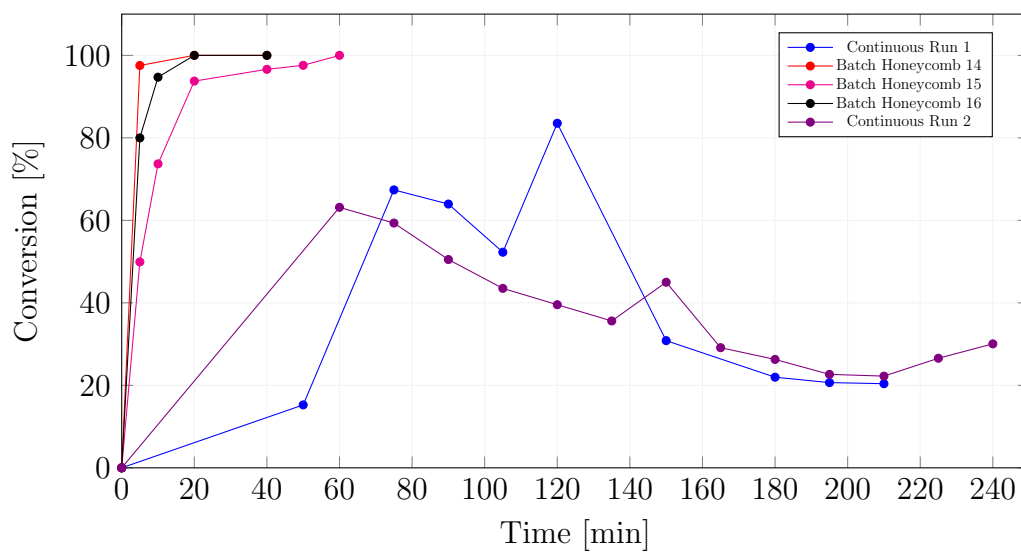

Figure 6.33: Comparison of the reactions carried out with the honeycombs 14, 15 and 16. The first continuous run was carried out at 80 °C, 0.4 ml/ min and 34 bar. The attached batch experiments of each honeycomb were performed at 75 °C. The reaction conditions for second continuous experiment were 80 °C, 0.35 ml/ min and 34 bar.

to vaporize. The best performance of the honeycombs was recorded at reaction 6 with a flow rate of $0.3\,\mathrm{ml/\,min}$ at $80\,°\mathrm{C}$ and a pressure of $34\,\mathrm{bar}$.

To check the leaching and the permanent deactivation of the honeycombs, the monoliths 14, 15 and 16 were tested in a batch experiment after the first run. The results indicate that the activity of the honeycombs can be fully reactivated in the furnace as shown in Figure 6.33. The second runs of all three honeycombs are comparable with the second run of honeycomb 9 or 10, which was also completed after $20\,\mathrm{min}$. The result indicates that the amount of leached palladium over the time of the continuous experiment ($200\,\mathrm{min}$) is similar to the amount in batch experiments (ordinary $30\,\mathrm{min}$). The batch reactions were performed simultaneously at a temperature of $75\,°\mathrm{C}$.

6.4.4 Conclusion

For the continuous experiments it can be concluded that honeycombs are highly suitable for continuous reaction setups. The results of Figure 6.33 show that monoliths offer a high durability and recyclability. The reactivity of the honeycombs does not suffer from long reaction times or from re-usage and recycling. The temperature, the pressure and primarily the flow rate affect the reaction rate notably. A low flow rate to achieve a high residence time is recommendable.

The reactor design is not optimal balanced with honeycombs. A new system has to be implemented which can use the actual reactor as a basis. With an alternate fluid flow through every channel of the honeycomb the residence time and the flow regime could be improved. A higher residence time can lead to higher conversion and yield. According to the modular design of the reactor, two new cover inlets could be implemented, as in the free space under and above the honeycombs. Channels in the cover can provide a guidance through every channel of the honeycomb. The honeycomb will act as a long tubular reactor. For example, a $1\,\mathrm{cm}$ strand with 64 channels could be set up as a $64\,\mathrm{cm}$ tubular reactor. Other possibilities to increase the contact between the fluid and the catalysts and to reduce the high volume of the reactor could be the deployment of inert stuffings, such as silica spheres.

7 Summary and outlook

The goal of this thesis was the immobilization of $Ce-Sn-Pd$ catalyst particles on the surface of cordierite monoliths and the implementation of the new catalytic system in a continuous synthesis process environment. A very easy and fast single step coating process with a high gain of surface area was developed in the thesis. The key facts of the immobilization are:

- Average immobilized mass per honeycomb: $0.0817\,g$

- Average amount of palladium per kg honeycomb: $314.47\,mg\,kg^{-1}$

- Average surface area: $0.8382\,m^2\,g^{-1}$

- Average gained m^2: $1.4879\,m^2\,g^{-1}$

According to the microscopy and batch results honeycombs should be coated at least twice to minimize free surface areas. The distribution on the cordierite surface can be described as consistent, whereas in some areas cluster formation can occur. The immobilization process for honeycombs has a lot of potential for other surfaces. Beside of honeycombs, metal foams and alloys are other possible application for the catalysts.

The batch experiments could be performed with high conversion, yield and selectivity up to 100%. According to the different reaction rates of the substrate it is necessary for an optimal lifetime of the catalyst to define which reaction should be carried out first. The conversion and yield highly depends on the used substrate. The selectivity can be described as stable over run cycles.

Honeycombs, which are partly or deactivated over time, can be successfully re-coated. Previous conversions ($\sim$60%) after several runs can be restored up to 90% by re-coating. The results of the re-coating experiments show that it is not

necessary to dissolve the immobilized Pd from the surface of the monoliths. The difference of directly re-coated honeycombs and ornately re-coated honeycombs is small. A direct re-coating process is as successful as the dissolution routine.

The heterogeneity of the catalysts was tested in batch experiments with recyclability studies and hot filtration tests. The recyclability studies show that, with an increasing number of coatings and a higher recovery temperatures, the reactivity drop of the immobilized catalysts can be minimized and the recyclability can be increased significantly. A re-usage rate of the honeycombs with high conversion and yield could be obtained up to a minimum of eight runs, if all recovery processes were performed. For a maximum lifetime in batch, the following points should be considered:

- Recover honeycombs with a temperature of $550\,°C$ in a muffle furnace

- Washing with EtOH and water after every run

- Reactions with a low reaction rate should be performed first

- Minimum requirement for the durable coating: double coated

- Re-coating is recommended after several runs

The hot filtration test was performed with three honeycombs. All honeycombs show a quite similar conversion. The monoliths were removed after $60\,min$ at a conversion of about 60%. In the following $120\,min$ the conversion increased in all three cases up to 80% which indicates that small amounts of Pd leached or particles were set free from the surface. The reaction solution was not filtered for hot filtration test, because it was assumed that the re-movement of the honeycomb out of the reaction solution will remove the catalyst particles from the reaction. All three reactions were completed after about $600\,min$. According to the ICP/MS measurements Pd is detectable in the reaction solution and the products. The amounts of about $0.069\,mg\,kg^{-1}$ for batch and $0.17\,mg\,kg^{-1}$ for continuous mode are small, but, as Lichtenegger et al. have discovered, very small amounts of Pd are enough to carry out a Suzuki-Miyaura reaction.

The continuous reactions were performed with a novel honeycomb housing. The residence time distribution classifies the flow behavior of reactor 2 as arbitrarily.

The flow regime is created by the shape of the inlet and outlet, from the free space below and above the honeycombs, as well as from the plug flow behavior of the honeycombs itself. All these different flow regimes lead to a non-ideal behavior of the reactor. As described in the conclusion for the continuous experiments, the regime and the performance can be improved with some modular changes of the reactor. New covers for the honeycomb which can be planned as inlets for the reactor, could change the flow regime and increase the residence time. A higher conversion for new flow controls can be assumed. Nevertheless, the results of the continuous experiments allow the statement that honeycombs are highly suitable for the synthesis in flow. The monoliths with immobilized catalyst show a high reactivity and recyclability ability. The most important factors for a successful synthesis in flow for the current reactor are

- A high temperature

- A high pressure is favorable

- A low flow rate is beneficial

Honeycombs are highly recommendable for fine chemical synthesis. The high residence and inertness of the ceramic against chemicals, mechanical influences, temperature changes and the ability to change the shape of the cordierite make monoliths and their surfaces very suitable, as carriers for catalysts and for challenging chemical reactions. Further investigations have to be performed to define the optimal process conditions, such as, for example, the shape of the honeycomb or the flow regime.

Bibliography

[1] Jun-ichi Yoshida, Yusuke Takahashi, and Aiichiro Nagaki. "Flash chemistry: flow chemistry that cannot be done in batch". In: *Chem. Commun.* 49 (85 2013), pp. 9896–9904. DOI: 10.1039/C3CC44709J. URL: http://dx.doi.org/10.1039/C3CC44709J (cit. on p. 1).

[2] *FDA Perspective on Continuous Manufacturing.* Jan. 2012. URL: https://www.fda.gov/downloads/AboutFDA/CentersOffices/OfficeofMedicalProductsandTobacco/CDER/UCM341197.pdf (visited on 01/06/2018) (cit. on p. 1).

[3] Roderick Bates. *Organic Synthesis Using Transition Metals.* Second Edition. Wiley-VCH Verlag GmbH & Co. KGaA, 2012. ISBN: 978-1-119-94286-3. DOI: 10.1002/978-1-119-94286-3 (cit. on pp. 4, 14).

[4] *14.7: Catalysis.* 2018. URL: https://chem.libretexts.org/Textbook_Maps/General_Chemistry_Textbook_Maps/Map%3A_Chemistry%3A_The_Central_Science_(Brown_et_al.)/14%3A_Chemical_Kinetics/14.7%3A_Catalysis (visited on 01/08/2018) (cit. on p. 4).

[5] Hans Peter Latscha and Helmut Alfons Klein. *Anorganische Chemie.* 9. Auflage. Springer-Verlag Berlin Heidelberg, 2007. ISBN: 978-3-540-69863-0. DOI: 10.1007/978-3-540-69865-4 (cit. on pp. 3, 4).

[6] Josef K. Felixberger. *Chemie für Einsteiger.* Springer-Verlag GmbH Deutschland, 2017. ISBN: 978-3-662-52821-1. DOI: 10.1007/978-3-662-52821-1 (cit. on pp. 3–7, 9).

[7] Ass. Prof. Dipl.-Ing. Dr. Heidrun Gruber-Wölfler. *Pharmaceutical Engineering I.* Version WS 2014/15. TU Graz, 2014 (cit. on pp. 4–8, 12–14).

[8] Helmut Knözinger and Karl Kochloefl. "Heterogeneous Catalysis and Solid Catalysts". In: *Ullmann's Encyclopedia of Industrial Chemistry.* Wiley-VCH

Bibliography

Verlag GmbH & Co. KGaA, 2003. ISBN: 978-3-5273-0673-2. DOI: `10.1002/14356007.a05_313`. URL: `http://dx.doi.org/10.1002/14356007.a05_313` (cit. on pp. 6, 9–11).

[9] Piet W.N.M. van Leeuwen. *Homogeneous Catalysis*. Understanding the Art. Kluwer Academic Publishers, 2004. ISBN: 1-4020-2000-7 (cit. on p. 7).

[10] Dr. habil. Marko Hapke. "Homogeneous vs. heterogeneous catalysis". Lecture. Leibzig Institut für Katalyse e.V., 2015 (cit. on p. 8).

[11] Wladimir Reschetilowski. *Einführung in die Heterogene Katalyse*. Springer-Verlag Berlin Heidelberg, 2015. ISBN: 978-3-662-46984-2. DOI: `10.1007/978-3-662-46984-2` (cit. on pp. 8–11).

[12] Calvin H Bartholomew. "Mechanisms of catalyst deactivation". In: *Applied Catalysis A: General* 212.1 (2001). Catalyst Deactivation, pp. 17–60. ISSN: 0926-860X. DOI: `https://doi.org/10.1016/S0926-860X(00)00843-7`. URL: `http://www.sciencedirect.com/science/article/pii/S0926860X00008437` (cit. on pp. 9–12).

[13] J.A Moulijn, A.E van Diepen, and F Kapteijn. "Catalyst deactivation: is it predictable: What to do". In: *Applied Catalysis A: General* 212.1 (2001). Catalyst Deactivation, pp. 3–16. ISSN: 0926-860X. DOI: `https://doi.org/10.1016/S0926-860X(00)00842-5`. URL: `http://www.sciencedirect.com/science/article/pii/S0926860X00008425` (cit. on pp. 9, 12).

[14] X.S. Zhao et al. "Immobilizing catalysts on porous materials". In: *Materials Today* 9.3 (2006), pp. 32–39. ISSN: 1369-7021. DOI: `https://doi.org/10.1016/S1369-7021(06)71388-8`. URL: `http://www.sciencedirect.com/science/article/pii/S1369702106713888` (cit. on pp. 12, 13).

[15] Florian Schröper. "Optimierte Immobilisierung von Redoxproteinen an funktionale Elektrodenoberflächen für die molekulare Bioelektronik". Dissertation. Universität Aachen, 2009 (cit. on pp. 12, 13).

[16] Sudhanshu Sharma and M. S. Hegde. "Single step direct coating of 3-way catalysts on cordierite monolith by solution combustion method: High catalytic activity of Ce 0.98Pd0.02O2-δ". In: *Catalysis Letters* 112.1 (Nov. 2006), pp. 69–75. ISSN: 1572-879X. DOI: `10.1007/s10562-006-0166-z`. URL: `https://doi.org/10.1007/s10562-006-0166-z` (cit. on p. 14).

[17] E.D. Banus et al. "Catalytic coating synthesized onto cordierite monolith walls. Its application to diesel soot combustion". In: *Applied Catalysis B: Environmental* 132-133.Supplement C (2013), pp. 479–486. ISSN: 0926-3373. DOI: `https://doi.org/10.1016/j.apcatb.2012.12.020`. URL: `http://www.sciencedirect.com/science/article/pii/S0926337312005887` (cit. on p. 14).

[18] Christos Agrafiotis et al. "Evaluation of sol-gel methods for the synthesis of doped-ceria environmental catalysis systems. Part I: preparation of coatings". In: *Journal of the European Ceramic Society* 22.1 (2002), pp. 15–25. ISSN: 0955-2219. DOI: `https://doi.org/10.1016/S0955-2219(01)00246-1`. URL: `http://www.sciencedirect.com/science/article/pii/S0955221901002461` (cit. on p. 14).

[19] Pedro Avila, Mario Montes, and Eduardo E. Miró. "Monolithic reactors for environmental applications: A review on preparation technologies". In: *Chemical Engineering Journal* 109.1 (2005), pp. 11–36. ISSN: 1385-8947. DOI: `https://doi.org/10.1016/j.cej.2005.02.025`. URL: `http://www.sciencedirect.com/science/article/pii/S1385894705000793` (cit. on pp. 14, 26–28).

[20] Jay K. Kochi. "Homo coupling, disproportionation and cross coupling of alkyl groups. Role of the transition metal catalyst". In: *Journal of Organometallic Chemistry* 653.1 (2002), pp. 11–19. ISSN: 0022-328X. DOI: `https://doi.org/10.1016/S0022-328X(02)01265-2`. URL: `http://www.sciencedirect.com/science/article/pii/S0022328X02012652` (cit. on p. 14).

[21] *PALLADIUM-CATALYZED CROSS COUPLINGS IN ORGANIC SYNTHESIS*. Scientific Background on the Nobel Prize in Chemistry 2010. 2010. URL: `https://www.nobelprize.org/nobel_prizes/chemistry/laureates/2010/advanced-chemistryprize2010.pdf` (visited on 01/09/2018) (cit. on pp. 15, 16).

[22] Thomas Colacot and et. al. *New Trends in Cross-Coupling. Theory and Applications*. Catalysis Series. The Royal Society of Chemistry, 2015, P001–864. ISBN: 978-1-84973-896-5. DOI: `10.1039/9781782620259`. URL: `http://dx.doi.org/10.1039/9781782620259` (cit. on p. 16).

[23]   Ataualpa A. C. Braga, Gregori Ujaque, and Feliu Maseras. "A DFT Study of the Full Catalytic Cycle of the Suzuki-Miyaura Cross-Coupling on a Model System". In: *Organometallics* 25.15 (2006), pp. 3647–3658. DOI: 10.1021/om060380i. URL: http://dx.doi.org/10.1021/om060380i (cit. on p. 16).

[24]   Peter Dinka and Alexander S. Mukasyan. "In Situ Preparation of Oxide-Based Supported Catalysts by Solution Combustion Synthesis". In: *The Journal of Physical Chemistry B* 109.46 (2005). PMID: 16853808, pp. 21627–21633. DOI: 10.1021/jp054486n. eprint: http://dx.doi.org/10.1021/jp054486n. URL: http://dx.doi.org/10.1021/jp054486n (cit. on p. 17).

[25]   Kashinath C. Patil, S.T. Aruna, and Tanu Mimani. "Combustion synthesis: an update". In: *Current Opinion in Solid State and Materials Science* 6.6 (2002), pp. 507–512. ISSN: 1359-0286. DOI: https://doi.org/10.1016/S1359-0286(02)00123-7. URL: http://www.sciencedirect.com/science/article/pii/S1359028602001237 (cit. on p. 17).

[26]   Sergio González-Cortés and Freddy Imbert. "ChemInform Abstract: Fundamentals, Properties and Applications of Solid Catalysts Prepared by Solution Combustion Synthesis (SCS)". In: 452 (Apr. 2013), pp. 117–131. DOI: 10.1016/j.apcata.2012.11.024 (cit. on p. 17).

[27]   O. Levenspiel. *Chemical reaction engineering*. Third Edition. Wiley, 1999. ISBN: 978-0-471-25424-9. URL: https://books.google.at/books?id=X4svAQAAIAAJ (cit. on pp. 17, 18, 21, 23–25).

[28]   Ass. Prof. Dipl.-Ing. Dr. Heidrun Gruber-Wölfler. *Continuous Processes*. Version SS 2016. TU Graz, 2016 (cit. on pp. 17, 19, 22).

[29]   Fabrizio Caccavale et al. *Control and Monitoring of Chemical Batch Reactors*. 1st ed. Springer-Verlag London, 2011. ISBN: 978-0-85729-195-0. DOI: 10.1007/978-0-85729-195-0 (cit. on pp. 18, 23).

[30]   CHEMGAROO. *Verweilzeit-Verteilung*. URL: http://www.chemgapedia.de/vsengine/vlu/vsc/de/ch/7/tc/vwz/praktikum/vwz_praktikum.vlu/Page/vsc/de/ch/7/tc/vwz/praktikum/einfuehrung/vwz_spektrum.vscml.html (cit. on p. 20).

[31]   Univ.- Prof. Dipl.-Ing. Dr.techn. Matthäus Siebenhofer, Dipl.-Ing. Dr.techn. Susanne Lux, and Dipl.-Ing. Daniela Painer. *Reaktionstechnik II*. Version SS 2014. TU Graz, 2014 (cit. on pp. 22–25).

Bibliography

[32] H. Scott Fogler. *Elements of Chemical Reaction Engineering*. 4th Edition. Prentice Hall, 2006. Chap. Distributions of Residence Times for Chemical Reactors. ISBN: 978-0-131-86383-5 (cit. on p. 22).

[33] Intellishare Enviromental. *Ceramic Monolith Catalyst*. URL: `http://www.intellishare-env.com/product/ceramic-monolith-catalyst/#` (cit. on p. 26).

[34] Shaibal Roy et al. "Monoliths as multiphase reactors: A review". In: *AIChE Journal* 50.11 (2004), pp. 2918–2938. ISSN: 1547-5905. DOI: `10.1002/aic.10268`. URL: `http://dx.doi.org/10.1002/aic.10268` (cit. on pp. 26, 28).

[35] T.A Nijhuis et al. "Monolithic catalysts as more efficient three-phase reactors". In: *Catalysis Today* 66.2 (2001). Catalysis in multiphase reactors, pp. 157–165. ISSN: 0920-5861. DOI: `https://doi.org/10.1016/S0920-5861(00)00621-0`. URL: `http://www.sciencedirect.com/science/article/pii/S0920586100006210` (cit. on p. 29).

[36] Andrzej Stankiewicz. "Reactive separations for process intensification: an industrial perspective". In: *Chemical Engineering and Processing: Process Intensification* 42.3 (2003), pp. 137–144. ISSN: 0255-2701. DOI: `https://doi.org/10.1016/S0255-2701(02)00084-3`. URL: `http://www.sciencedirect.com/science/article/pii/S0255270102000843` (cit. on p. 29).

[37] F Aguero et al. "MnCu/Cordierite Monolith used for Catalytic Combustion of Volatile Organic Compounds". In: 36 (Sept. 2013) (cit. on p. 29).

[38] Alejandra Devard, María Alicia Ulla, and F. Albana Marchesini. "Synthesis of Pd/Al2O3 coating onto a cordierite monolith and its application to nitrite reduction in water". In: *Catalysis Communications* 34 (2013), pp. 26–29. ISSN: 1566-7367. DOI: `https://doi.org/10.1016/j.catcom.2013.01.005`. URL: `http://www.sciencedirect.com/science/article/pii/S156673671300006X` (cit. on p. 29).

[39] Cortes Nicole Salgado. *Fluorescence Microscopy*. URL: `https://www.slideshare.net/nisalgadoc/fluorescence-microscopy-introduction` (cit. on p. 32).

[40] UCLA Brain Research Institute. *UCLA BRAIN RESEARCH INSTITUTE MICROSCOPY CORE FACILITIES*. URL: `http://www.gonda.ucla.edu/bri_core/homepage.htm` (cit. on p. 32).

Bibliography

[41]   Hayley Anderson. *Brightfield Microscopy*. URL: `https://www.microscopem aster.com/brightfield-microscopy.html` (cit. on p. 32).

[42]   Abramowitz Mortimer and Davidson Michael W. *Reflected/Transmitted light microskopy*. URL: `https://www.olympus-lifescience.com/en/microscop e-resource/primer/anatomy/reflected/` (cit. on p. 33).

[43]   Rottenfusser Rudi, Wilson Erin E., and Davidson Michael W. *Education in Microscopy and Digital Imaging*. URL: `http://zeiss-campus.magnet.fsu. edu/articles/basics/reflected.html` (cit. on p. 33).

[44]   *High Performance Liquid Chromatography (HPLC) : Principle, Types, Instrumentation and Applications*. 2018. URL: `https://laboratoryinfo.com/ hplc/` (visited on 02/12/2018) (cit. on p. 33).

[45]   *Chromatography*. URL: `https://upload.wikimedia.org/wikipedia/comm ons/4/4c/Kromatografia.png` (visited on 02/12/2018) (cit. on p. 33).

[46]   *High purity water for ICP-MS*. URL: `https://www.merckmillipore.com/ AT/de/water-purification/learning-centers/applications/inorg anic-analysis/icp-ms/_e2b.qB.s7QAAAFAniQQWTtN,nav` (visited on 02/14/2018) (cit. on p. 35).

[47]   *The 30-Minute Guide to ICP-MS*. URL: `https://www.perkinelmer.com/PD Fs/Downloads/tch_icpmsthirtyminuteguide.pdf` (visited on 02/14/2018) (cit. on p. 36).

[48]   Micromeritics Instrument Corporation. *TriStar II 3020 Analyzer*. 2009 (cit. on p. 36).

[49]   Georg J. Lichtenegger et al. "Continuous Suzuki-Miyaura Reactions with Novel Ce-Sn-Pd Oxides and Integrated Crystallization as Continuous Downstream Protocol". In: 6.3 (Aug. 2016), pp. 244–251. ISSN: 2063-0212. DOI: `10.1556/1846.2016.00021` (cit. on pp. 39, 40, 73, 74, 88).

[50]   G.J. Lichtenegger et al. "Suzuki-Miyaura coupling reactions using novel metal oxide supported ionic palladium catalysts". In: *Journal of Molecular Catalysis A: Chemical* 426.Part A (2017), pp. 39–51. ISSN: 1381-1169. DOI: `https://doi.org/10.1016/j.molcata.2016.10.033`. URL: `http: //www.sciencedirect.com/science/article/pii/S1381116916304563` (cit. on pp. 39, 40).

[51]   Tetsuo Iwasawa et al. "Homogeneous Palladium Catalyst Suppressing Pd Black Formation in Air Oxidation of Alcohols". In: *Journal of the American Chemical Society* 126.21 (2004). PMID: 15161274, pp. 6554–6555. DOI: 10. 1021/ja031936l. eprint: `https://doi.org/10.1021/ja031936l`. URL: `https://doi.org/10.1021/ja031936l` (cit. on p. 55).